TH-172

HYDROGENATION OF NITROBENZENE ON COPPER CHROMITE : STUDIES IN REACTION MODELLING AND ADSORPTION OF POISON (THIOPHENE)

A THESIS SUBMITTED TO THE

UNIVERSITY OF BOMBAY

FOR THE DEGREE OF

DOCTOR OF PHILOSOPHY

in

Physical Chemistry

BY

S. D. SANSARE

NATIONAL CHEMICAL LABORATORY
POONA-411 008 (India)

MARCH 1981

Statement required to be submitted under rule 0.413 of the University of Bombay

No part of this thesis has been submitted for a degree or diploma or other academy award. The literature concerning the problems investigated has been surveyed and all the necessary references are given in the thesis. The present work has been clearly indicated separately. The experimental work has been carried out entirely by me. In accordance with the usual practice due acknowledgement has been made wherever the work presented is based on the results of other workers.

(Dr. L. K. Doraiswamy)
Research Guide

(S. D. Sansare)
Candidate

.....

ACKNOWLEDGEMENT

I wish to put on record my deep-felt sense of gratitude to Dr. L.K. Doraiswamy, Director, N.C.L. Pune, for guiding me in the research work for the Ph.D. degree. But for his inspired guidance I could not have brought the investigation to a successful conclusion. I am also grateful to him for permitting me to carry out the research work.

Dr. V.R. Choudhary, Scientist, Chemical Engineering Division, very willingly guided me in the part of investigation in which the Gas Chromatographic technique was employed for studying adsorption. I am extremely grateful to him for this guidance.

Dr. B.D. Kulkarni, Scientist, Chemical Engineering Division, made his knowledge and time readily available to me and helped me to prepare this thesis. I am extremely thankful to him for this help.

Dr. R.A. Rajadhyaksha, Reader in Chemical Engineering, UDCT, Matunga, Bombay, helped me with the computation of experimental and other data, for which I am indebted to him.

I also take this opportunity to thank all my colleagues and friends who always offered their help unhesitatingly.

(S. D. SANSARE)

MARCH
1981

CONTENTS

....

....

....

LIST OF FIGURES

.....

.....

.....

.....

LIST OF TABLES

....

SUMMARY AND CONCLUSIONS

SUMMARY AND CONCLUSION

Hydrogenation of nitrobenzene to aniline is a well known reaction. Commercially available nitrobenzene contains thiophene as an impurity which affects the activity and hence the life of the catalyst. Literature on the reduction of nitrobenzene to aniline reaction deals mainly with the kinetics and reaction mechanism under conditions of no poisoning. Hence the present work has been undertaken to analyse the kinetics of the deactivation. The first step in the study of deactivation kinetics is as investigation of kinetics of main reaction occurring on the pure catalyst and the first part deals with this aspect. The second part is concerned with the deactivation of the catalyst due to thiophene. In the present case the deactivation is due to the adsorption of thiophene on the catalyst surface and hence a detailed study of the adsorption pattern on the catalyst surface has been made.

KINETICS OF REACTION ON UNPOISONED CATALYST

Experimental data has been collected in an integral reactor in temperature range 180°C-260°C, the range of reciprocal space velocity being 20-240. Experimental data obtained has been further used to test well known models viz. power law and the heterogeneous Hougen-Watson model.

By power law analysis it has been found that the hydrogenation that the order of reaction is 1.4 with respect to nitrobenzene. Two methods have been followed to determine the constants A and E, viz. (1) by analysing the data at each temperature separately and then applying Arrhenius law to get the constants and (2) by analysing the data at all the temperatures together to obtain the constants. Values of constants obtained by both the methods have been found comparable.

Hougen-Watson approach is then adopted to achieve the possible mechanism. Six models have been considered. The estimation of model parameters is carried out using linear and non-linear least square analysis. Suitability of the best model has been confirmed by comparing observed and calculated rates. The temperature dependence of rate constant (k) and adsorption equilibrium constant (K_A) has been studied and activation energy (E) is determined from it. The best fitted model suggests the adsorption of nitrobenzene to be thecontrolling step with dual site mechanism.

STUDIES IN POISONING

After evaluating a model equation for the reaction on the unpoisoned catalyst, experiments have been conducted to study the effects of feed poisoning. The conditions of the

experiments were kept same as those in the study for obtaining kinetic model. A known amount of thiophene has been introduced into the nitrobenzene and the contaminated nitrobenzene fed to the reactor. Samples have been analysed at different time intervals. It is observed that initial fall of conversion is rapid but this slows down with time to a constant non-zero value. This can be explained as follows: with increasing time thiophene adsorption also increases irreversibly which reflects as a rapid fall in conversion. A stage is eventually reached when thiophene in gas phase remains in equilibrium with that adsorbed on the catalyst. Irreversible adsorption now stops and reversible adsorption starts as indicated by non-zero value.

In the present case separable type of deactivation equations have been proposed, in which the deactivation term and activity terms are separable. Activity is found to have an exponential dependence on time. In the present case terms for poison concentration, conversion and time have been included in the deactivation equation. The constants of the equation have been evaluated by graphical and regression analysis methods. Two sets of values of the constants are obtained by each method indicating that only one set of value is not enough to predict the activity pattern throughout the entire time interval. The validity of the equation has been confirmed by comparing predicted and observed rates. The

poisoning study points to a two-stage adsorption of thiophene on the catalyst. The first being the irreversible adsorption and second the reversible one. Both the modes of adsorption play an important role in the poisoning phenomenon.

ADSORPTION OF THIOPHENE ON COPPER CHROMITE CATALYST

Adsorption of thiophene on the catalyst has been studied at conditions close to those used in the reduction of nitrobenzene to aniline (i.e. at temperature of 150° to 300°C and in the presence of hydrogen) by using the gas chromatography technique. Both the irreversible and the reversible adsorptions have been studied and they exhibit an unusual behaviour.

The rate of irreversible adsorption of thiophene is found to be influenced by the quantity of chemisorbed thiophene. The extent of reversible adsorption on the catalyst surface with partially saturated irreversible adsorption sites, is also found to depend upon the initial surface coverage, as both the two adsorption are probably due to the modifications of the existing sites and/or creation of new active sites on the surface. The adsorption isotherms have been determined by a peak maxima method using the pulse technique. It has been found to follow the Freundlich adsorption equation. The isosteric heat of adsorption has been determined from the isotherms and found to be dependent on the surface coverage.

...

poisoning study points to a two-stage adsorption of thiophene on the catalyst. The first being the irreversible adsorption and second the reversible one. Both the modes of adsorption play an important role in the poisoning phenomenon.

ADSORPTION OF THIOPHENE ON COPPER CHROMITE CATALYST

Adsorption of thiophene on the catalyst has been studied at conditions close to those used in the reduction of nitrobenzene to aniline (i.e. at temperature of 150° to 300°C and in the presence of hydrogen) by using the gas chromatography technique. Both the irreversible and the reversible adsorptions have been studied and they exhibit an unusual behaviour.

The rate of irreversible adsorption of thiophene is found to be influenced by the quantity of chemisorbed thiophene. The extent of reversible adsorption on the catalyst surface with partially saturated irreversible adsorption sites, is also found to depend upon the initial surface coverage, as both the two adsorption are probably due to the modifications of the existing sites and/or creation of new active sites on the surface. The adsorption isotherms have been determined by a peak maxima method using the pulse technique. It has been found to follow the Freundlich adsorption equation. The isosteric heat of adsorption has been determined from the isotherms and found to be dependent on the surface coverage.

...

CHAPTER 1

GENERAL INTRODUCTION

CHAPTER 1

GENERAL INTRODUCTION

Deactivation of the catalyst in fixed bed reactors is widely encountered in practice. It often plays an important role in determining the overall kinetics of catalytic reactions. As in the case of reactor analysis, the study of catalyst deactivation involves three major considerations: chemical nature of the catalyst deactivation, behaviour of a pellet as a whole under conditions of deactivation, and reactor design for a deactivating catalyst.

1.1 TYPES OF DEACTIVATION

Deactivation is a general term used to denote the loss in catalyst activity which may be due to the formation of coke (fouling), due to the impurity present in the feed stream (poisoning), or it may be due to structural modification or sintering of the catalyst. Deactivation due to coke formation represents perhaps the most common type of deactivation and several theoretical and experimental studies taking into account the complexities of the rate equations for the main and the fouling reactions have been reported in the literature. The case of impurity-poisoning is also common but systematic experimental studies for this case are somewhat scarce. In the case of sintering decay is independent of the concentration of the material in the gas phase, but dependent on the length of time

spent in the high temperature atmosphere.

Many heterogeneous reactions of industrial importance such as cracking, isomerization, dehydrogenation of hydrocarbons etc. are accompanied by gradual decrease in the catalyst activity. This decrease in the activity in many cases may be due to the formation of carbonaceous material (coke), or due to the presence of small amounts of impurity in the feed stream. A few such important examples (deactivation due to coke formation and poisoning) are summarized in Table I.

1.2 STUDIES ON DEACTIVATION

Several recent studies dealing with catalyst deactivation discuss the effect of various types of deactivation. Butt (7) has reviewed the literature on various aspects of deactivation.

1.2.1 Studies on a single pellet

Deactivation studies have been commonly reported either on a single pellet or in a reactor containing a number of pellets. Many investigators in this field have used single pellet diffusion reactors (3,8,20-24,27-29,55,56) for the measurement of concentration and temperature profiles. However, most of these studies are concerned with deactivation due to coke formation. Hegedus and Petersen (24) have reviewed several studies in the single pellet diffusion reactor and shown that it can be used in studying the interactions between diffusion, reaction and deacti-

TABLE 1

Examples of deactivation due to coke formation and poisoning

S.No.	Reaction	Remarks	Reference
1	2	3	4
1.	Hydrogenation of an unsaturated glyceride on finely divided Nickel.	Traces of carbon monoxide acted as an impurity.	E.B. Maxted (34)
2.	Hydrogenation of ethylene on copper.	Pressure of carbon monoxide found to reduce the activity	R.N. Pease L. Stewart (40)
3.	Synthesis of ammonia on iron.	Small amount of oxygen in feed mixture reduced the NH_3 concentration	J.A. Almquist (1)
4.	Synthesis of ammonia on iron.	Water vapour acted as a poison for the iron catalyst	D.H. Emmett S. Brunauner (14)
5.	Liquid phase hydrogenation of crotonic acid and olive oil on platinum and nickel catalysts.	Catalysts were poisoned by thiophene.	Maxted E.B. Evans H.C. (35)
6.	Hydrogenation of phenol, naphthalene, quinolens on Raney	Sulphur compounds in five different stages of oxidation	A.G. Deem J.I. Kaveckis (10)

contd..

1	2	3	4
	nickel.	were found to affect the activity.	
7.	Para hydrogen conversion on tungsten surface.	Adsorbed oxygen on tungsten surface acted as a poison.	Eley E.K. Rideal (13)
8.	Aromatization of aliphatic compound on molybdenum supported on alumina.	Deactivation of the catalyst was found due to polymer formation on catalyst surface.	E.F.G. Herington E.K. Rideal (26)
9.	Cracking of a gas oil on an acid activated monomorillonite clay.	Presence of poison in feed such as sulphur compounds and metals like iron, nickel, copper, vanadium found to reduce the activity.	B.J. Dutly N.M. Hart (12)
10.	Petroleum cracking on acid treated natural clay and synthetic silica alumina catalyst.	Deactivation was due to coke formation (cracking).	F.H. Blandins (4)
11.	Oxidation of carbon monoxide on nickel oxide catalyst.	Excess concentration of oxygen was found to reduce the activity.	G. Parravano (39)

contd..

1	2	3	4
12.	Aromatization of cyclohexane on molybdenum-alumina hydro-forming catalyst.	Deposition of coke reduced the activity exponentially.	C.G. Rudershausen C.C. Watson (47)
13.	Gas oil cracking on natural and synthetic catalysts.	Coke formation reduced the activity.	Voorhies (42)
14.	Cracking of cumene on silica-alumina cracking catalyst.	Deactivation was due to coke formation.	C.D. Prater R.M. Lago (44)
15.	Hydrogenation of isobutylene on nickel.	Polymerization of isobutylene during hydrogenation was responsible for deactivation.	A.L. Pozzi H.F. Rase (43)
16.	Dehydrogenation of 1-1.3 cyclohexane on platinum-alumina.	Coke formation was the cause of deactivation.	Germain Maurel (17)
17.	Conversion of cyclohexane to benzene.	Introduction of thiophene in feed reduced the catalyst activity.	Kh.M. Minachev G.V. Isaghlyants (37)

contd...

1	2	3	4
18.	Dehydrogenation of butene on chromia-alumina.	Coke formation was due to cracking of 1-butene, coke deposit was analysed with micro-balance flow reactor.	L. Forni et al. (16)
19.	Alkylation of benzene by cyclohexane on zeolite.	Deactivation was due to the di and tri alkyl benzene which was trapped in the void space of zeolite crystals.	C.H. Tan O.M. Fuller (50)
20.	Hydrogenation of ethylene on Cu-MgO catalyst.	Introduction of water vapour in feed was found to reduce the activity.	F. Gioia (19)
21.	Hydrogenation of benzene on Ni Kieselguhr.	Thiophene was used as pioson. Temperature profiles were measured along the reactor length.	H.S. Weng et al. (53)
22.	Dehydrogenation of n-butane on chromia and alumina.	Dehydrogenation was more effective on chromia while coke formation occurred on both.	R. Toei et al. (51)

contd..

1	2	3	4
23.	Thermal cracking of n-octane.	Stainless steel tubular reactor was used. Deactivation was due to coke formation.	Y.T. Shah et al. (48)
24.	Dehydrogenation of 1-butene to butadiene on Cr_2O_3 - Al_2O_3 catalyst.	Deactivation was due to coke formation which was analysed by thermobalance.	F.J. Dumerz G.F. Froment (11)

vation. The single pellet reactor has also been used to study deactivation due to poisoning, for example the poisoning of $Ni/SiO_2-Al_2O_3$ by O_2 in ethylene hydrogenation (28) and thiophene poisoning of Ni Kiselguhr in benzene hydrogenation (8,27).

1.2.2 Studies on using bulk quantities of catalyst

Experimental studies on deactivation using bulk quantities of catalyst (as opposed to single pellets) have also been reported in the literature and several equations relating rates, concentration, time and temperature to the activity of the catalyst are available. Rudershausen and Watson (47) studied the coke formation on molybdena-alumina catalyst, and observed an exponential decay in the activity. Pozzi and Rase (43) have developed the rate expressions as well as the technique for isolation of fouling. The activity in this work was based on the conversion. Rates were related to the number of active centres, partial pressures and temperature. Froment and Bischoff (15) have accounted for the decrease in the catalyst activity by relating the rate coefficients to the carbon content of the catalyst rather than to the time. Anderson and Whitehouse (2) examined the distribution of poison along the catalyst bed, and suggested poisoning equations, relating relative activity to the poison concentration on the catalyst surface. Szepe and Levenspiel (49) have reviewed several types of decay equations. Levenspiel (32) and Khang et al. (30) have presented various types of decay mechanisms. Gioia (19) studied the influence of reversible poison (water vapour) on the deacti-

vation rate of Cu-MgO porous catalyst which was used in the hydrogenation of ethylene. Toei et al. (51) studied the catalyst fouling in dehydrogenation of n-butane both theoretically and experimentally and observed that dehydrogenation occurred on chromia, whereas coke could be formed on γ-alumina as well as on chromia. In a recent work Hegedus and Summers (25) have investigated the poisoning of noble metals in the oxidation of CO and hydrocarbons. Correlations were given for poison penetration and effectiveness as a function of time. Mikus et al. (36) have studied the temperature profiles and exit conversion for different inlet CS_2 (poison) concentrations. Recently detailed reactor modelling studies of dynamics as they are influenced by poisoning have been reported by Blaum (5) and some experiments in which parallel poisoning is the mechanism of deactivation have been reported by Weng et al. (53), Price and Butt (45) and Butt et al. (9) for hydrogenation of benzene on Ni/Kiselguhr with thiophene poison. They measured the axial temperature profiles, and rate and the deactivation equations were presented separately.

Another industrially important reaction prone to impurity poisoning is the hydrogenation of nitrobenzene to aniline. Commercially available nitrobenzene contains thiophene as an impurity which affects the activity of the catalyst. Several studies have been reported on this reaction in order to investigate the mechanism and the kinetics of reaction.

Brown and Henke (6) studied the vapour phase reduction of nitrobenzene on nickel and copper catalyst, and found that nickel reduced nitrobenzene to ammonia and cyclohexane giving low yields of aniline, while copper catalyst gave fairly high yields of aniline. Gharda et al. (18) found that under certain conditions, copper catalysts were stable. However, sulphur compounds, especially thiophene in feed, deactivated the catalyst. Their proposed rate model showed the rate controlling step to be surface reaction between absorbed hydrogen and nitrobenzene. The fluidized bed technique (38) has also been used to investigate the effect of catalyst particle size, mole ratio of reactants in the feed, space velocity and temperature on conversion. Several catalysts have been screened by Rihani et al. (46), and they recommended a suitable rate expression in power law form. Kinetics and mechanism of reaction have also been studied on nickel foil and copper catalyst (41) as well as on nickel copper alloy (42).

It has generally been observed that (18,38) the activity of the catalyst falls during the course of reaction. This fall in activity could be due to the impurity in the feed, mainly sulphur compounds, or due to the high particle temperature.

1.3 PRESENT STUDY

As stated earlier the literature on the reduction of nitrobenzene to aniline deals mainly with the kinetics and reaction mechanism under conditions of no deactivation. The

present study was undertaken to examine quantitatively the deactivation of the catalyst (copper chromite) used in the vapour phase hydrogenation of nitrobenzene to aniline.

1.3.1 Methods of studies in deactivation

Both direct and indirect methods can be used to study deactivation. In the direct method, it is necessary to measure the poison concentration analytically which is often impracticable. Hence indirect methods are more common. In some cases a fresh sample of catalyst is first exposed to a specific concentration of poison for a certain length of time and then the conversion or rate is calculated by passing a pure feed. In other cases, feed is contaminated with poison of different concentrations and then the contaminated feed is passed over the catalyst bed. The latter method seems to be preferable, since in practice poison species are deposited along with the reactant on the catalyst surface in many cases.

The first step in a study of deactivation kinetics is obviously an investigation of the kinetics of the main reaction on the pure unpoisoned catalyst. This can be carried out by passing pure feed over the catalyst bed and studying the kinetics of the reaction, the results are presented in Chapter 2. The second part requires addition of a continuity equation involving the poison concentration and time. This is discussed in Chapter 3.

1.3.2 Studies in adsorption of thiophene

Adsorption of thiophene on the catalyst surface deactivates the active centres on the catalyst. Hence it is necessary to study the adsorption pattern of thiophene on the catalyst surface.

In recent years the gas chromatographic technique has been widely used (31) to obtain physico-chemical information. The present work uses the gas chromatographic method (dynamic method) to determine the adsorption behaviour of thiophene on the catalyst surface, maintaining the conditions close to reaction conditions. The theoretical aspects of this study are covered in Chapter 4, while the experimental technique used and results obtained are discussed in Chapter 5.

...

REFERENCES

1. Almauist, J.A., Blank, C.A., J. Am. Chem. Soc., 48, 2814 (1926)

2. Andersen, R.B., and Whitehouse, A.M., Ind. Eng. Chem., 53, 1011 (1961)

3. Balder, J.R., and Petersen, E.E., Chem. Eng. Sci., 23, 1287 (1968)

4. Blanding, F.H., Ind. Eng. Chem., 45, 1186 (1953)

5. Blaum, E., Chem. Eng. Sci., 29, 2263 (1974)

6. Brown, O.W. and Henke, C.O., J. Phy. Chem., 26, 161, 273, 715 (1922)

7. Butt, J.B., Adv. Chem. Ser., 109, 259 (1972)

8. Butt J.B., Downing, D.M., and Lee J.W., Ind. Eng. Chem., (Fundal), 16, 270 (1977)

9. Butt, J.B., Weng, H.S., Eigenbarger, G., International Chem. Eng., 17, 35 (1977)

10. Deem, A.G., Kaveckis, J.I., Ind. Eng. Chem., 33, 1373 (1941)

11. Dumez, F.J., Forment, G.F., Ind. Eng. Chem., (Proc. Des. Dev.), 15, 291 (1976)

12. Dutty, B.J., Hart, H.M., Chem. Eng. Progr., 48, 344 (1952)

13. Eley, D.D., Rideal, E.K., Proccd. Roy. Soc., (London) A, 178, 429 (1941)

14. Emmett, P.H., Brunauner, S., J. Am. Chem. Soc., 52, 2682 (1930)

...

15. Froment, G.F., and Bischoff, K.B.,
Chem. Eng. Sci., 16, 189 (1961)

16. Forni, L., Zanderighi, L., Cavenaeni, C., Carra, S.,
J. Catal. 15, 153 (1969)

17. Germain Maurel,
Comptes, Rendus, 247, 1854 (1958)

18. Gharda, K.H., Sliepcavich, C.W.,
Ind. Eng. Chem., 52, 417 (1960)

19. Gioia Francisco,
Ind. Eng. Chem. (Fundl), 10, 204 (1971)

20. Hegedus, L.L., Petersen, E.E.,
Ind. Eng. Chem. (Fundl), 11, 579 (1972)

21. Hegedus, L.L., Petersen, E.E.,
Chem. Eng. Sci., 28, 69 (1973)

22. ibid , 28, 345 (1973)

23. Hegedus, L.L., Petersen, E.E.,
J. Catal. 28, 150 (1973)

24. Hegedus, L.L., Petersen, E.E.,
Catal. Rev. Sci.,Eng., 11, 245 (1974)

25. Hegedus, L.L., Summers, J.C.,
J. Catal. 48, 345 (1977)

26. Herington, E.F.G., Rideal, E.K.,
Proccd. Roy. Soc. (London) A 184, 434 (1945)

27. Hughes, R. and Koh, H.P.,
Chem. Eng. J., 20, 395 (1974)

28. Hughes, R. and Koh, H.P.,
AIChEJ, 20, 395 (1974)

29. Kehoe, J.P.G. and Butt, J.B.,
AIChEJ., 18, 347 (1972)

...

30. Khang, S.J., Levenspiel, O.,
Ind. Eng. Chem. (Fundl), 12, 185 (1973)

31. Kobayashi, R., Chappelear, P.S., Deans, H.A.,
Ind. Eng. Chem., 59, 63 (1967)

32. Levenspiel, O.,
J. Catal., 25, 265 (1972)

33. Masamune, S. , Smith, J.M.,
AIChEJ., 12, 384 (1966)

34. Maxted, E.B.,
Trans. Far. Soc., 13, 36 (1917)

35. Maxted, E.B., Evan, H.C.,
J. Chem. Soc., 603 (1937)

36. Mikus, O., Pour, V., and Hlavacek, V.,
J. Catal., 48, 98 (1977)

37. Minachev, K.h. M., Isagulgants, a.V.,
Proccd. 3rd Int. Cong. Catâ.Part I, 309 (1965)

38. Murthy, M.S., Deshpande, P.K., Kuloor, N.P.,
Chemical Age of India, 14, 653 (1963)

39. Parravano, G.,
J. Am. Chem. Soc., 75, 1448 (1953)

40. Pease, R.N., Stewart, L.,
J. Am. Chem. Soc., 47, 1235 (1925)

41. Pogorelov, V.V., Vigdorovich, F.L., Gel'bshtein, A.I.,
Kinetics and Catalysis Part I, 17, 587 (1976)

42. Pogorelov, V.V. and Gel'bshtein, A.I.,
Kinetics and Catalysis Part II, 17, 1287 (1977)

43. Pozzi, A.L., Rase, H.F.,
Ind. Eng. Chem., 7, 1075 (1958)

...

44. Prater, C.D., Lago, R.M.,
Adv. Cat. 8, 293 (1956)

45. Price, T.H., Butt, J.B.,
Chem. Eng. Sci., 32, 393 (1977)

46. Rihani, D.N., Narayanan, T.K., Doraiswamy, L.K.,
Ind. Eng. Chem. (Procc. Des. Dev.), 4, 403 (1965)

47. Rudershausen, C.G., Watson, C.C.,
Chem. Eng.Sci., 3, 110 (1954)

48. Shah, Y.T., Stuart, E.B., Sheth, K.D.,
Ind. Eng. Chem. (Procc. Des. Dev.), 15, 519 (1976)

49. Szepe, S., Levenspiel, O.,
Chem. React. Eng., 165, Sept. (1968)

50. Tan, C.H., Fuller, O.M.,
Cand. J. Chem. Eng., 48, 174 (1970)

51. Toei, R., Nakanishi, K., Yamada, K., Okazaki, M.,
J. Chem. Eng. Japan, 8, 131 (1975)

52. Voorhies, A. Jr.,
Ind. Eng. Chem. 37, 318 (1945)

53. Weng, H.S., Eigenberger, G., Butt, J.B.,
Chem. Eng.Sci., 30, 1341 (1975)

54. Wheeler,
Adv. Cat. 2, 250 (1951)

55. Wolf, E. and Petersen, E.E.,
Chem. Eng. Sci., 29, 1500 (1974)

56. Wolf, E. and Petersen, E.E.,
J. Catal, 46, 190 (1977)

....

CHAPTER 2

REACTION MODELLING ON UNPOISONED CATALYST

CHAPTER 2

REACTION MODELLING ON UNPOISONED CATALYST

2.1 INTRODUCTION

As stated in the earlier chapter, as a precursor to the study of the deactivation kinetics, it is necessary first to investigate the kinetics of the main reaction on the unpoisoned catalyst. This chapter aims at providing the kinetics on the unpoisoned catalyst. The experimental kinetic data have been analyzed, and a power law model as well as a suitable Hougen-Watson model in the temperature range 453°-533°K have been proposed.

2.2 EXPERIMENTAL

2.2.1 Raw materials

Nitrobenzene: Nitrobenzene used was of pure analytical grade and free from thiophene contamination.

Hydrogen: Hydrogen used was free from other impurities (obtained from Industrial Oxygen Ltd., India).

Nitrogen: Nitrogen used was also free from other impurities (obtained from Industrial Oxygen Ltd., India).

Catalyst: Copper chromite catalyst was used (CuO. $CuCr_2O_4$, prepared in the laboratory, Ref: N.C.L. Report 1975) for the reduction of nitrobenzene.

2.2.2 Experimental set-up

The experimental set-up is shown in Fig. 2.1. It consists of a hydrogen gas supply system, nitrobenzene feed device and the reactor assembly. Nitrobenzene was fed into the reactor through a burette from a constant flow device as shown in Fig. 2.1. The function of burette was to provide sufficient head of the liquid to take care of the pressure fluctuations.

Reactor assembly

The reactor assembly consisted of (i) outer jacket of the reactor (ii) reactor tube, and (iii) cyclone to minimize the loss of fluidizing solids (bauxite) as shown in Fig. 2.1.

The outer jacket was provided with the heating coil and contained the fluidizing medium. The bauxite in the fluidized state ensured uniform heating of the reactor tube throughout its length. The details of reactor are shown in Fig. 2.1.

The feed stream containing a mixture of hydrogen and nitrobenzene was preheated in coil before entering the reactor tube. Then the vapours of nitrobenzene and hydrogen entered the reactor tube through the sintered disc and reacted in the catalyst bed. Vapour consisting of the products and un-converted reactants were first passed through the air condenser

1 HYDROGEN REGULATOR
2 ABSORBER
3 MANOMETER
4 BURETTE
5 CONSTANT FEED DEVICE
6 NITROBENZENE RESERVOIR
7 REACTOR OUTER JACKET
8 JACKET HEATING COIL
9 REACTOR TUBE
10 AIR INLET FOR FLUIDIZATION
11 SINTERED DISC
12 COILED PREHEATER
13 CATALYST PARTICLE
14 THERMOWELL
15 CYCLONE
16 THERMOCOUPLE
17 COILED WATER CONDENSER
18 RECEIVER

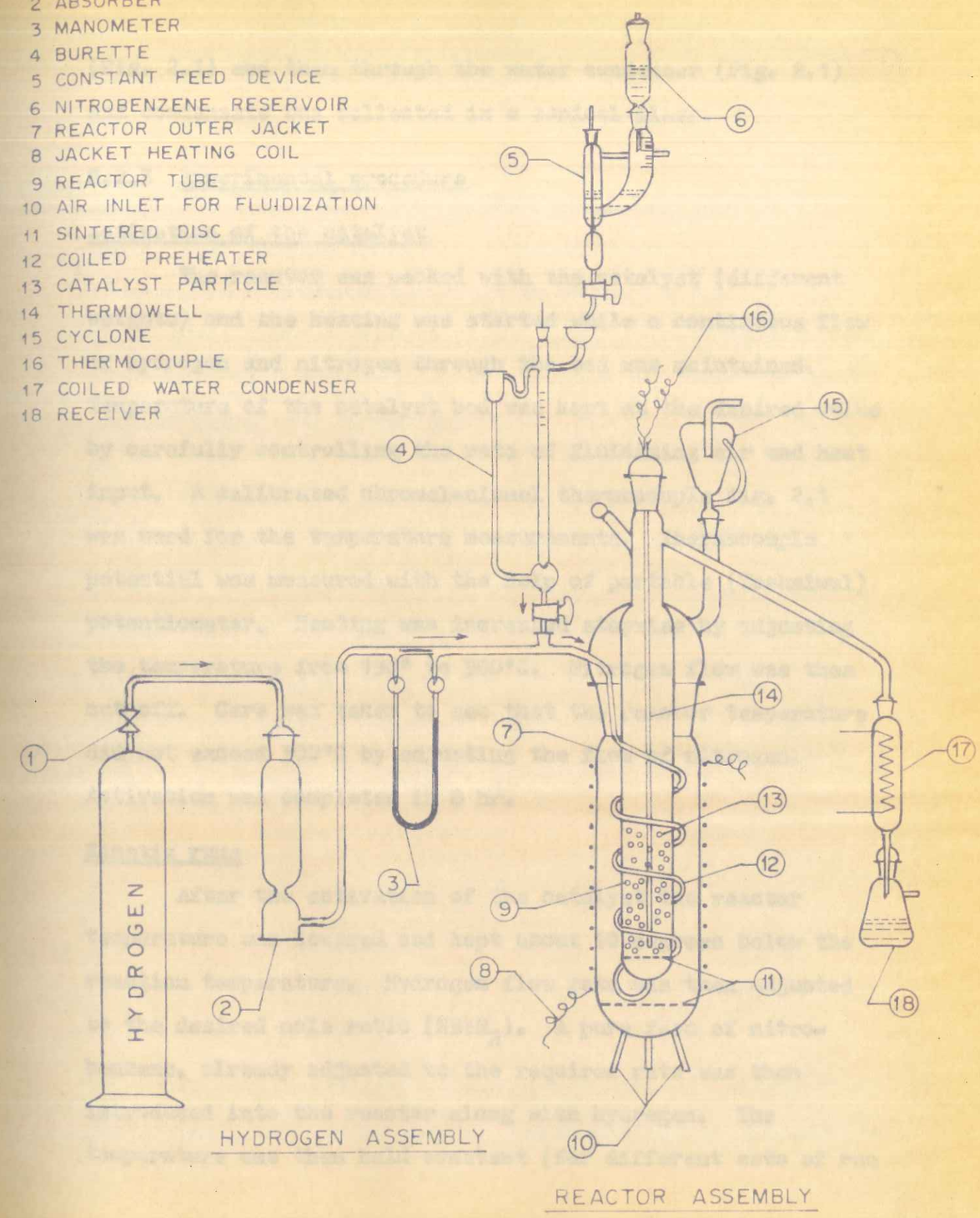

FIG. 2·1. EXPERIMENTAL SET-UP

(Fig. 2.1) and then through the water condenser (Fig. 2.1) and condensate was collected in a conical flask.

2.2.3 Experimental procedure

Activation of the catalyst

The reactor was packed with the catalyst (different weights) and the heating was started while a continuous flow of hydrogen and nitrogen through the bed was maintained. Temperature of the catalyst bed was kept at the desired value by carefully controlling the rate of fluidizing air and heat input. A calibrated chromel-alumel thermocouple Fig. 2.1 was used for the temperature measurements. Thermocouple potential was measured with the help of portable (Toshniwal) potentiometer. Heating was increased stepwise by adjusting the temperature from 150° to 300°C. Nitrogen flow was then cut off. Care was taken to see that the reactor temperature did not exceed 300°C by adjusting the flow of nitrogen. Activation was completed in 8 hr.

Kinetic runs

After the activation of the catalyst the reactor temperature was lowered and kept about 10 degrees below the reaction temperature. Hydrogen flow rate was then adjusted to the desired mole ratio (NB:H_2). A pure feed of nitrobenzene, already adjusted to the required rate was then introduced into the reactor along with hydrogen. The temperature was then held constant (for different sets of run

180°, 220°, 240° and 260°C) by carefully controlling the fluidizing air and heat input. The reaction was allowed to proceed for about 6.0 hr. The temperature gradient along with the length of the catalyst bed was checked by moving thermocouple up and down the thermowell. The temperature difference was found to be negligible ($\simeq$ 3°C). About three samples were withdrawn after the attainment of steady state with respect to temperature, flow rate of gas and outlet concentration.

2.2.4 Analysis

Product samples were analysed on a gas chromatograph (AMIL NCL made) provided with a thermal conductivity detector (TCD). The conditions of analysis were as follows:

Column length	11 ft.
Column material	S E 30 on Chromosorb W
Injection temperature	180°C
Column temperature	160°C
T.C.D. temperature	180°C
Hydrogen (carrier) gas flow rate	60 ml/min
Chart speed	15 mm/min
Attenuation	6

Synthetic mixtures of aniline (5, 20, 40, 60 wt.%) in nitrobenzene were prepared. The percentage of aniline was

then determined by calculating the area of the chromatogram for aniline in the synthetic mixture and that in the sample obtained under identical conditions. A representative chromatogram containing 67% aniline and 33% nitrobenzene is shown in Fig. 2.2.

2.2.5 Experimental results

Plots of experimental data, reciprocal space velocity (W/F) vs. fractional conversion (x) at four reaction temperature (180°-260°C) are shown in graphical form in Fig.2.3.

The rate of reaction was calculated by using the relation:

$$r_o = \frac{d\,x}{d\,(W/F)} \qquad (1)$$

The rate was calculated from the graph by taking slopes of the curves at different points and for different temperatures. These are represented in Table 2.1.

2.3 CONTROLLING MECHANISMS

Any catalytic gas-solid reaction can be broadly divided into three main classes. One class where the physical phenomenon is involved, another class where physical as well as chemical steps are involved and third class where only chemical process is involved. Physical phenomenon

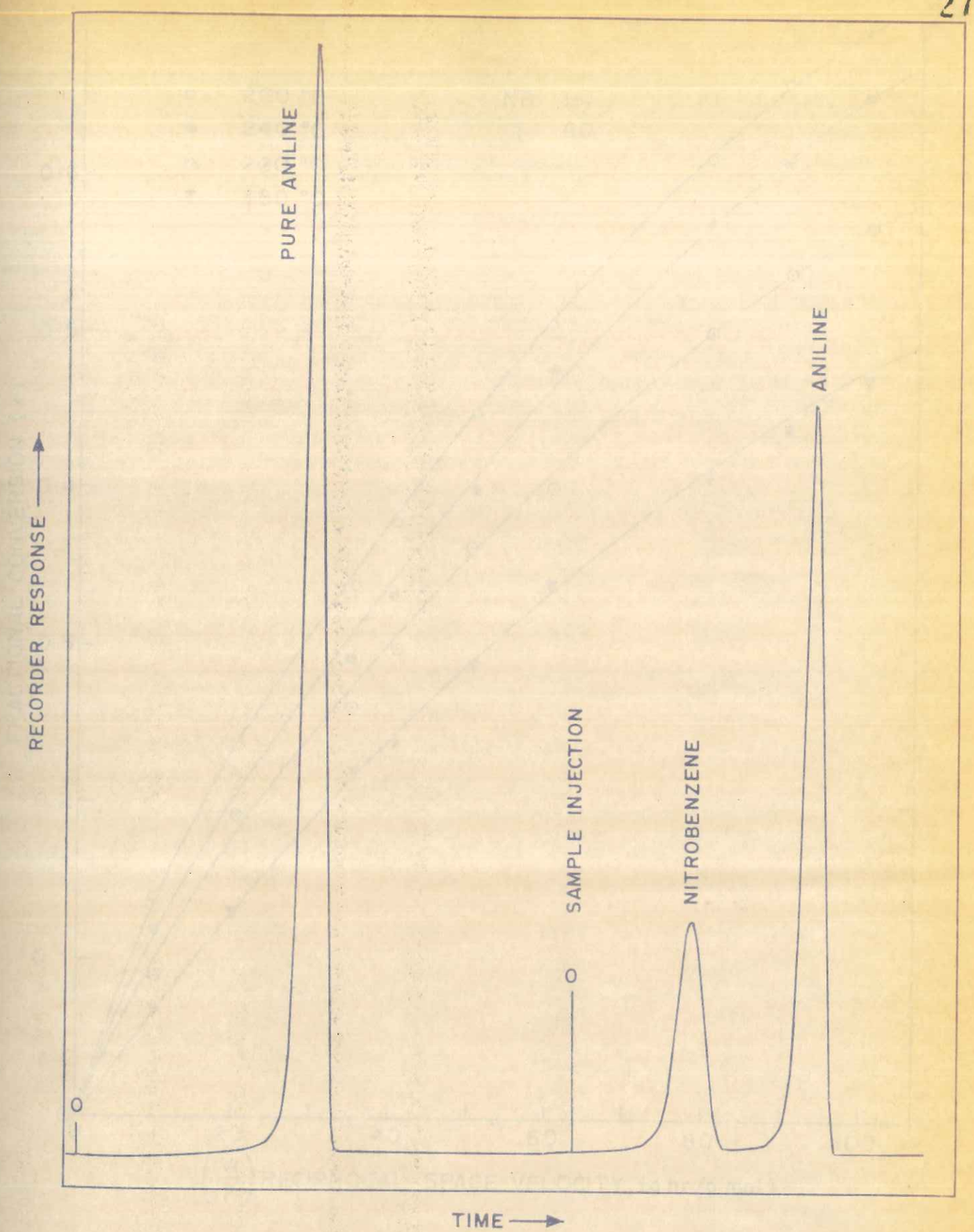

FIGURE 2·2: REPRESENTATIVE CURVE FROM CHROMATOGRAM

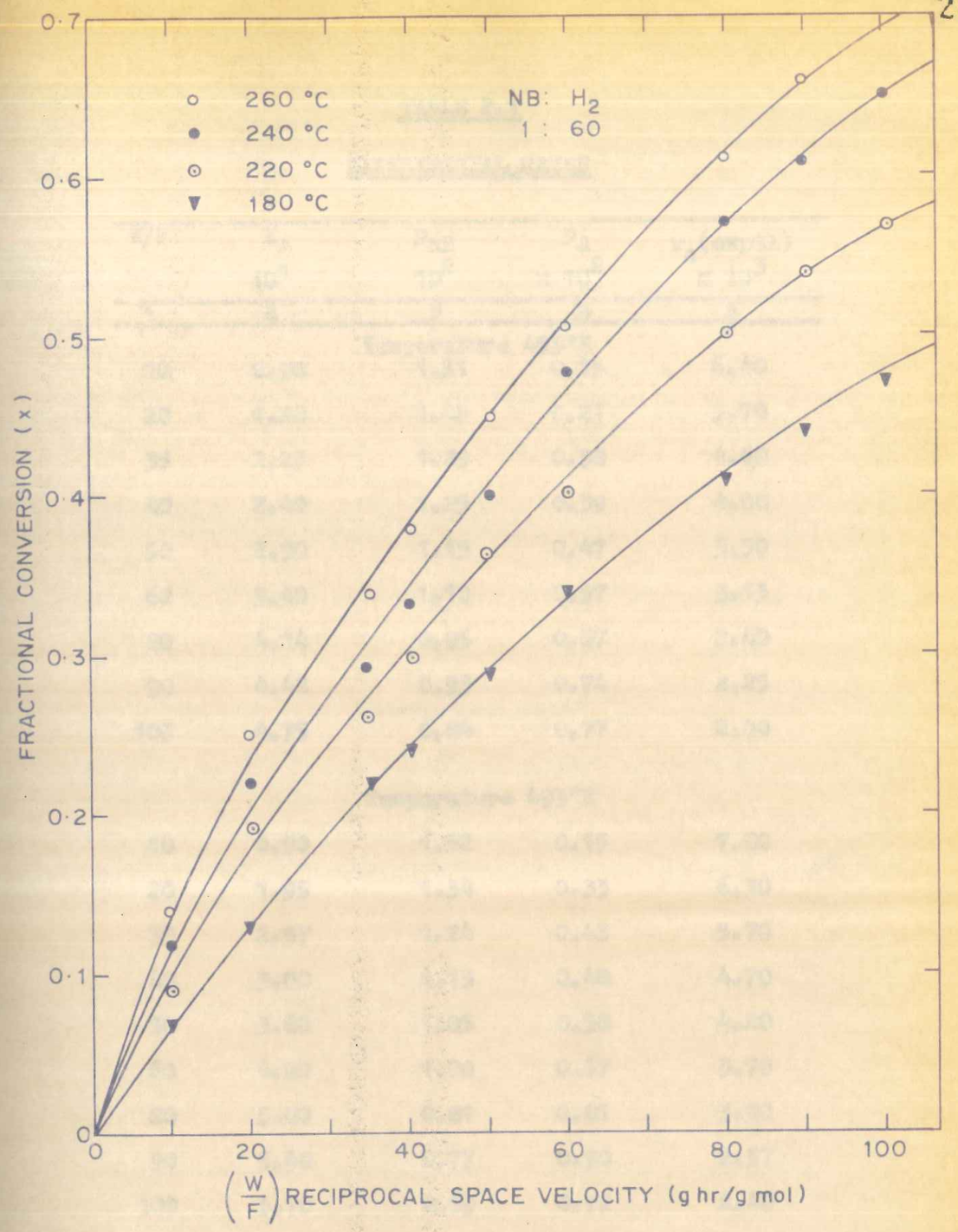

FIGURE 2·3: PLOTS OF EXPERIMENTAL DATA (x vs $^{W}/_{F}$)

TABLE 2.1

EXPERIMENTAL RATES

W/F	X_A 10^1	p_{NB} 10^2	p_A x 10^2	r_o(exptl) x 10^3
1	2	3	4	5
		Temperature 453°K		
10	0.70	1.51	0.15	6.40
20	1.28	1.45	0.21	5.70
35	2.25	1.29	0.38	4.60
40	2.40	1.25	0.39	4.00
50	2.90	1.15	0.47	3.50
60	3.40	1.10	0.57	3.15
80	4.14	0.95	0.67	2.40
90	4.42	0.93	0.74	2.25
100	4.75	0.84	0.77	2.00
		Temperature 493°K		
10	0.90	1.52	0.15	7.80
20	1.95	1.34	0.33	6.30
35	2.57	1.24	0.43	5.70
40	3.00	1.13	0.48	4.70
50	3.60	1.05	0.58	4.20
60	4.00	1.00	0.67	3.70
80	5.00	0.81	0.81	3.00
90	5.40	0.77	0.90	2.57
100	5.70	0.69	0.92	2.40

...

1	2	3	4	5
		Temperature 513°K		
10	1.20	1.47	0.20	8.60
20	2.28	1.29	0.38	7.00
35	2.90	1.18	0.48	6.00
40	3.35	1.10	0.54	5.55
50	4.00	0.96	0.65	4.65
60	4.85	0.86	0.81	4.10
80	5.75	0.68	0.92	3.00
90	6.09	0.65	1.01	2.70
100	6.55	0.54	1.05	2.10
		Temperature 533°K		
10	1.40	1.43	0.23	10.45
20	2.50	1.25	0.42	8.60
35	3.45	1.05	0.58	7.00
40	3.80	1.00	0.61	6.20
50	4.50	0.89	0.73	5.50
60	5.00	0.83	0.83	4.55
80	6.15	0.62	0.99	3.51
90	6.60	0.57	1.10	3.00
100	6.95	0.49	1.12	2.52

includes the transfer of reactant compounds upto the catalyst surface, diffusion at the reactants into the interior of the pellet, diffusion of the product back to the exterior of the surface and finally transfer of the product from exterior to the main stream of gas. Chemical steps involved are the adsorption of reactants, surface reaction and desorption of the products. Any of the above three types of processes can be the rate controlling step.

These three controlling regimes in the heterogeneous catalysed reaction can be identified by studying the effect of temperature on the apparent rate constant. At relatively low temperatures, the surface reaction rate is quite low and hence the chemical reaction is normally the controlling mechanism. As the temperature increases chemical reaction rate increases much faster while pore diffusion rate increases slowly. Here the chemical reaction rate is much faster than diffusion, hence pore diffusion is the controlling mechanism. As the temperature further increases, the rates of chemical reaction and pore diffusion become much faster than external film diffusion and the latter becomes the controlling mechanism.

Mass transfer

As discussed earlier any gas-solid reaction is accompanied with external and internal mass transfer effects. In order to obtain accurate kinetic data, experiments must be

carried out in such conditions where these effects are negligible.

In the present investigations external film diffusion resistance was minimised by using a high gas velocity. It was further confirmed by obtaining same conversions at fixed reciprocal space velocity but by varying weight of catalyst and nitrobenzene feed rate correspondingly.

2.4 MODELLING

Reaction rate models can be broadly divided into two groups: (1) emirical power law models and (2) semi-theoretical mechanistic rate models (heterogeneous models) based on the theory of adsorption.

2.4.1 Power law analysis of kinetic data

A simple design equation based on the power law analysis can be obtained by (1) analysing the kinetic data at different temperatures separately and then arriving at a general rate equation which fits the data at all the temperatures and (2) by analysing the kinetic data at all the temperatures together.

Analysis of data at single temperatures (Method I)

Power law equation for the reduction of nitrobenzene to aniline can be written as

$$r = k\ p_{NB}^{n} \qquad (2)$$

Partial pressure term for hydrogen has not been included since it is in far excess. Above expression can be written in the linear form as

$$\text{Log}\ (r) = \text{Log}\ (k) + n\ \text{Log}\ (p_{NB}) \qquad (3)$$

The constants of the above equation such as k and n, reaction rate constant, order of reaction with respect to nitrobenzene respectively, were evaluated by plotting Log r vs. Log p_{NB} at each temperature separately (Fig.2.4). The values of the above parameters are shown in Table 2.2.

The temperature dependency of the rate constant has been expressed in the form of the Arrhenius equation

$$k = A\ e^{-E/RT} \qquad (4)$$

Plots of Log (k) vs. 1000/T are shown in the Fig. 2.5. The activation energy was determined from the slopes of the

TABLE 2.2

RATE PARAMETERS OBTAINED BY (I) METHOD

Temperature °K	Rate constant k	order of reaction with respect to nitrobenzene
453	2.27	1.45
493	3.00	1.44
513	3.59	1.42
533	4.13	1.39
Activation Energy (E) Kcal/g mol	- 4.05	
Frequency factor (A) (g mol/hr g atm)	199.12	

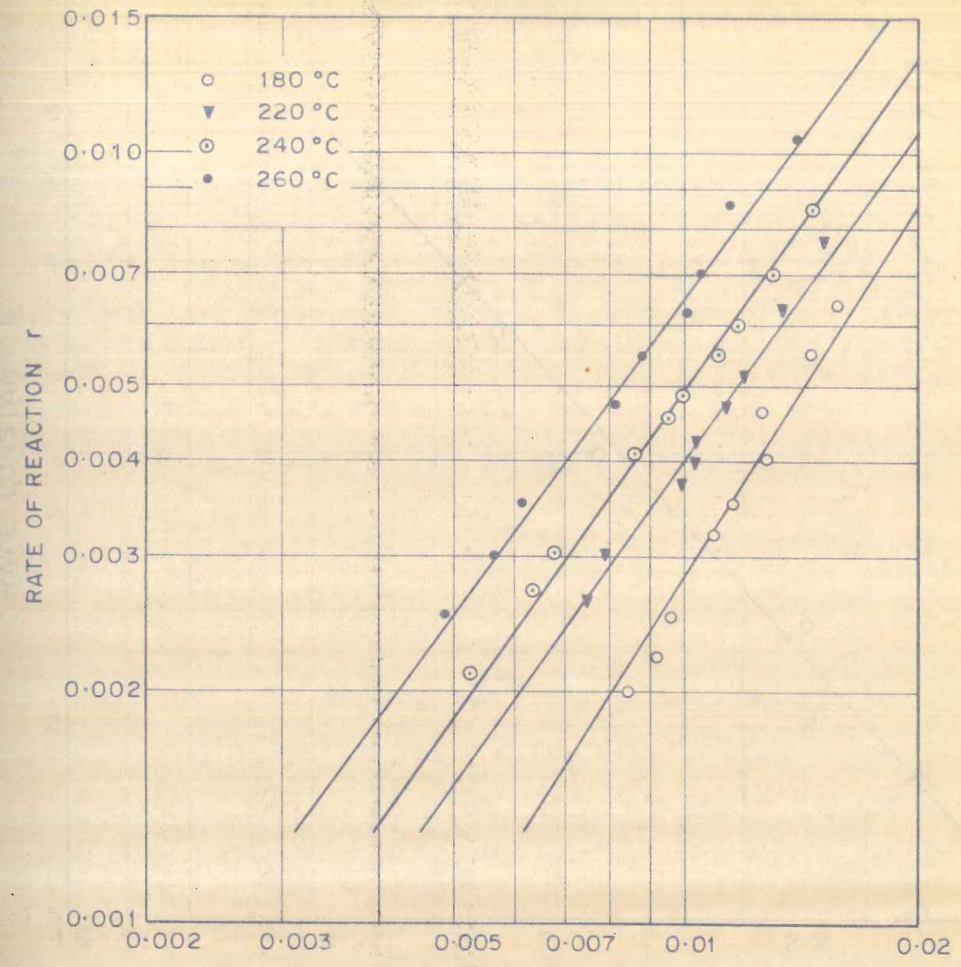

FIGURE 2·4: PLOTS TO DETERMINE ORDER OF REACTION AND RATE CONSTANTS IN Eq. (3)

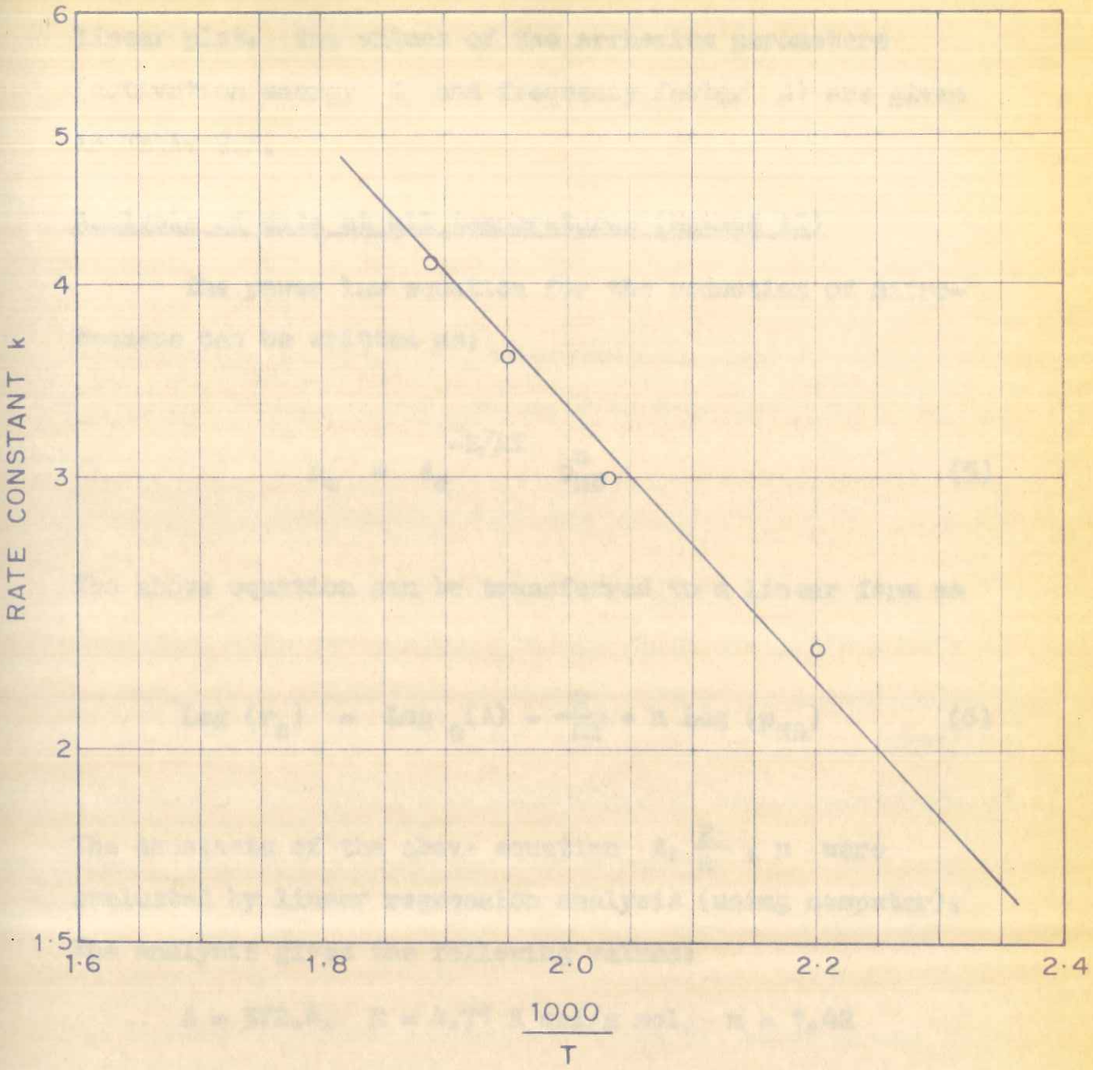

FIGURE 2·5: TEMPERATURE DEPENDENCY OF RATE CONSTANT

linear plot. The values of the Arrhenius parameters (activation energy E and frequency factor A) are given in Table 2.2.

Analysis of data at all temperatures (Method II)

The power law equation for the reduction of nitrobenzene can be written as:

$$r_o = A e^{-E/RT} p_{NB}^{n} \qquad (5)$$

The above equation can be transferred to a linear form as

$$\text{Log}\,(r_o) = \text{Log}_e(A) - \frac{E}{RT} + n\,\text{Log}\,(p_{NB}) \qquad (6)$$

The constants of the above equation A, $\frac{E}{R}$, n were evaluated by linear regression analysis (using computer). The analysis gives the following values:

A = 372.4, E = 4.71 K cal/g mol, n = 1.42

By substituting the evaluated parameters in the above equation it becomes:

$$r_o = 372.4\ e^{(-2387/T)}\ p_{NB}^{1.42}$$

or

$$r_o = 372.4 \exp(-2387/T) \times p_{NB}^{1.42}$$

The validity of the power law equation was further tested by comparing the estimated rates from the rate equation with the experimental rates. A comparison of the predicted rates with the observed rates has been made in Fig. 2.6. Table 2.3 contains the observed rate and predicted rate data at four temperatures of study.

It can be seen from this, that the corresponding values of rate parameters obtained by both the methods are quite comparable.

2.4.2 Heterogeneous rate models

The heterogeneous rate models can in general be classified into two groups. In the first group the models are based on a simplified theory of adsorption (chemisorption). In the second group, the models are based on a more realistic appreciation of the physical situation at the catalyst surface.

Langmuir-Hinshelwood models

There are two methods generally used to determine the controlling mechanisms of solid catalysed reaction, one due to Hougen-Watson (12) and other due to Balandin and coworkers (1), (2). Since they are based on the Langmuir-Hinshelwood adsorption theory they have common assumptions such as (i) only one type of active centres are present on the catalyst surface; (ii) the adsorption of the reactant forms a monolayer of adsorbate (iii) the heat of adsorption

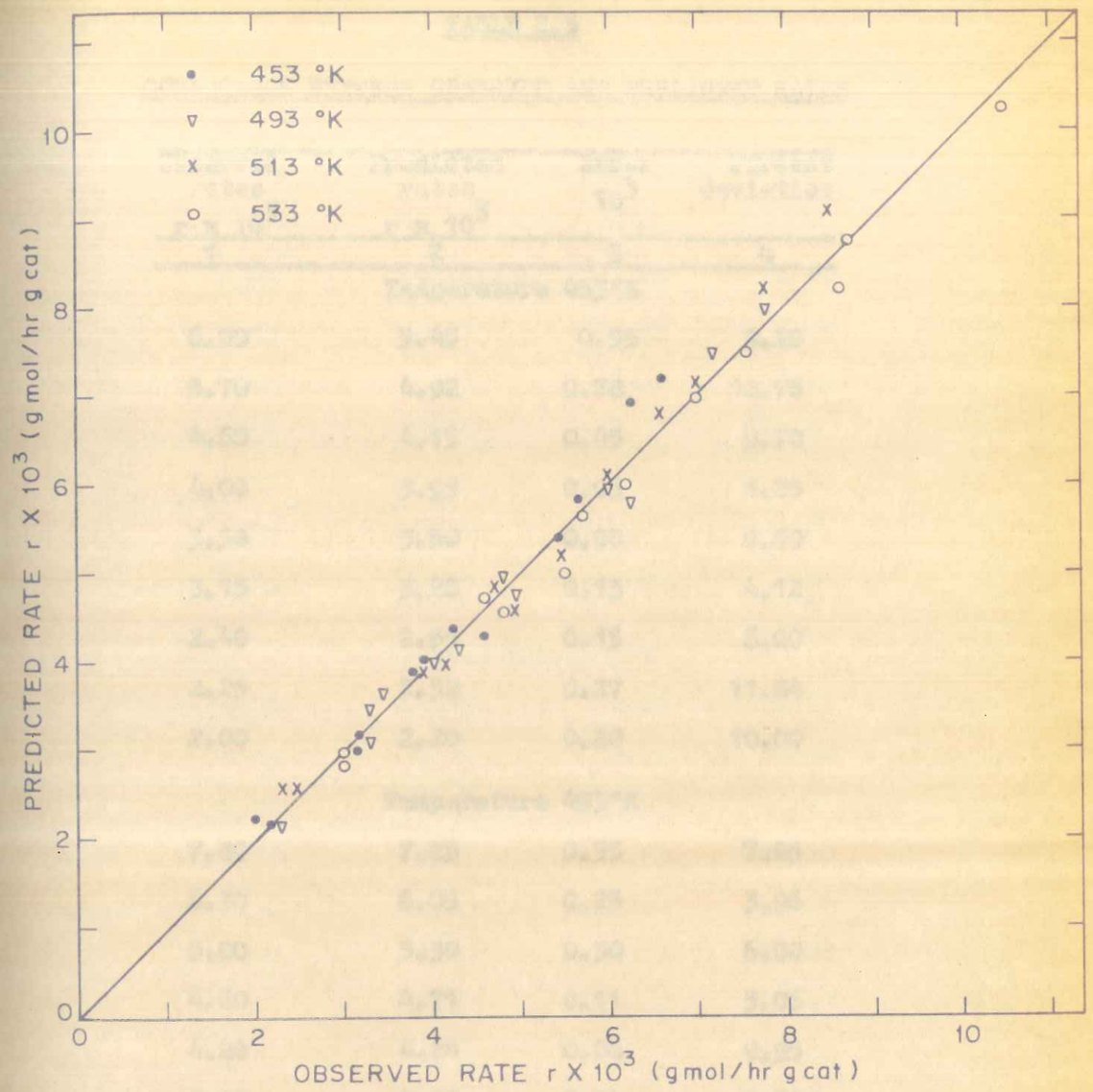

FIGURE 2·6: COMPARISON OF OBSERVED AND PREDICTED RATES AS CALCULATED BY POWER LAW MODEL

TABLE 2.3

COMPARISON BETWEEN OBSERVED AND PREDICTED RATES

Observed rates $r \times 10^3$	Predicted rates $r \times 10^3$	Error 10^3	Percent deviation
1	2	3	4
	Temperature 453°K		
6.00	5.45	0.55	9.20
5.70	4.92	0.78	12.76
4.60	4.15	0.45	9.70
4.00	3.95	0.05	1.25
3.50	3.50	0.00	0.00
3.15	3.28	0.13	4.12
2.40	2.55	0.15	6.00
2.25	2.52	0.27	11.84
2.00	2.20	0.20	10.00
	Temperature 493°K		
7.80	7.25	0.55	7.05
6.30	6.05	0.25	3.96
5.00	5.30	0.30	6.00
4.60	4.71	0.11	5.06
4.20	4.24	0.04	0.95
3.70	3.95	0.25	6.72
3.00	2.92	0.08	2.66
2.57	2.71	0.14	5.40
2.40	2.33	0.07	2.91

....

1	2	3	4
	Temperature 513°K		
8.50	8.96	0.46	5.41
7.00	7.44	0.44	6.28
6.00	6.56	0.56	9.33
5.55	5.94	0.39	7.02
4.65	4.89	0.24	5.16
4.10	4.19	0.09	2.19
3.00	3.00	0.00	0.00
2.70	2.81	0.11	4.07
2.10	2.16	0.06	2.86
	Temperature 533°K		
10.45	11.26	0.81	7.75
8.60	9.34	0.74	8.60
7.00	7.23	0.23	3.28
6.20	6.85	0.65	10.40
5.50	5.83	0.33	6.00
4.85	5.29	0.44	9.07
3.51	3.53	0.02	0.57
3.00	3.13	0.13	4.30
2.52	2.54	0.02	0.79

is constant with respect to surface coverage (i.e. there is no interaction between adsorbed molecules) and (iv) the catalyst has uniform adsorption capacity.

A. Hougen-Watson models

The Hougen-Watson approach is based on the assumption that one of the elementary steps, viz. adsorption of one of the reactants, surface reaction, or desorption of one of the products, offers the controlling resistance in the overall reaction system. The possibility of one or more of the reactants or products and the fact that some of them may not be adsorbed are also included in the Hougen-Watson analysis. These models are more flexible in fitting the data.

B. Balandin models

In the Balandin models, it is assumed that chemisorption of reactant takes place on more than one adjacent active sites with the product adsorbed on the site initially occupied by the reactant and with the release of hydrogen or water molecules without adsorbed. These models are more recent than Hougen-Watson models, but they are restricted to the catalytic processes in the dehydrogenation of hydrocarbon, amines and alcohols and in the dehydration of alcohols.

C. Other complex models

Since Langmuir-Hinshelwood models are based on ~~the~~ several assumptions, many efforts have been made to develop models based on the more realistic physical situations.

Models where two steps of kinetic sequence are assumed to be controlling have been developed by Bischoff and Froment (3), Hutchinson et al. (13) and Happel (9). Kolboe (15) developed a model with the assumption that instead of all the active sites on the catalyst surface being equal, two different sets of active centers exist on the catalyst. With this model he was able to obtain a better fit to the data reported by Thodos and Thaller (16).

2.4.3 Heterogeneous modelling in the present work

The Hougen-Watson models based on the assumption that only one step out of three elementary steps is controlling, the other two steps being in equilibrium, are considered for the mechanisms involving single and dual sites in the above elementary steps. The corresponding rate models for the above controlling mechanisms along with their linear forms are presented in Table 2.4.

Parameter estimation

The estimation of the model parameters is usually done by using least square methods. Least square analysis

is classified as (a) linear least square and (b) non-linear least square analysis.

Linear least square method for parameter estimation

According to the principle of the least squares the parameters to be estimated are chosen such that some of squares of the residuals of experimental and estimated rates i.e. $\sum(y_i - r_i)^2$ is minimum. Hougen-Watson models are generally non-linear while this technique need the model in its linearised form. Hence the model is rearranged to obtain an equation linear in its parameters and then the regression analysis is performed. This technique however, does not give the best estimate of the model parameters since the function minimised here consists of some combination of dependent and independent variables.

$$\text{i.e.} \sum\left(\frac{p_{NB}}{r\,(obs)} - \frac{p_{NB}}{r\,(estim)}\right)^2$$

instead of minimising the residual sum of square of the dependent variable i.e. $\sum\left(r_{(obs)} - r_{est)}\right)^2$.

Non-linear least square analysis

Non-linear analysis gives more precise estimates of the model parameters because this method deals directly with the sum of squares of the residuals by minimising it

instead of minimising the residuals of some combination of variables as in the case of linear analysis. All the fitting of the data need not be restricted to the isothermal conditions.

Two basic techniques for least squares analysis of non-linear parameters are used: (i) a linearization of the model using Taylor series expansion about the previous estimates of the parameters and (ii) the method of steepest descent.

Taylor series expansion method

Gauss (8) suggested an interactive procedure consisting basically of a Taylor series expansion of the rate equation about an initial set of parameter values. By retaining only the linear term, the non-linear model can be linearised by a Taylor expansion:

$$y_i = f(x,K) + \sum_{j=1}^{p} \frac{\delta(x_i,K)\, h_j}{\delta K_j} \qquad (8)$$

where f is evaluated at the initial guess of vector K

$$K = (K_1^\circ , K_2^\circ \ldots\ldots\ldots K_p^\circ), \text{ and}$$

$$h_j = K_j - K_j^\circ \quad (\text{where } j = 1,2 \ldots\ldots p) \qquad (9)$$

The values of all the terms in equation are known except the coefficients h, which appear linearly and hence the equation can be solved for h. Now by knowing the values of h, a set of values of K can be obtained from equation (9). These new values of K can be used as K° and the procedure is repeated until the correction vector h approaches zero. If initial guesses are sufficiently close to the true values of the parameters, the process might converge, otherwise it diverges. Convergence is generally prevented by the non-linearities in the model and the poor initial parameter estimates.

Method of steepest descent

The steepest descent method is generally used when Taylor series expansion method fails to give the desired convergence. In this method the residual sum of squares is considered to be a response surface in space in which the parameters are available. One can then apply steepest descent procedures (4,5) to determine the parameter values, yielding the minimum of the sum surface.

Magnitude of the estimated parameters

Further step in the analysis involves the examination of the parameter values thus obtained. Following criteria should be used to select the model (1) the estimated adsorption rate constants should be positive, (2) plot of log of rate constant with reciprocal of the

absolute temperature should be linear with negative slope (3) plot of logarithm of adsorption equilibrium constant with reciprocal absolute temperature should be linear with positive slope and generally with negative intercept.

Parameter estimation in the present work

In the present case, the parameters of the six Hougen-Watson models (Table 2.4) were estimated initially by linear least square analysis (using computer). The parameter values thus obtained are summarised in Table 2.5. On examination of the above parameter values, it can be seen that the model numbers 2,3,5 and 6 have the negative adsorption equilibrium constants. These four models were therefore rejected on the ground that they are associated with negative adsorption equilibrium constants. Recently Kittrell and Mezaki (14) have pointed out that non-linear least squares for screening the rival models is not strongly recommended due to more effort required for exploring the sum of residual squares. They have suggested that initial screening of the rival models can be done by other means, and then close attention may be given to the additional data required for careful discrimination among remaining models. Here first four models have been rejected after screening through the linear least square analysis. Among the remaining two rival models (model numbers 1 and 4) model (4)

TABLE 2.4

HOUGEN-WATSON MODELS

Model No.	Controlling step	Rate model (non-linear form)	Rate model (linear form)
		Single site mechanism	
1.	Adsorption of nitrobenzene	$r = \frac{k\, p_{NB}}{1 + K_A\, p_A}$	$\frac{p_{NB}}{r} = \frac{1}{k} + \frac{K_A}{k}\, p_A$
2.	Surface reaction	$r = \frac{k\, p_{NB}}{1 + K_A p_A + K_{NB} p_{NB}}$	$\frac{p_{NB}}{r} = \frac{1}{k} + \frac{K_A p_A}{k} + \frac{K_{NB}}{k}\, p_{NB}$
3.	Desorption of aniline	$r = \frac{k\, p_{NB}}{1 + K_{NB}\, p_{NB}}$	$\frac{p_{NB}}{r} = \frac{1}{k} + \frac{K_{NB}}{k}\, p_{NB}$
		Dual site mechanism	
4.	Adsorption of nitrobenzene	$r = \frac{k\, p_{NB}}{(1 + K_A\, p_A)^2}$	$\sqrt{\frac{k_{NB}}{r}} = \frac{1}{\sqrt{k}} + \frac{K_A}{\sqrt{k}}\, p_A$
5.	Surface reaction	$r = \frac{k\, p_{NB}}{(1 + K_A p_A + K_{NB} p_{NB})^2}$	$\sqrt{\frac{p_{NB}}{r}} = \frac{1}{\sqrt{k}} + \frac{K_A}{\sqrt{k}}\, p_A + \frac{K_{NB}}{\sqrt{k}}\, p_{NB}$
6.	Desorption of aniline	$r = \frac{k\, p_{NB}}{(1 + K_{NB} p_{NB})^2}$	$\sqrt{\frac{p_{NB}}{r}} = \frac{1}{\sqrt{k}} + \frac{k_{NB}}{\sqrt{k}}\, p_{NB}$

TABLE 2.5

ESTIMATED PARAMETER VALUES BY LINEAR LEAST SQUARE ANALYSIS

Model No.	Model	Temp. °K	Parameter values k	K_{NB}	K_A
1.	$r = \frac{kp_{NB}}{1 + K_A p_A}$	453	0.781	-	401
		493	1.042	-	393
		533	1.081	-	169
2.	$r = \frac{k\, p_{NB}}{1+K_A p_A+K_{NB} p_{NB}}$	453	0.715	366.8	-7.384
		493	1.124	420.0	6.066
		533	1.551	262.3	33.39
3.	$r = \frac{k\, p_{NB}}{1 + K_{NB}\, p_{NB}}$	453	0.128	-50.92	-
		493	0.189	-45.14	-
		513	0.405	-17.30	-
		533	0.419	-28.25	-
4.	$r = \frac{k\, p_{NB}}{(1 + K_A\, p_A)^2}$	453	0.661	-	222
		493	0.880	-	114
		513	0.830	-	64
		533	1.000	-	58
5.	$r = \frac{k\, p_{NB}}{(1+K_A p_A+K_{NB} p_{NB})^2}$	453	0.887	116.02	-2.60
		493	0.964	111.409	6.72
		533	1.051	69.25	8.39
6.	$r = \frac{k\, p_{NB}}{(1 + K_{NB} p_{NB})^2}$	453	0.583	-34.05	-
		493	0.642	-30.42	-
		513	0.800	- 9.85	-
		533	0.797	-19.64	-

was selected since it gave the minimum sum of squares as compared to Model No. 1.

The parameters of the model No.4 were further accurately determined by non-linear least square analysis by using the method of Taylor series expansion (Himmelblau (11)), and was found to give good convergence with the initial parameter values obtained by linear least square analysis. The parameter values thus obtained at four different temperatures are presented in Table 2.6.

The proposed model (No.4) suggests that the adsorption of nitrobenzene is a controlling step in the hydrogenation of nitrobenzene with a dual site mechanism.

Validity of the proposed model

Residual analysis

A residual is defined as the difference between the observed and predicted values of some response of interest, such as the reaction rate. Difference between the observed and predicted rate is attributed solely to the experimental error and the plots of this residual vs. any independent variable should exhibit all the characteristics of this error. The validity of the model is further confirmed by comparing the estimated rates with the experimental (observed) rates. The deviations of the estimated rates from the corresponding observed rates are given in Table 2.8 and the plot of estimated

TABLE 2.6

PARAMETER VALUES OBTAINED AFTER NON-LINEAR ANALYSIS FOR THE PROPOSED MODEL

$$r_o = \frac{k\, p_{NB}}{(1 + K_A\, p_A)^2}$$

No.	Temp., °K	k	K_A
1.	453	0.600	100.00
2.	493	0.7524	60.52
3.	513	0.7805	44.80
4.	533	0.9208	40.36

rates vs. observed rates is shown in Fig. 2.7. As seen from the results (Table 2.7 and Fig. 2.7) an excellent agreement between the estimated and observed rates exists which proves the validity of the proposed model.

Comparison between the model parameters estimated by linear and non-linear least squares

The comparison between the parameters (k, K_A) of the proposed model estimated by the linear and non-linear least square analysis of the rate model has been presented in Table 2.8.

As seen from the table, the sum of squares in case of non-linear analysis is always less than that of linear analysis. Thus the values of parameters obtained by non-linear least square method are more accurate than those by linear least squares method.

Temperature depending of model parameters

The temperature dependence of the model parameters can be expressed by usual Arrhenius equation.

The temperature dependence of rate constant k has been shown in Fig. 2.8. The activation energy thus estimated from the negative slope of the line gives the value as 2.56 k cal/g mol.

The temperature dependency of adsorption equilibrium constant for aniline K_A (or Van't Hoft plot) has been shown

TABLE 2.7

COMPARISON BETWEEN OBSERVED AND PREDICTED RATES

Observed rate $r \times 10^3$	Predicted rate $rx10^3$	Error 10^3	Percent deviation
1	2	3	4
	Temperature 453°K		
6.07	6.72	-.65	10.75
5.70	5.92	-.22	3.72
4.60	4.28	0.32	7.47
4.00	3.89	0.11	2.95
3.50	3.20	0.30	8.70
3.15	3.16	-.01	0.36
2.40	2.15	0.25	10.41
2.25	2.08	0.12	5.48
2.00	1.94	0.06	3.00
	Average percent deviation 5.86		
	Temperature 493°K		
7.80	8.02	-.22	2.80
6.30	6.13	0.17	2.60
5.70	5.87	-.17	2.98
4.70	5.10	-.60	8.51
4.20	4.32	-.12	3.05
3.70	3.81	-.11	3.20

.....

1	2	3	4
3.00	2.76	0.24	8.00
2.57	2.43	0.14	5.22
2.40	2.16	0.24	10.74

Average percent deviation 5.23

Temperature 513°K

8.60	9.60	-1.00	11.60
7.00	7.33	-0.33	4.70
6.00	6.23	-0.23	3.80
5.55	5.57	-0.02	0.36
4.65	4.72	-0.07	1.50
4.10	4.30	-0.20	4.93
3.00	2.67	0.33	11.28
2.70	2.48	0.22	8.15
2.10	1.96	0.14	6.67

Average percent deviation 5.88

Temperature 533°K

10.45	11.00	-0.65	6.10
8.60	8.49	0.11	1.28
7.00	6.69	0.32	4.62
6.20	6.46	-0.26	4.27
5.50	5.34	0.16	2.93
4.55	4.30	0.25	5.49

.....

1	2	3	4
3.21	2.98	0.23	7.16
3.00	2.98	0.02	0.65
2.52	2.28	0.24	8.00

Average percent deviation 4.50

TABLE 2.8

COMPARISON BETWEEN THE MODEL PARAMETERS
BY LINEAR AND NON-LINEAR LEAST SQUARE ANALYSIS

Temp., °K	Model parameters				Sum of squares	
	Linear		Non-linear			
	k	K_A	k	K_A	10^3 linear	10^3 non-linear
453	0.661	222	0.600	100.00	52.90	1.96
493	0.88	114	0.752	60.52	65.80	2.89
513	0.83	64	0.781	44.80	60.80	2.30
533	1.00	58	0.921	40.36	63.18	3.41

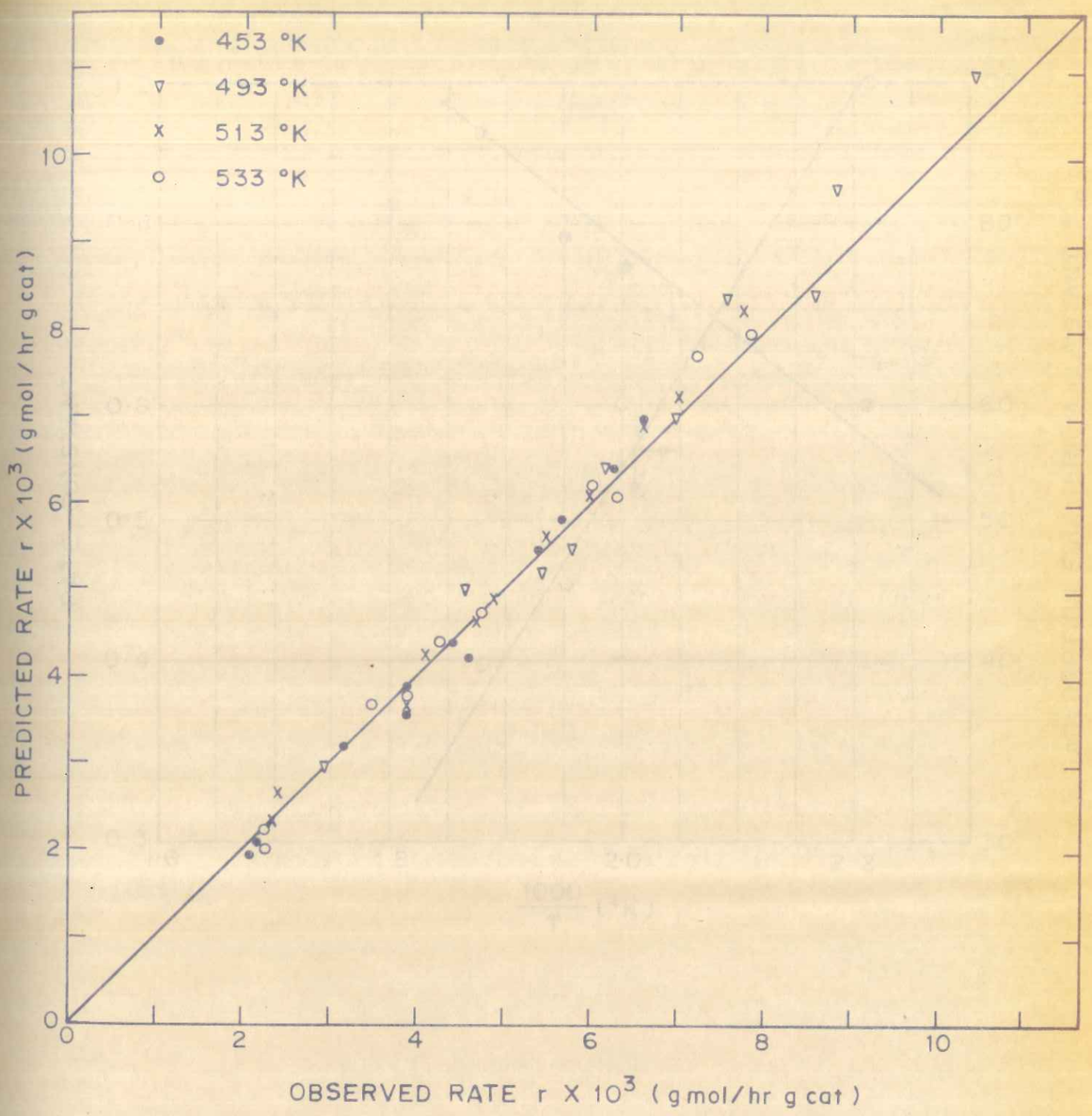

FIGURE 2·7: COMPARISON BETWEEN OBSERVED AND PREDICTED RATES

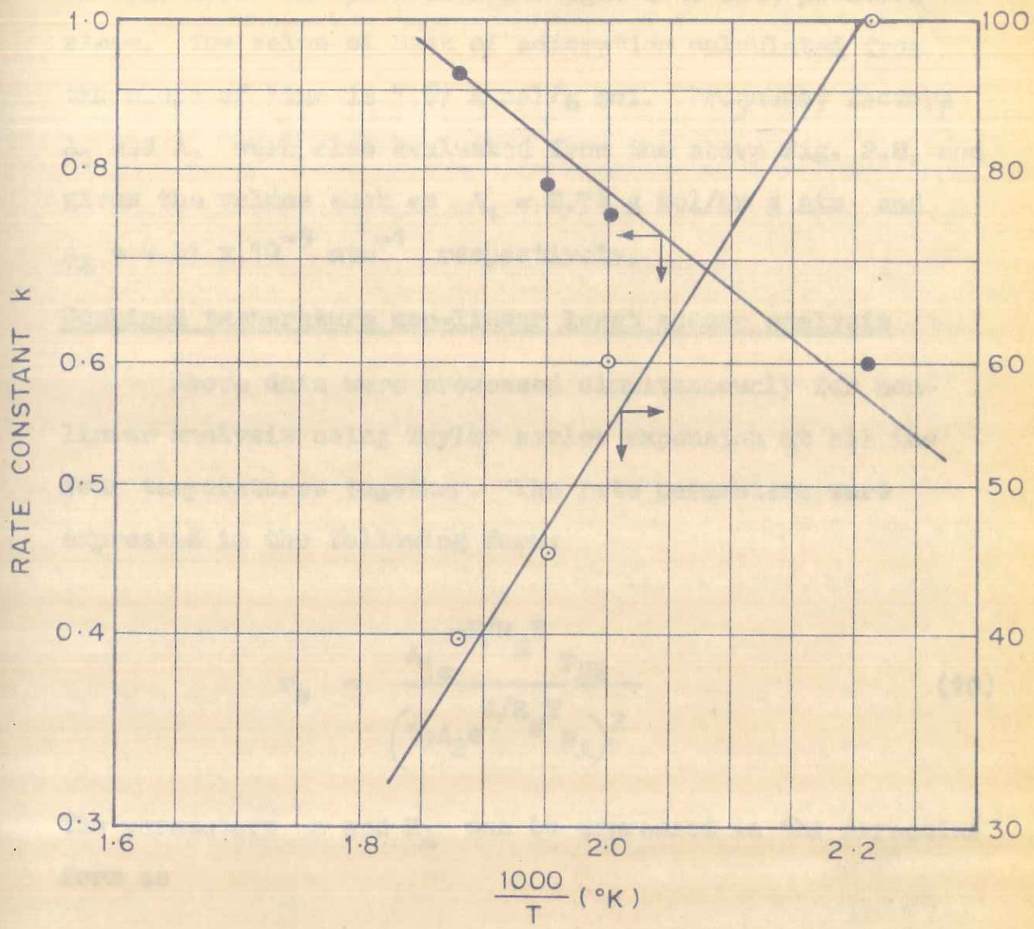

FIGURE 2·8: TEMPERATURE DEPENDENCY OF RATE AND ADSORPTION EQUILIBRIUM CONSTANT

in Fig. 2.8. The plot is a straight line with positive slope. The value of heat of adsorption calculated from the slope of line is 7.67 k cal/g mol. Frequency factors A_1 and A_2 were also evaluated from the above Fig. 2.8, and gives the values such as $A_1 = 8.74$ g mol/hr g atm and $A_2 = 4.51 \times 10^{-3}$ atm^{-1} respectively.

Combined temperature non-linear least square analysis

Above data were processed simultaneously for non-linear analysis using Taylor series expansion at all the four temperatures together. The rate parameters were expressed in the following form:

$$r_o = \frac{A_{1e}^{-E/R_gT} p_{NB}}{\left(1+A_2 e^{E/R_gT} p_A\right)^2} \qquad (10)$$

The parameters k and K_A can be expressed in the Arrhenius form as

$$k = A_1 \exp(-E_1/RT) \quad \text{and} \qquad (11)$$

$$K_A = A_2 \exp(E_2/RT) \qquad (12)$$

The parameter values obtained by combined temperature analysis and by the plots of $\log_e k$ vs. $\frac{1}{T}$ are summarised

in Table 2.9. I can be seen from the table values that the values obtained by both the methods are comparable.

The activation energy for the reaction is very low which is suggestive of interphase mass transfer intrusion. However, experiments were carried out to insure absence of mass transfer limitations. Such low activation energies have been reported in the literature for different systems. Hawthorn et al. (10) fitted a similar model for the dehydrogenation of methyl cyclohexane and found that the activation energy was 3 k cal/g mol while the heat of adsorption was 30 k cal/g mol. Cerni and Pasek (7) studied the hydrogenation of nitrobenzene on a copper silica catalyst and have reported an activation energy of 3.4 k cal/g mol.

2.5 CONCLUSION

The experimental data, as analysed first for power law models, suggests that the reaction is 1.4 order with respect to nitrobenzene.

Comparison between different possible heterogeneous Hougen-Watson models, reveals that only one model is possible which indicates the rate controlling step to be the adsorption of reactant (nitrobenzene with dual site mechanism).

...

TABLE 2.9

COMPARISON BETWEEN THE ARRHENIUS PARAMETERS OBTAINED BY TWO APPROACHES

Model parameters	Separate temperature method	Combined temperature method
Activation energy (E_1)(K cal/g mol)	-2.55	-2.63
Frequency factor (A_1)(g mol/hr g atm)	8.74	8.77
Activation energy (E_2)(K cal/g mol)	7.67	8.04
Frequency factor (A_2)(atm 1)	4.51×10^{-3}	2.63×10^{-3}

NOMENCLATURE

A	Frequency factor (g mol/hr g)
A_1	Constant of equation 11 (g mol/hr g atm)
A_2	Constant of equation 12 (atm^{-1})
E	Activation energy (cal/g mol)
F	Feed rate of reactant (g mol/hr)
k	Reaction rate constant (g mol/hr g cat)
K_A	Adsorption equilibrium constant for aniline (atm^{-1})
K_{NB}	Adsorption equilibrium constant for nitrobenzene (atm^{-1})
p_A	Partial pressure of aniline (atm)
p_{NB}	Partial pressure of nitrobenzene (atm)
R	Gas constant (cal/g mol °K)
r_o	Rate of reaction on unpoisoned catalyst (g mol/ hr g cat)
T	Absolute temperature (°K)
W	Weight of the catalyst (g)
X_A	Fractional conversion to aniline

...

REFERENCES

1. Balandin, A.A., and Ponomarev, A.A., J. Gen. Chem. (SSSR), 26, 1301 (1956)

2. Balandin, A.A., 'Adv. Catalysis', 10, 96 (1958)

3. Bischoff, K.B., and Forment, G.F., Ind. Eng. Chem. (Fundl), 1, 195 (1962)

4. Box, G.E.P., and Conite, G.A., Proccd. Inst. Elect. Eng. (London), Pt. 13103, (1) Suppl. 100 (1956)

5. Box, G.E.P., Cox, D.R., J. Roy. Statist. Soc. Ser., B 26 (2), 211 (1944)

6. Bradshaw, R.W., and Davidson, 19, Chem. Eng. Sci., 24, 1519 (1969)

7. Cerni, J., and Pasek, J. 'Design of a reactor for catalytic hydrogenation of nitrobenzene to aniline', Dept. of Organic Tech.; Adv. School of Chemistry, Prauge (1966)

8. Gauss, C.F., 'Theory of least squares', English translation by Trotter, F., Priceton Univ. Statistics technical research group, Tech. Report No. 5.

9. Happed, J.J., Res. Inst. Cat. Hokkuido uni, 16, 305 (1968)

10. Hawthorn, R.D., Ackerman, G.H., Nixon, A.C., AIChEJ, 14, 69 (1968)

11. Himmelblau, D.M., 'Process Analysis by Statistical Methods', John Wiley and Sons, Newyork (1970)

....

12. Hougen, O.A., and Watson, K.M.,
'Chemical Process Principles Vol. III',
John Wiley and Sons, Inc. New York (1947)

13. Hutchinson, H.L., Barrick, D.L., Brown, L.F.,
Chem. Eng. Prog. Ser., 63, 18 (1967)

14. Kittrel, J.R., and Mezaki, R.,
AIChEJ, 14, 513 (1968)

15. Kolboe, S.,
Ind. Chem. Eng. (Fundl), 6 (2), 169 (1967)

16. Thodos, G., and Thaller, L.H.,
AIChEJ, 6, 369 (1960)

.....

CHAPTER 3

CATALYST POISONING

CHAPTER 3

CATALYST POISONING

3.1 INTRODUCTION

The poisoning of the catalyst occurs due to preferential adsorption of certain species (impurities) which are present in the reacting system. These species are firmly held to the catalyst surface because of the formation of strong adsorptive bonds. In some cases these bonds are highly specific and chemical in nature. The poison is then said to be irreversibly adsorbed. Passing of pure feed over the catalyst does not help in regaining the original activity of the catalyst in this case. In certain other cases the adsorptive bonds may not be so strong, and the removal of the adsorbed poison may occur when a pure feed is passed over the catalyst surface (1,2,3,4).

3.1.1 Methods of poisoning

Poisoning in a fixed bed reactor can be studied by three different methods: (i) by using prepoisoned catalyst, (ii) by using pulses of poison, and (iii) by introducing poison in the feed.

In the case of prepoisoning of the catalyst, the catalyst is immersed in the solution containing a known concentration of poison for a certain length of time. Then

the prepoisoned catalyst is introduced into the reactor and the pure feed is passed over it. Here the distribution of poison is not a function of bed length. The results obtained by this method can be more easily interpreted, but the data cannot be extrapolated to in situ poisoning. However, it can be readily interpreted in terms of surface area available at the time of poisoning.

Pulse addition of poison to a fixed bed of catalyst is also a convenient method, chiefly due to the possibility of on-line tracking of the poison using a chromatograph.

Experiments with continuous addition of poison with the feed over the catalyst surface reflect the practical situation more closely. Usually a known quantity of poison is introduced into the feed, either as a solution or by passing the feed gas through a saturator containing the poison and maintained at the desired temperature. In in situ poisoning experiments, the catalyst is pretreated and conditioned with pure feed, and then the feed containing a known quantity of poison is introduced. Often it is desirable to use large poison concentrations so that the poisoning experiment can be completed during the period of constant relative activity of the catalyst.

3.2 EXPERIMENTAL

3.2.1 Raw materials

Hydrogen gas: Hydrogen gas was free from impurities and was obtained from Industrial Oxygen Ltd. (Bombay, India).

Nitrogen gas: Nitrogen gas was also obtained from Industrial Oxygen Ltd.

Nitrobenzene: Nitrobenzene used was pure and of analytical grade (free from thiophene).

Thiophene: Thiophene used was of Riedeal grade and free from impurities.

Catalyst: Same catalyst was used as in kinetic studies. (Chapter 1).

3.2.2 Experimental set-up

The experimental set-up (Fig. 2.1) was the same as described in Chapter 2.

3.2.3 Experimental procedure

Activation of the catalyst:

Catalyst activation was carried out before the poisoning experiments as described in Chapter 2.

Poisoning runs:

Conditioning of the catalyst with pure feed was not necessary since the activity of the catalyst was found to remain

constant throughout the experiment. Here the activity of the catalyst was tested only for 20 hr at a space velocity of 75 and at 260°C temperature.

After the activation of the catalyst, the temperature of the reactor was set a few degree below the reaction temperature. Hydrogen together with nitrobenzene feed contaminated with a known concentration of thiophene was then introduced into the reactor. The time of feed introduction was marked as zero. Temperature fluctuations due to poisoning were about 3°C. Product samples were collected at different time intervals. Poisoning runs were carried out at 260°C.

3.2.4 Analysis

Analysis of the samples collected was carried out on a gas chromatograph. The procedure was the same as described in Chapter 2.

3.2.5 Experimental data

Experiments were carried out at different reciprocal space velocities (W/F) and thiophene concentrations. The experimental data were plotted as fractional conversion (x) vs. time (t) for different W/F and poison (thiophene) concentrations, and are shown in Figs. 3.1, 3.2, 3.3, 3.4. From the above plots (i.e. x vs. t) conversions at different space velocities can be obtained for different times (t) and

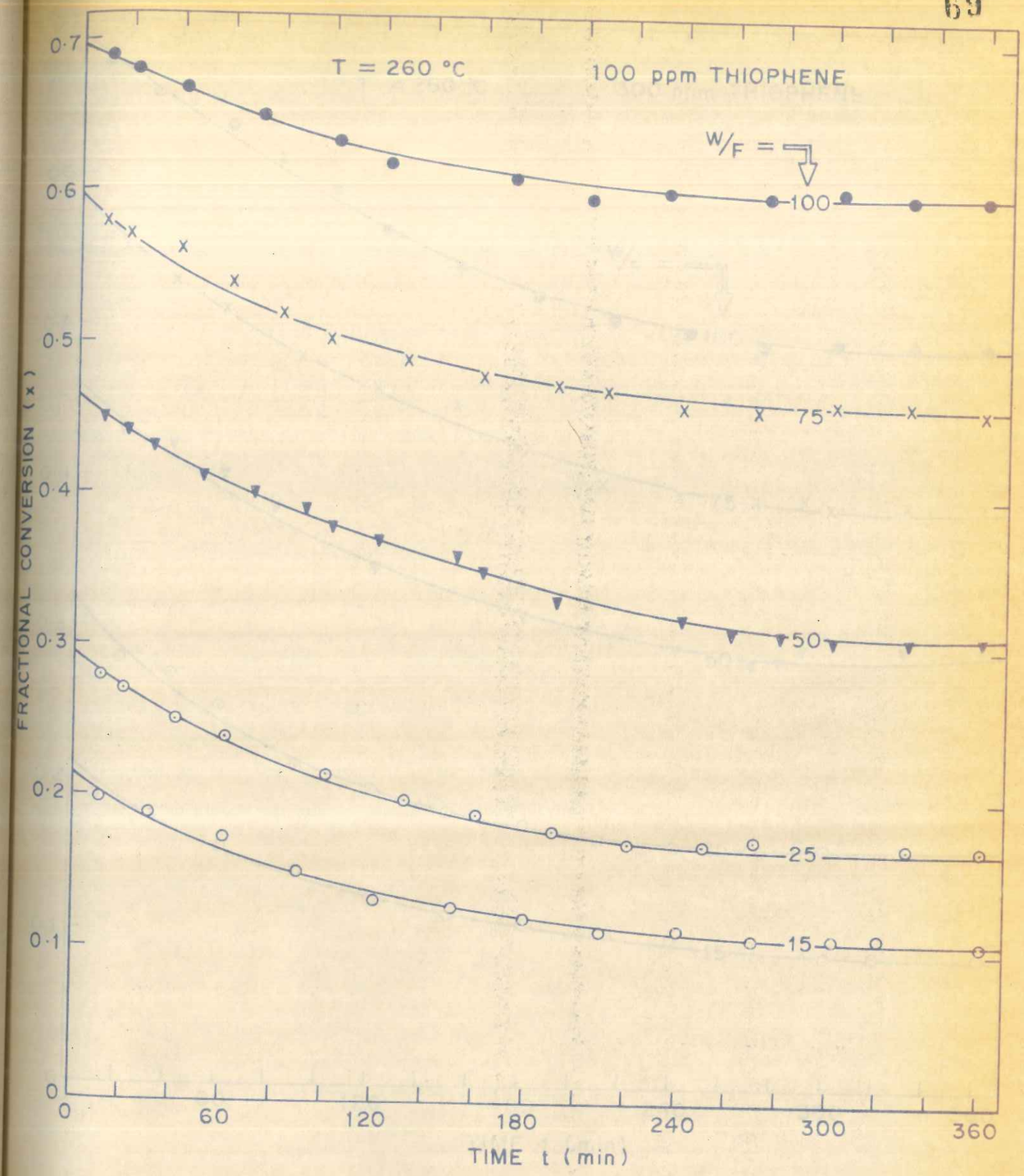

FIGURE 3·1: PLOTS FOR EXPERIMENTAL DATA (x vs t)

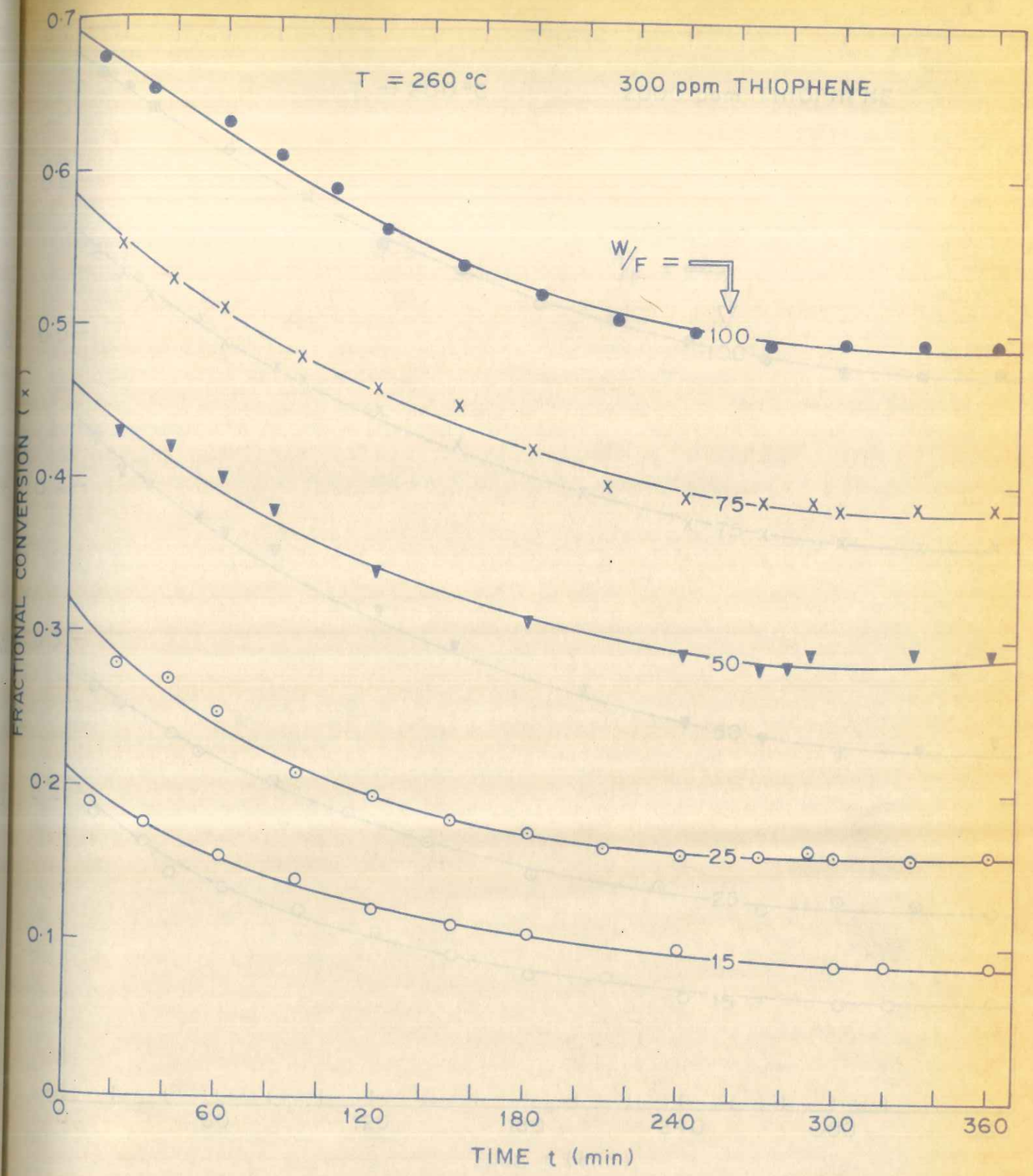

FIGURE 3·2: PLOTS FOR EXPERIMENTAL DATA (x vs t)

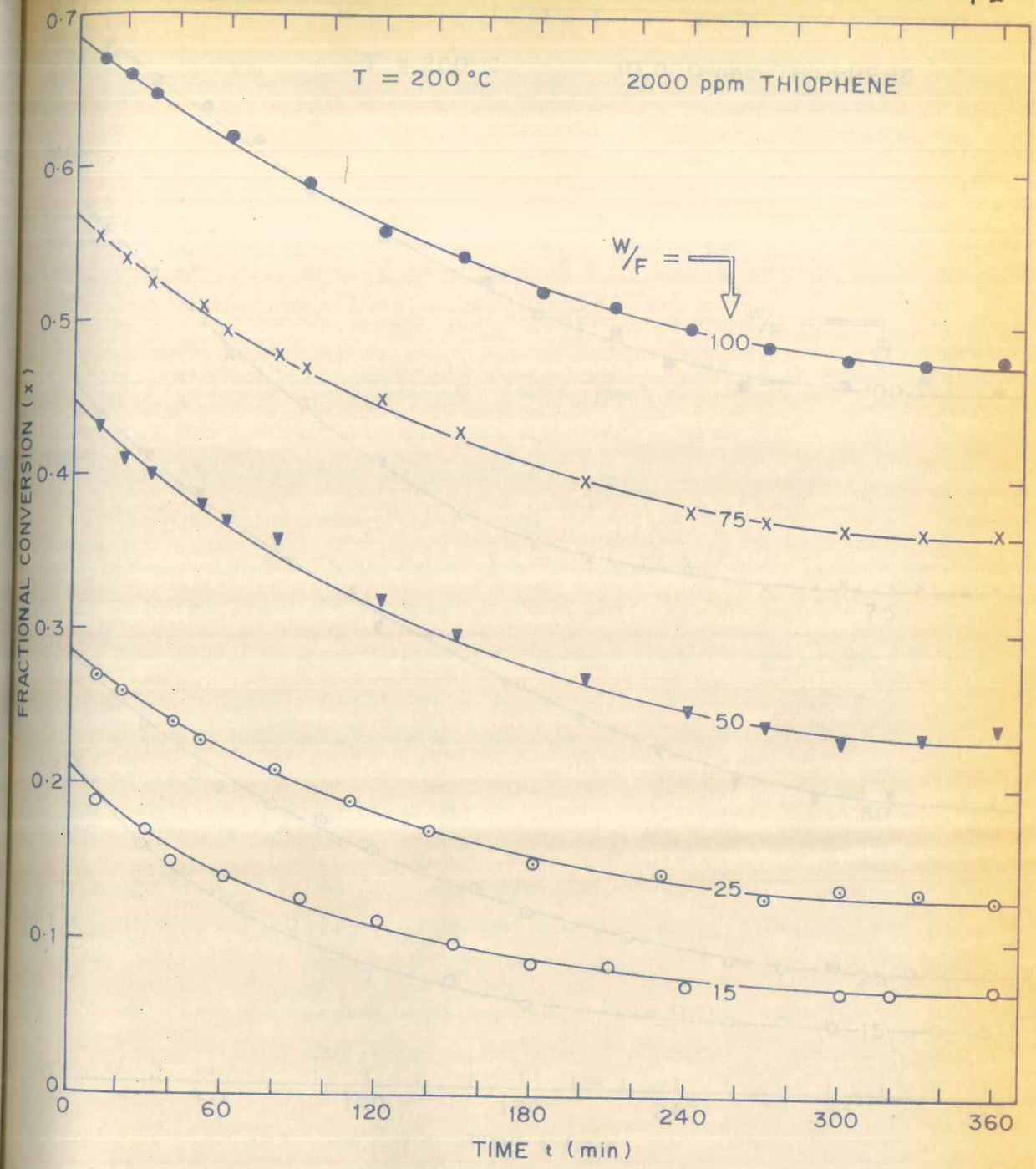

FIGURE 3·3: PLOTS FOR EXPERIMENTAL DATA (x vs t)

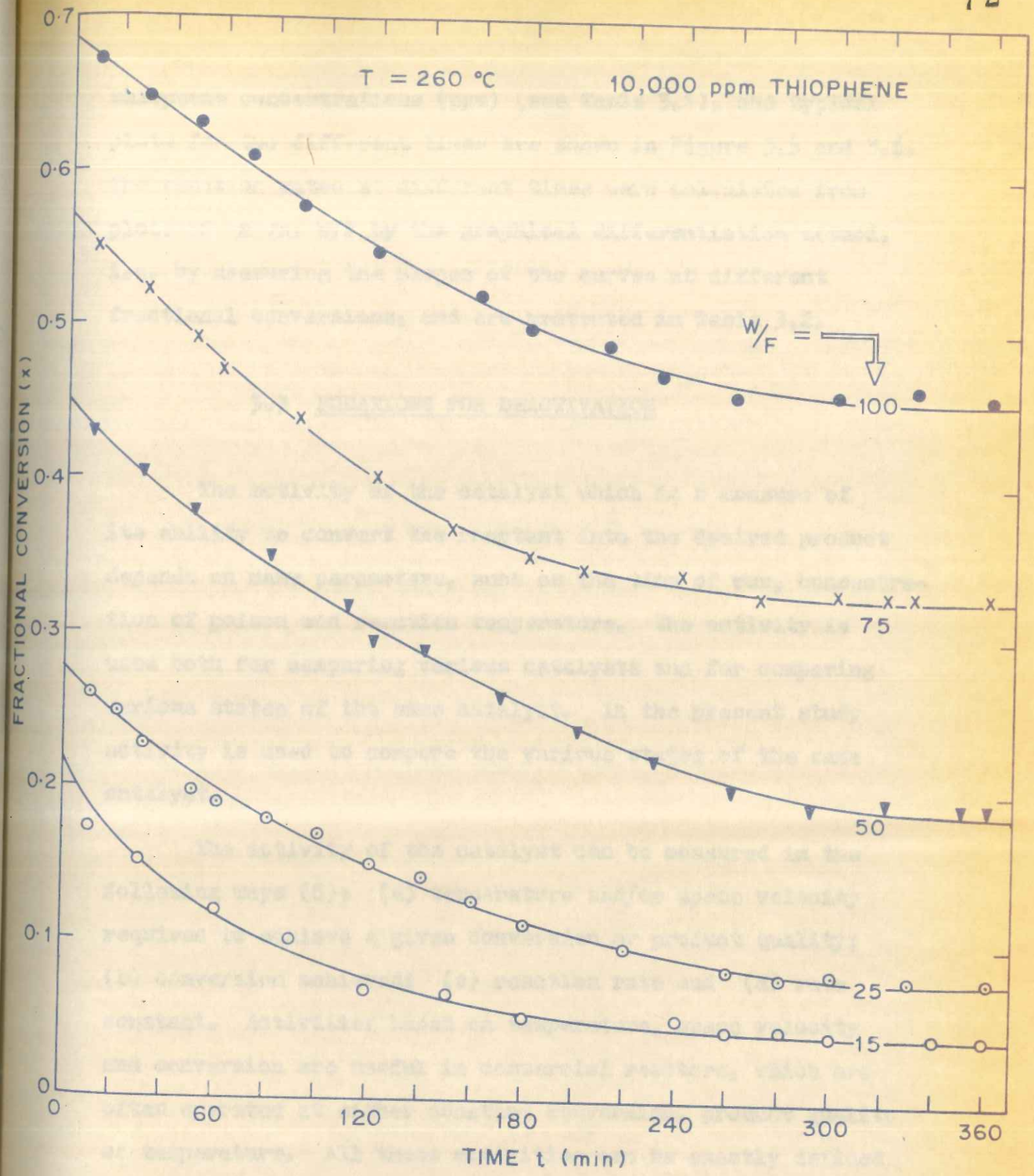

FIGURE 3·4: PLOTS FOR EXPERIMENTAL DATA (x vs t)

thiophene concentrations (ppm) (see Table 3.1), and typical plots for two different times are shown in Figure 3.5 and 3.6. The reaction rates at different times were calculated from plots of x vs. W/F by the graphical differentiation method, i.e. by measuring the slopes of the curves at different fractional conversions, and are presented in Table 3.2.

3.3 EQUATIONS FOR DEACTIVATION

The activity of the catalyst which is a measure of its ability to convert the reactant into the desired product depends on many parameters, such as the time of run, concentration of poison and reaction temperature. The activity is used both for comparing various catalysts and for comparing various states of the same catalyst. In the present study activity is used to compare the various states of the same catalyst.

The activity of the catalyst can be measured in the following ways (6): (a) temperature and/or space velocity required to achieve a given conversion or product quality; (b) conversion achieved; (c) reaction rate and (d) rate constant. Activities based on temperature, space velocity and conversion are useful in commercial reactors, which are often operated at either constant conversion, product quality or temperature. All these activities can be exactly defined

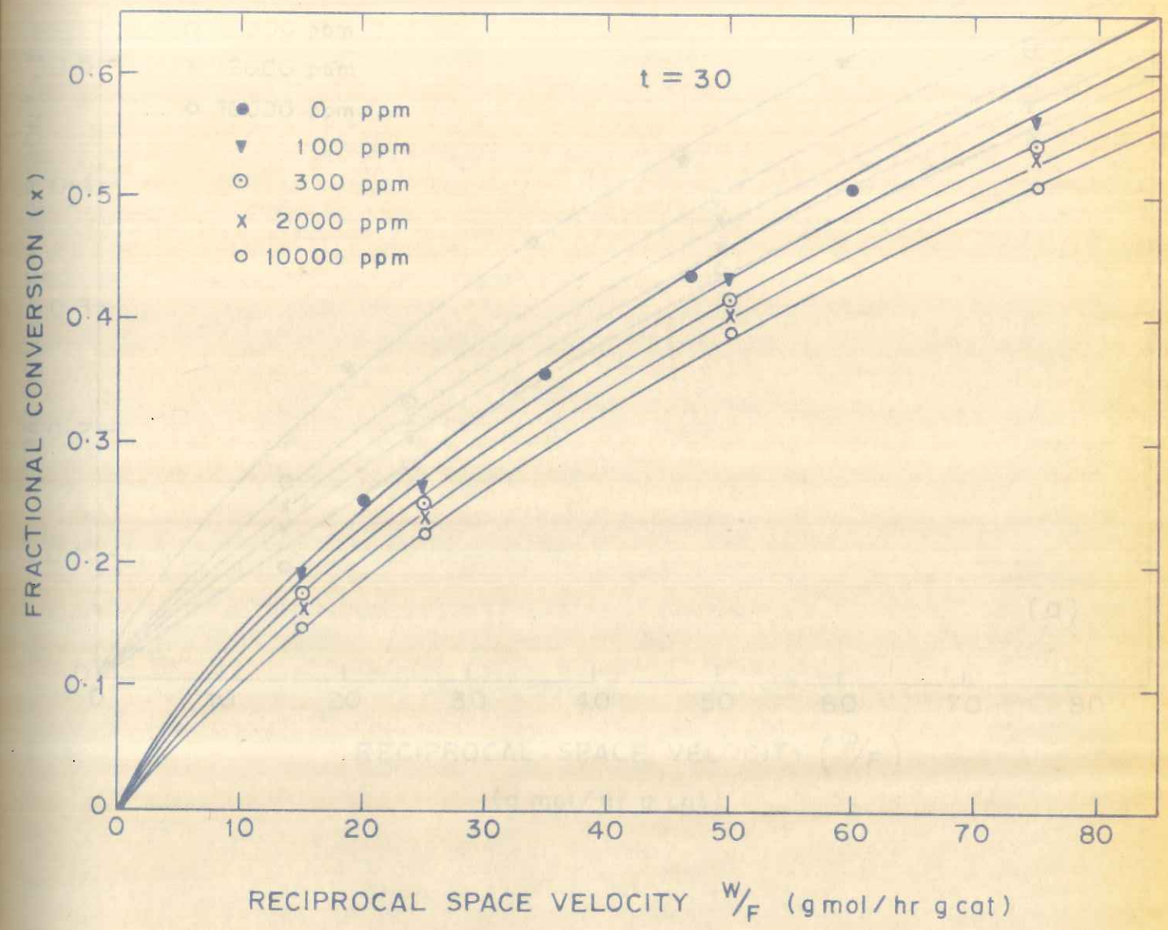

FIGURE 3·5: TYPICAL PLOTS OF (x vs W/F) FOR DIFFERENT TIME (t) AND THIOPHENE CONCENTRATIONS (ppm)

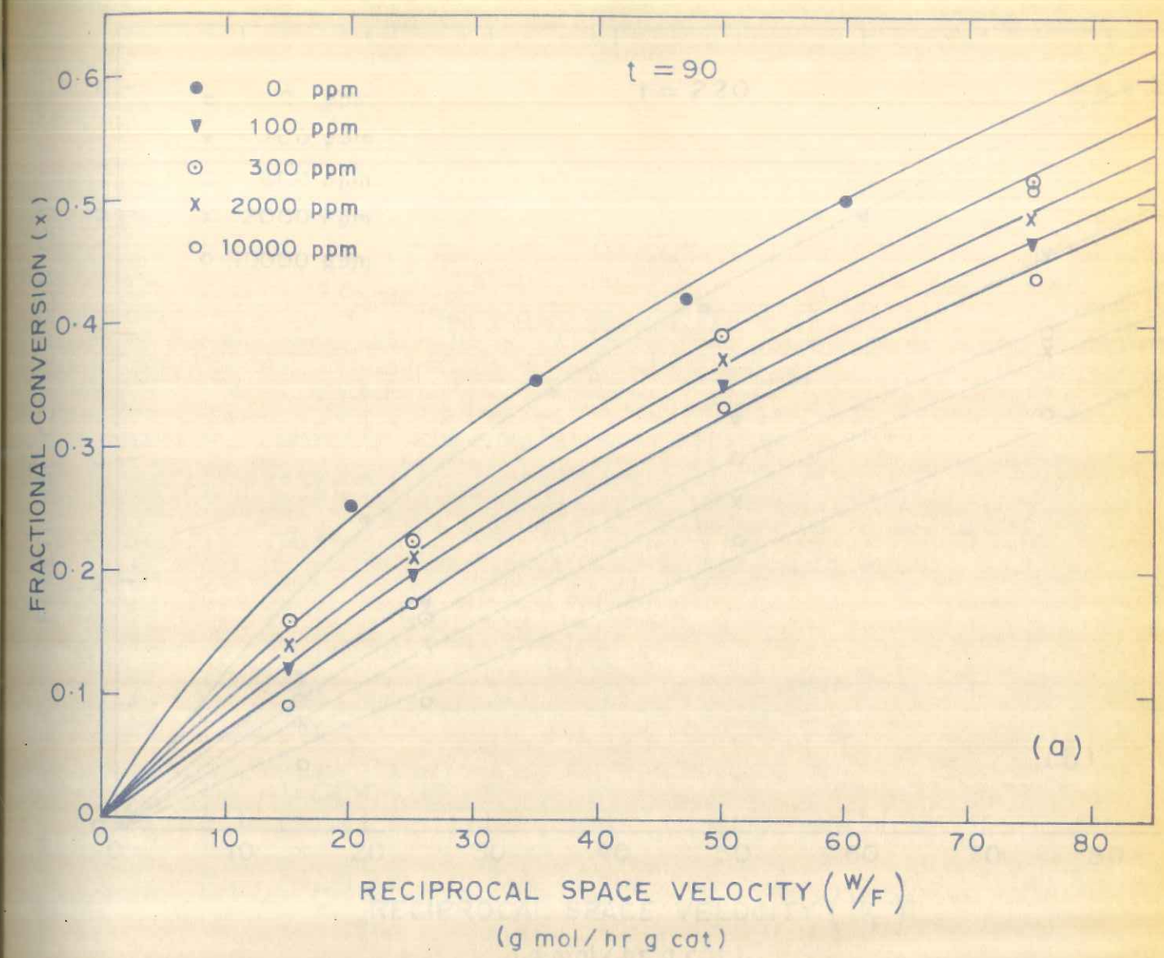

FIGURE 3·6a: TYPICAL PLOTS OF (x vs $^{W}/_{F}$) FOR DIFFERENT TIME (t) AND THIOPHENE CONCENTRATIONS (ppm)

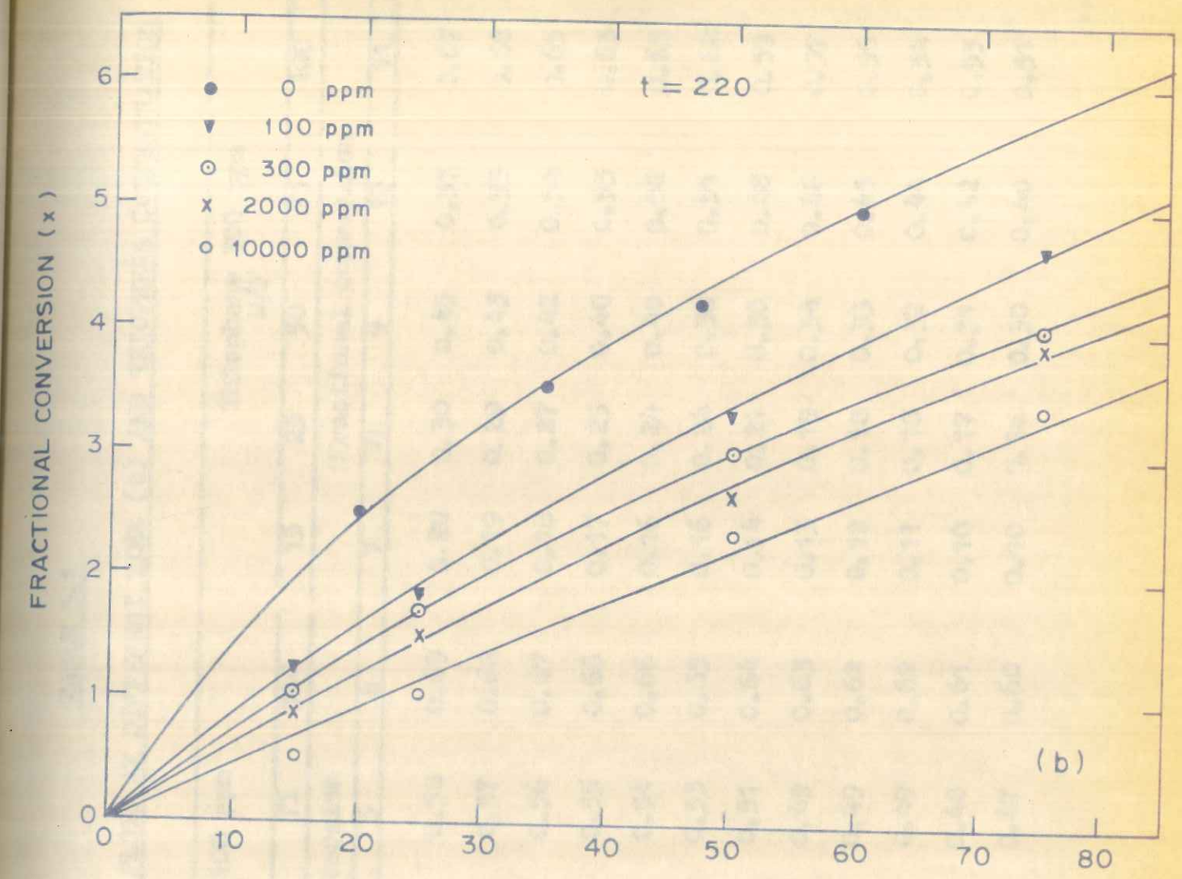

FIGURE 3·6b: TYPICAL PLOTS OF (x vs W/F) FOR DIFFERENT TIME (t) AND THIOPHENE CONCENTRATIONS (ppm)

TABLE 3.1

CONVERSION FROM x vs. W/F PLOTS AT DIFFERENT TIME (t) AND THIOPHENE CONCENTRATION

Time (min)	Thiophene 100 ppm W/F					Thiophene 300 ppm W/F				
	15	25	50	75	100	15	25	50	75	100
	Fractional conversion					Fractional conversion				
1	2	3	4	5	6	7	8	9	10	11
10	0.21	0.30	0.46	0.58	0.69	0.20	0.30	0.45	0.57	0.67
20	0.20	0.29	0.44	0.57	0.68	0.19	0.29	0.43	0.55	0.66
30	0.19	0.26	0.43	0.56	0.67	0.18	0.27	0.42	0.54	0.65
40	0.18	0.25	0.42	0.55	0.66	0.17	0.25	0.40	0.53	0.63
50	0.17	0.24	0.41	0.54	0.66	0.16	0.24	0.40	0.52	0.63
60	0.17	0.23	0.40	0.53	0.65	0.16	0.24	0.38	0.51	0.62
90	0.15	0.21	0.38	0.51	0.64	0.14	0.21	0.36	0.48	0.59
120	0.14	0.20	0.37	0.49	0.63	0.13	0.19	0.34	0.46	0.57
140	0.13	0.19	0.36	0.49	0.62	0.12	0.18	0.33	0.45	0.55
150	0.12	0.19	0.35	0.49	0.62	0.11	0.18	0.32	0.44	0.54
180	0.12	0.18	0.34	0.48	0.61	0.10	0.17	0.31	0.42	0.53
220	0.11	0.17	0.33	0.47	0.60	0.10	0.16	0.30	0.40	0.51

...

Table 3.1 contd..

1	2	3	4	5	6	7	8	9	10	11
260	0.11	0.17	0.31	0.47	0.60	0.09	0.16	0.28	0.39	0.50
300	0.11	0.17	0.31	0.47	0.60	o.09	0.16	0.28	0.39	0.50
			Thiophene 2000 ppm					Thiophene 10000 ppm		
10	0.19	0.27	0.43	0.56	0.67	0.18	0.26	0.43	0.55	0.67
20	0.18	0.26	0.42	0.54	0.65	0.17	0.24	0.41	0.54	0.66
30	0.17	0.25	0.40	0.52	0.64	0.15	0.23	0.40	0.52	0.64
40	0.16	0.24	0.39	0.51	0.63	0.14	0.22	0.39	0.50	0.63
50	0.15	0.23	0.37	0.50	0.62	0.13	0.21	0.37	0.49	0.62
60	0.14	0.22	0.36	0.49	0.61	0.12	0.20	0.36	0.48	0.61
90	0.12	0.20	0.34	0.47	0.59	0.09	0.17	0.33	0.44	0.58
120	0.11	0.18	0.31	0.44	0.56	0.08	0.15	0.30	0.40	0.55
140	0.10	0.17	0.30	0.43	0.55	0.07	0.14	0.29	0.38	0.53
150	0.09	0.16	0.29	0.42	0.54	0.06	0.13	0.28	0.37	0.52
180	0.08	0.15	0.28	0.40	0.52	0.05	0.12	0.25	0.35	0.50
220	0.07	0.14	0.26	0.38	0.50	0.05	0.10	0.23	0.33	0.48
260	0.07	0.14	0.24	0.37	0.48	0.05	0.08	0.21	0.33	0.47
300	0.07	0.14	0.24	0.37	0.48	0.05	0.08	0.20	0.33	0.47

TABLE 3.2

OBSERVED RATES FROM x vs. W/F PLOTS AT DIFFERENT THIOPHENE CONCENTRATIONS

Fractional conversion x	Observed rate : r x 10^3												
	Time (min)												
	10	20	30	40	50	60	90	120	140	150	180	220	260
1	2	3	4	5	6	7	8	9	10	11	12	13	14
							100 ppm						
0.1	11.40	11.19	10.86	10.65	10.47	9.82	9.25	8.69	8.44	8.12	7.80	7.49	7.49
0.2	9.46	9.22	3.98	8.70	8.43	7.78	7.56	7.11	6.90	6.77	6.63	6.49	6.49
0.3	7.37	7.24	7.02	6.89	6.72	6.65	6.52	6.23	6.14	6.08	5.90	5.67	5.67
0.4	6.39	6.23	6.02	5.86	5.63	5.26	5.20	4.80	4.66	4.56	4.35	3.93	3.93
							300 ppm						
0.1	11.27	10.91	10.53	10.20	9.80	9.34	8.62	7.96	7.79	7.42	7.06	6.64	6.64
0.2	9.39	9.15	8.84	8.52	8.02	7.73	7.29	6.90	6.63	6.43	6.18	5.88	5.88
0.3	7.32	7.13	6.89	6.70	6.48	6.33	6.02	5.72	5.56	5.45	5.29	5.13	5.13
0.4	6.32	6.19	5.92	5.75	5.41	4.99	4.80	4.47	4.25	4.13	3.93	3.56	3.56

.....

Table 3.2 contd...

1	2	3	4	5	6	7	8	9	10	11	12	13	14
					2000 ppm								
0.1	11.04	10.52	9.90	9.52	9.06	8.28	7.49	7.06	6.58	6.13	5.78	5.78	5.78
0.2	9.12	8.60	8.02	7.48	7,11	7.04	6.63	5.94	5.71	5.34	5.27	4.90	4.90
0.3	7.26	7.00	6.72	6.52	6.20	5.96	5.67	5.23	5.03	4.87	4.64	4.64	4.64
0.4	6.27	5.80	5.63	5.35	5.00	4.80	4.35	4.01	3.78	3.56	3.32	3.32	3.30
					10000 ppm								
0.1	10.52	9.82	9.15	8.20	7.42	6.78	5.66	4.63	4.36	4.28	3.52	3.52	3.52
0.2	8.99	8.34	7.56	7.04	6.57	6.12	5.37	4.53	4.14	3.70	3.16	3.16	3.16
0.3	7.13	6.70	6.15	5.84	5.39	5.28	4.83	4.29	3.95	3.65	3.54	3.54	3.54
0.4	6.18	5.86	5.41	5.05	4.65	4.43	4.01	3.56	3.22	3.03	2.80	2.80	2.80

even if the rate equation is not known. Activity defined on the basis of rate constant is more restrictive and is useful only if the rate expression is described by a power law function. Activity defined on the basis of rate is more useful in the present context. The importance of using this definition of activity has been stressed by Anderson and Whitehouse (5).

Deactivation equations of various forms, viz. linear, exponential, hyperbolic, have been reviewed by Levenspiel et al. (6) and are summarized in Table 3.3; any kinetic equation describing the deactivation behaviour should have the following features.

(1) It should be general enough to represent various types of deactivations observed in practice. (2) The parameters should be related in a simple way to the mechanism of deactivation. (3) It should have a simple form so as to determine the parameters directly from the experimental data. (4) The form should be useful in designing.

The deactivation equations are of two types, non-separable and separable. A separate type rate expression can be written as

$$r = r_o \text{ (present condition)} \quad q \text{ (past history)}$$

TABLE 3.3

TYPES OF DEACTIVATION EQUATIONS

Type of activity decay	Equation	Differential form	Exponent in the power law $-da/dt=ka^m$
Linear	$a = a_o - \beta_1 t$	$- da/dt = \beta_1$	0
Exponential	$a=a_o exp(- \beta_2 t)$	$- da/dt = \beta_2 a$	1
Hyperbolic	$1/a=1/a_o+ \beta_3 t$	$- da/dt = \beta_3 a^2$	2
Reciprocal power function	$a = At^{-\beta_5}$	$-da/dt= \beta_5 A^{1/\beta_5} a^{(\beta_5+1)/\beta_5}$	$(\beta_5+1)/\beta_5$
Voorhies equation	$a = A/\sqrt{t}$	$- da/dt = A^2 a^3/2$	3
Elovich equation	$dx/dt= \beta exp(-\beta_7 x)$	$-da/dt = \beta_7 a^2$	2

The activity of the catalyst at condition (T_1, C_1) and time t can be written as

$$a\,(T_1C_1t_1) = \frac{r\,(T_1C_1t_1)}{r\,(T_1C_1t_o)}$$

In the case of a separable rate expression, the activity will be a function of past history only, i.e. $a = q$. Therefore

$$r = r_o \underset{\text{reaction term}}{(\text{present condition})} \qquad a \underset{\text{activity term}}{(\text{past history})}$$

3.4 DEVELOPMENT OF A DEACTIVATION EQUATION FOR THE PRESENT CASE

As discussed earlier, to develop a deactivation equation, one must first define the term activity. In the present case the activity of the catalyst has been defined as the ratio of the rate of reaction on the poisoned catalyst to that on the fresh catalyst for the same conversion, and can be written as

$$a = \frac{\text{rate of reaction at time t on poisoned catalyst}}{\text{rate of reaction with fresh catalyst for the same conversion}}$$

i.e.
$$a = \frac{r_t}{r_o} \qquad (1)$$

Activity as a function of time has been plotted for $x = 0.1$ and the curves for different concentrations of poison (100 to 10,000 ppm) are shown in Fig. 3.7. It can be seen from the figure that the fall of activity is not linear but varies almost exponentially with time. Hence one can write the activity equation as

$$a = a_o \exp (- k_d t) \tag{2}$$

or

$$- \frac{d a}{d t} = k_d \tag{3}$$

where k_d is the deactivation constant. As stated earlier activity is not merely a function of time, but also depends upon other operating conditions, such as temperature, poison concentration (C_p), fractional conversion (x) and time of operation (t). The activity equation may thus be written as

$$a = a_o \exp (- k_d \, x \, C_p \, t) \tag{4}$$

A more general equation would be

$$a = a_o \exp (- k_d \, x^m \, C_p^n \, t^p) \tag{5}$$

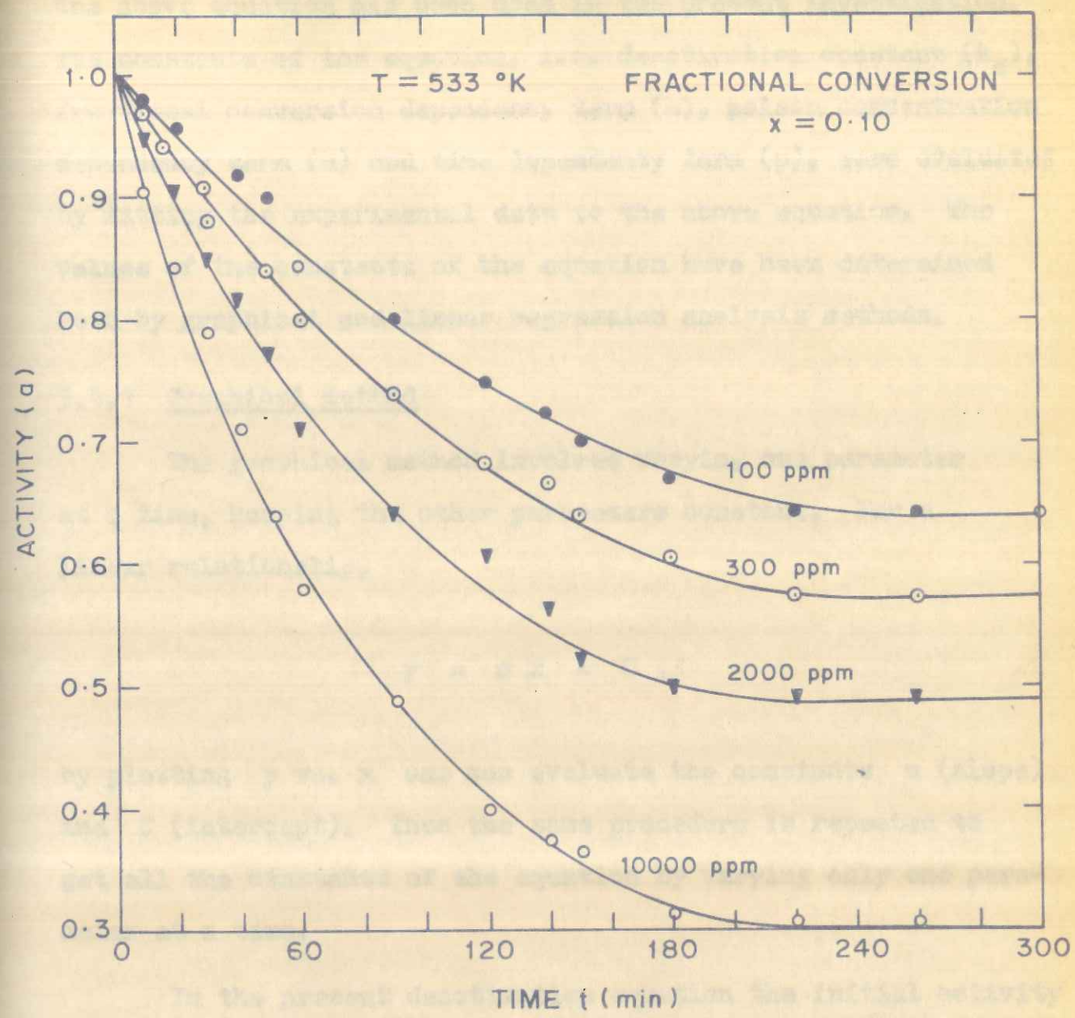

FIGURE 3·7: ACTIVITY AS A FUNCTION OF TIME

The above equation has been used in the present investigation. The constants of the equation, i.e. deactivation constant (k_d), fractional conversion dependency term (m), poison concentration dependency term (n) and time dependency term (p), were evaluated by fitting the experimental data to the above equation. The values of the constants of the equation have been determined both by graphical and linear regression analysis methods.

3.4.1 Graphical method

The graphical method involves varying one parameter at a time, keeping the other parameters constant. For a linear relationship,

$$y = m x + C ,$$

by plotting y vs. x one can evaluate the constants m (slope) and C (intercept). Thus the same procedure is repeated to get all the constants of the equation by varying only one parameter at a time.

In the present deactivation equation the initial activity of the catalyst is unity, hence

$$a = \exp (- k_d x^m C_p^n t^p) \qquad (6)$$

or

$$\ln (a) = - k_d x^m C_p^n t^p \qquad (6)$$

In the first stage poison concentration (C_p) and fractional conversion (x) were kept constant and only time was varied, i.e.

$$k_d \; x^m \; C_p^n = k_d'' = \text{constant} \qquad (7)$$

Thus the equation can be written as

$$\ln (a) = k_d'' \; t^p \qquad (8)$$

or

$$\text{Log } (\ln (a)) = \text{Log } k''_d + p \log t \qquad (8)$$

The values of log (ln(a)) were plotted against those of log t for different sets of poison concentrations and fractional conversions, and are shown in Figs. 3.8(a), 3.8(b), 3.8(c) and 3.8(d).

It can be seen from the plots that there are two straight lines for each set of poison concentrations and fractional conversions. The slopes give the value of k_d'' (i.e. k''_{d_1} and k''_{d_2}), while the intercepts give the values of p(i.e. p_1 and p_2). These values are summarized in Table 3.4. Two values of k_d'' and p clearly indicate that one set of values are applicable for $0 < t < 50$ and the other set of values for $t > 50$ min.

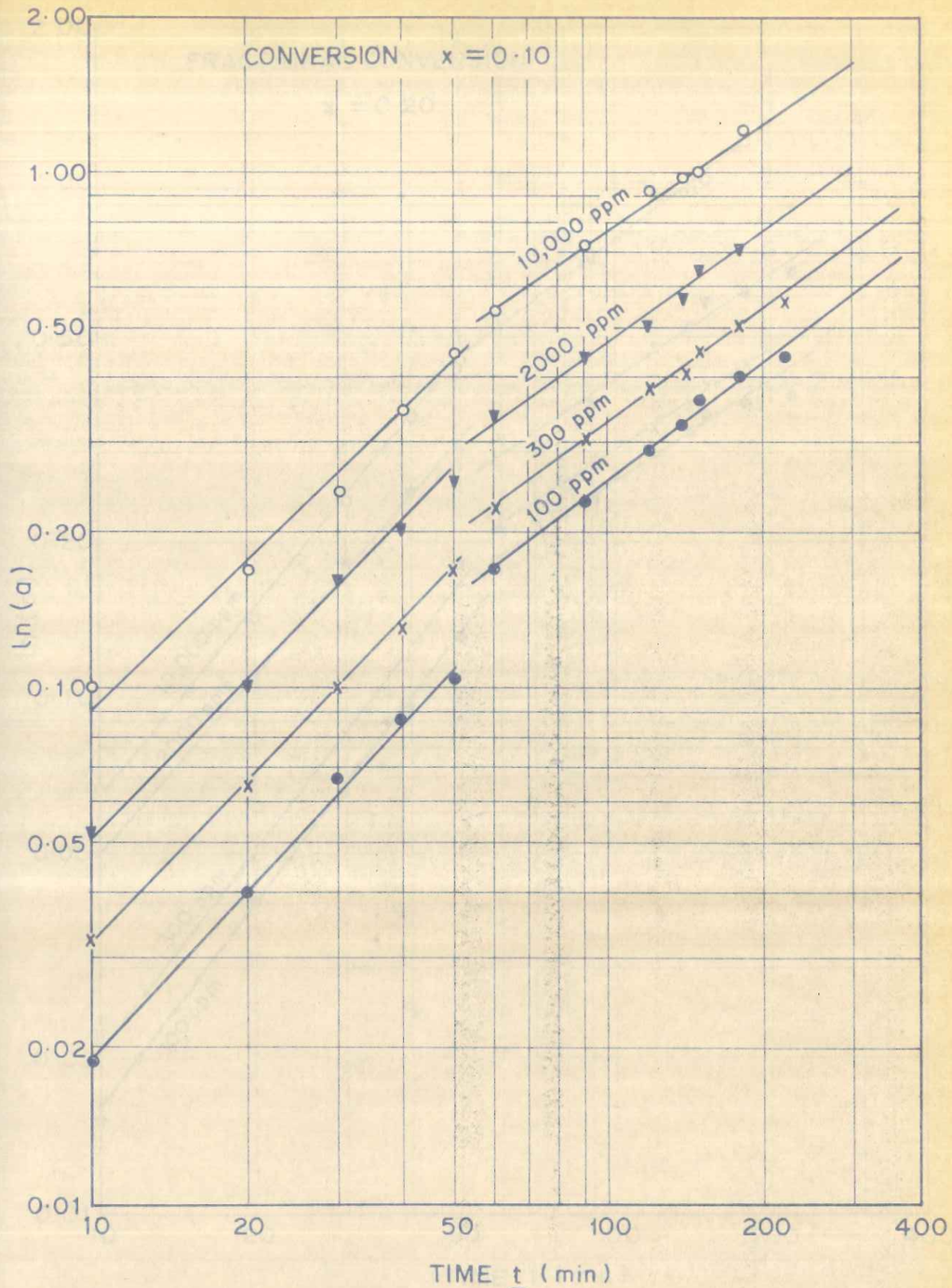

FIGURE 3·8a: PLOT FOR EQUATION (8)

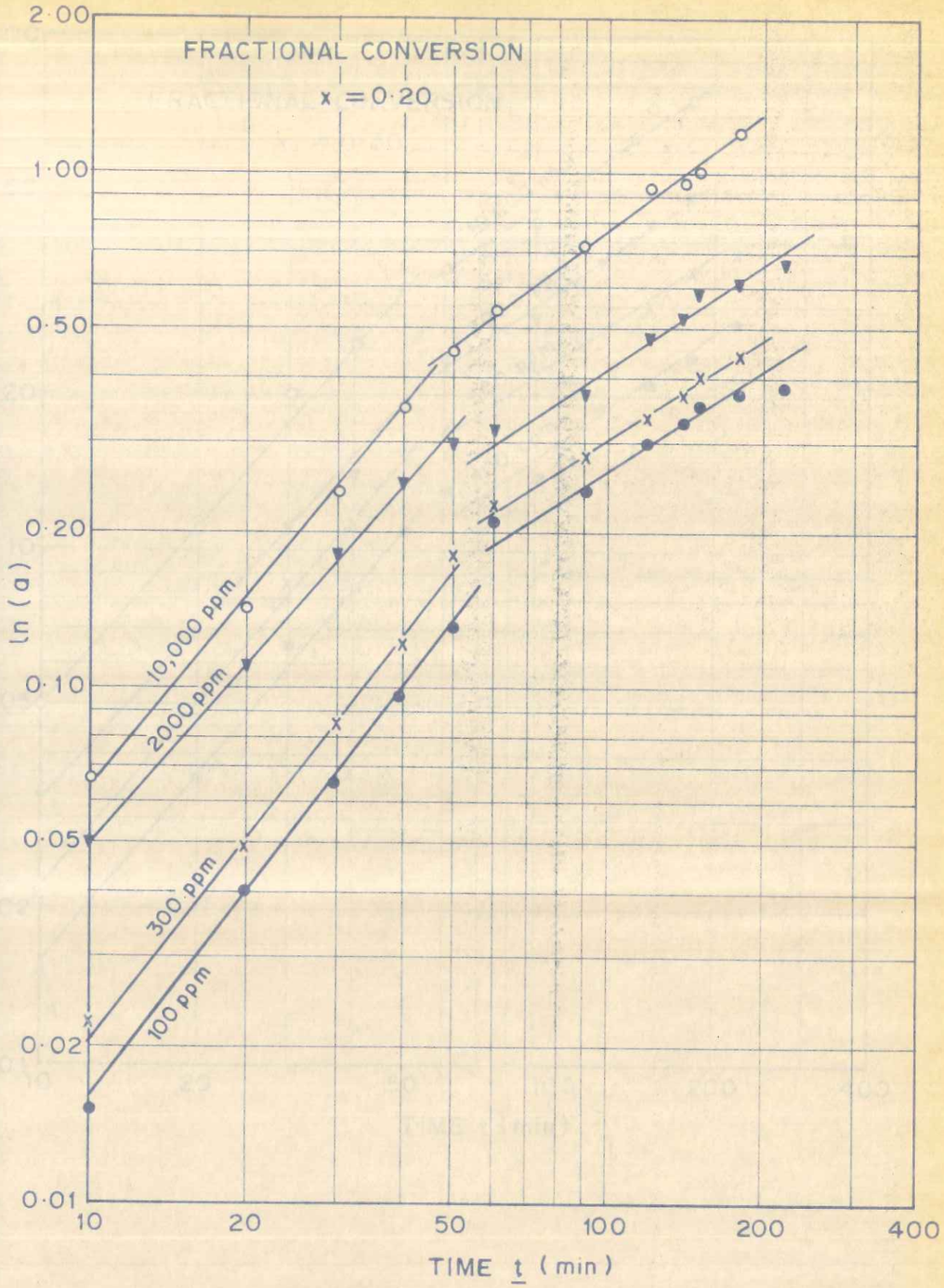

FIGURE 3·8b: PLOT FOR EQUATION (8)

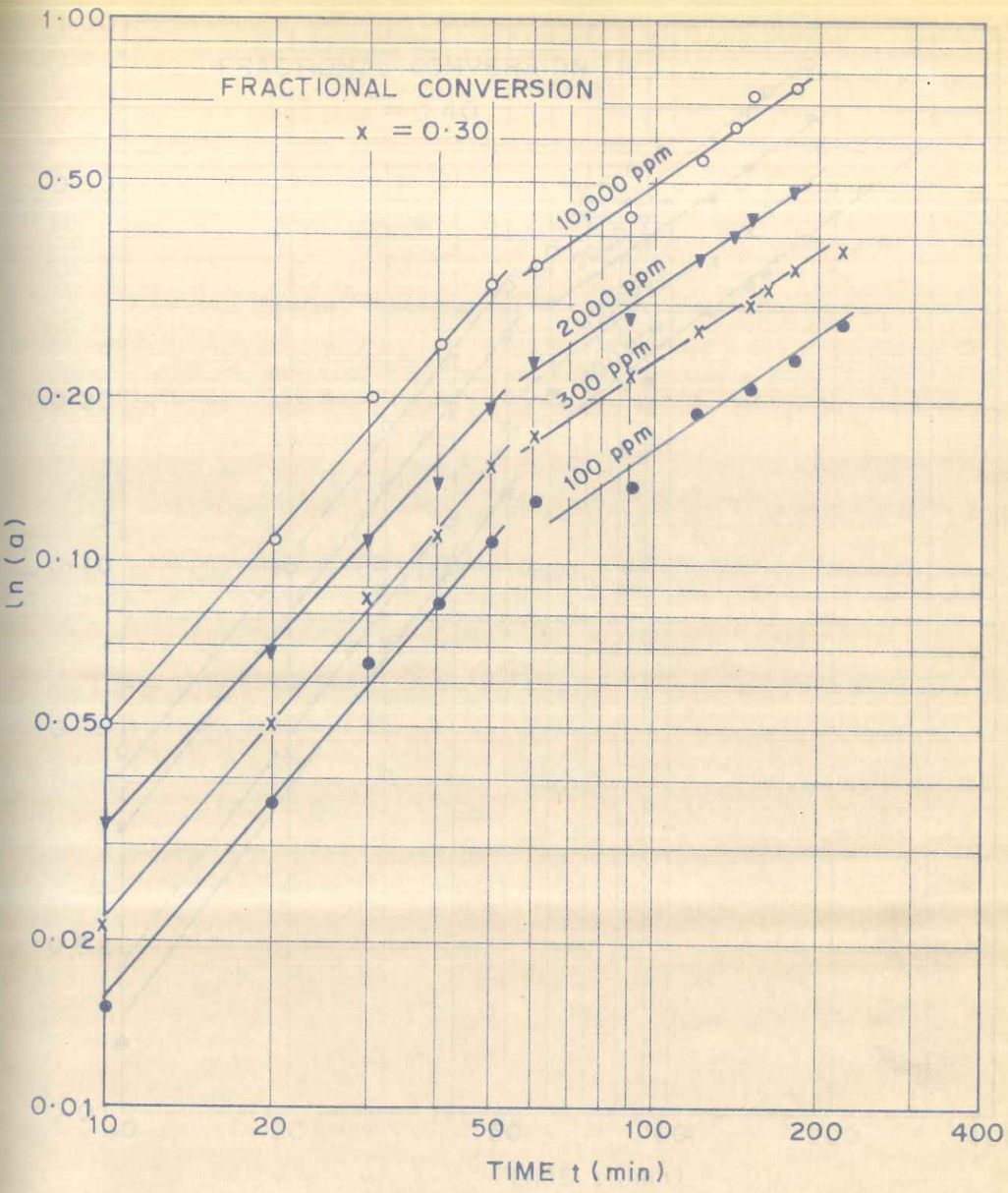

FIGURE 3·8c: PLOT FOR EQUATION (8)

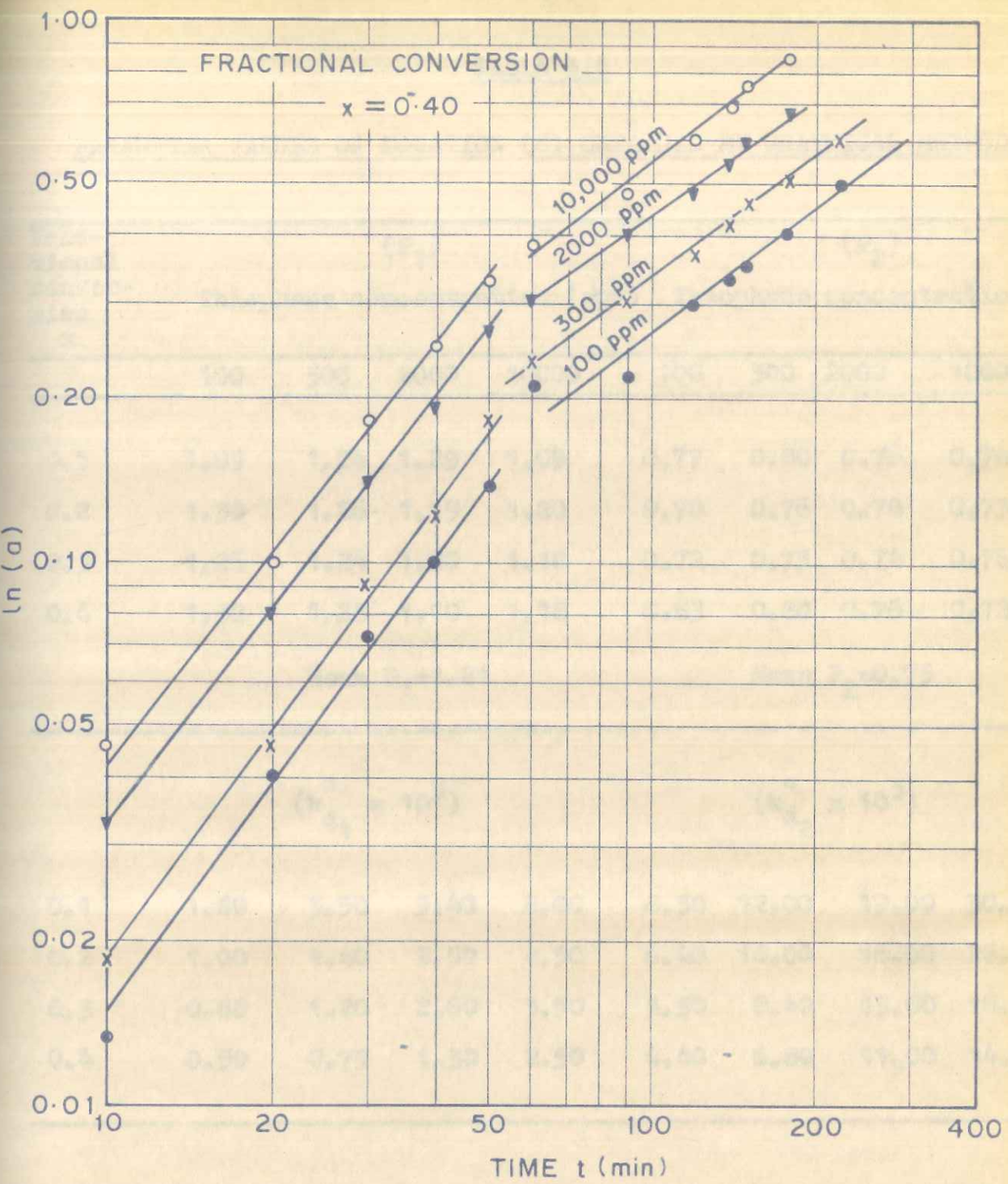

FIGURE 3·8d: PLOT FOR EQUATION (8)

TABLE 3.4

PARAMETER VALUES OF EQUATION (8) OBTAINED BY GRAPHICAL METHOD

Fractional conversion x	(P_1) Thiophene concentration (ppm)				(P_2) Thiophene concentration(ppm)			
	100	300	2000	10000	100	300	2000	10000
0.1	1.09	1.24	1.29	1.09	0.77	0.80	0.76	0.74
0.2	1.30	1.26	1.19	1.20	0.70	0.76	0.78	0.73
0.3	1.26	1.24	1.20	1.18	0.72	0.75	0.74	0.76
0.4	1.32	1.28	1.10	1.18	0.83	0.80	0.76	0.72
	Mean P_1=1.21				Mean P_2=0.75			
	$(k''_{d_1} \times 10^3)$				$(k''_{d_2} \times 10^3)$			
0.1	1.80	3.50	5.40	8.00	8.30	12.00	19.00	30.00
0.2	1.00	1.40	3.50	4.50	6.40	10.00	16.00	26.00
0.3	0.80	1.20	2.60	3.50	5.50	8.40	13.00	18.00
0.4	0.50	0.75	1.30	2.50	4.40	6.80	11.00	14.00

Now from the equation (7)

$$k_d'' = k_d \; x^m \; C_p^n$$

In the second stage fractional conversion (x) is kept constant and poison concentration (C_p) is varied, i.e.

$$k_d \; x^m = k_d' \qquad (9)$$

Hence

$$k_d'' = k_d' \; C_p^n \qquad (10)$$

or

$$\log \; k_d'' = \log \; k_d' + n \log C_p \qquad (10)$$

The values of $\log k_d''$ (obtained from the slope of the first plots) were plotted against poison concentration (C_p) for different values of fractional conversion (x). The plots are represented in Fig. 3.9. Slopes give the values of n and intercepts give the value of k_d. Here again two sets of values of constants are obtained and are given in Table 3.5.

In the third and last stage, the fractional conversion

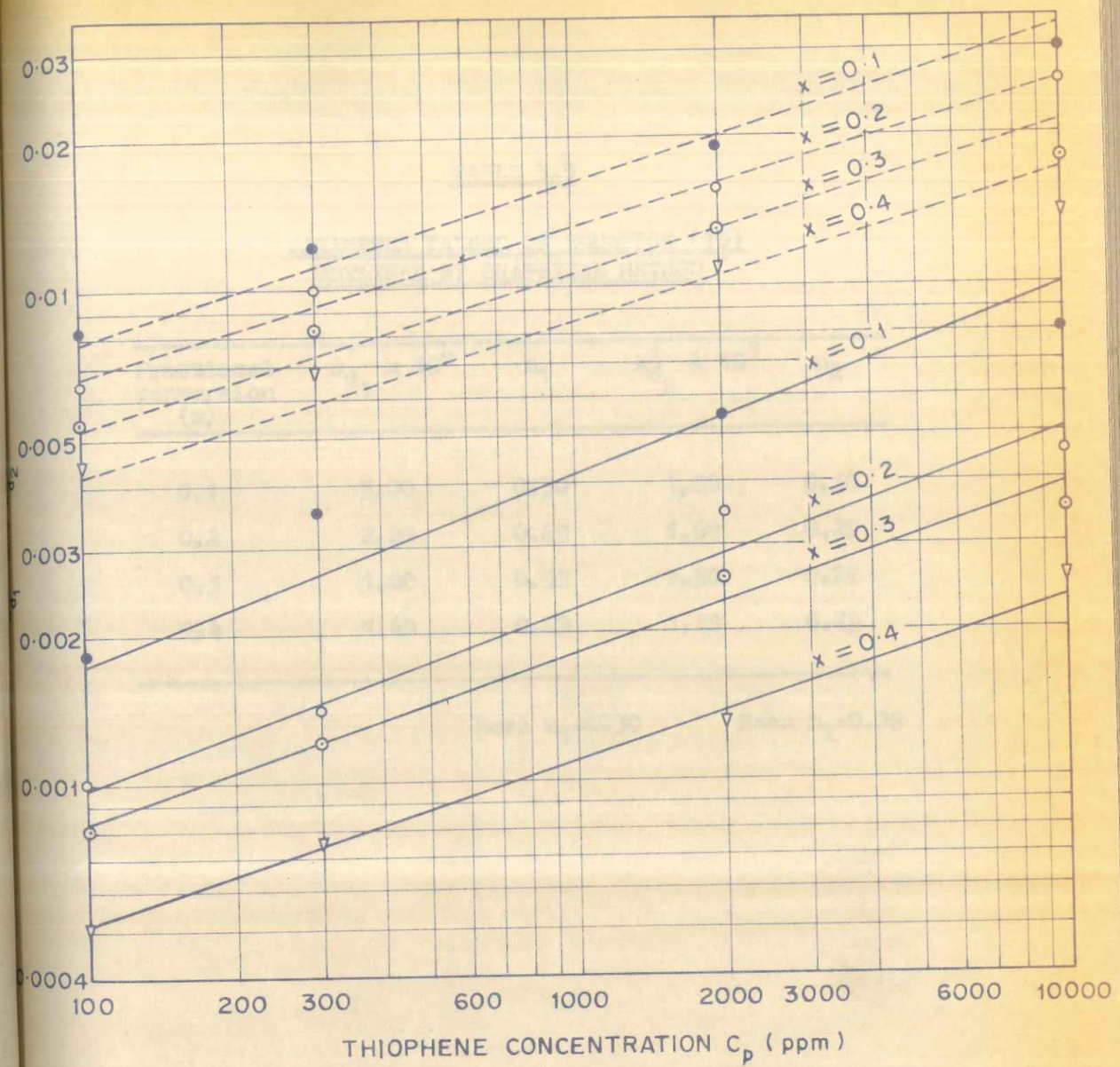

FIGURE 3·9: PLOTS FOR EQUATION (10)

TABLE 3.5

PARAMETER VALUES OF EQUATION (10)
OBTAINED BY GRAPHICAL METHOD

Fractional conversion (x)	$k'_{d_1} \times 10^4$	n_1	$k'_{d_2} \times 10^3$	n_2
0.1	3.00	0.30	1.80	0.30
0.2	2.20	0.29	1.60	0.29
0.3	1.80	0.32	1.30	0.28
0.4	1.40	0.29	1.20	0.29

Mean n_1=0.30 Mean n_2=0.29

(x) is varied keeping the other parameters constant. Hence from equation (9)

$$\text{i.e.} \qquad k_d' = k_d \; x^m \qquad (9)$$

$$\log k_d' = \log k_d + m \log x \qquad (11)$$

The values of $\log k_d'$ were plotted against $\log x$ for two sets of values of k_d (obtained from the previous plots) and the lines are shown in Fig. 3.10. Slopes of the lines give the value of m (i.e. m_1 and m_2) while intercepts give the value if k_d (i.e. k_{d_1} and k_{d_2}).

The two sets of values of the constants (k_d, m, n, p) thus obtained are summarized in Table 3.6.

Equation (6) can be further expanded to give

$$r_t = r_o \; \exp\left(- k_d \, C_p^n \, x^m \, t^p\right) \qquad (12)$$

$$\text{for} \quad a = \frac{r_t}{r_o} \quad \text{and} \quad a_o = 1$$

Hence for $0 < t < 50$ min.

$$r_t = r_o \; \exp\left(-1.16 \times 10^{-4} \, C_p^{0.30} \, . \; x^{-0.4} \, . \; t^{1.21}\right) \qquad (13)$$

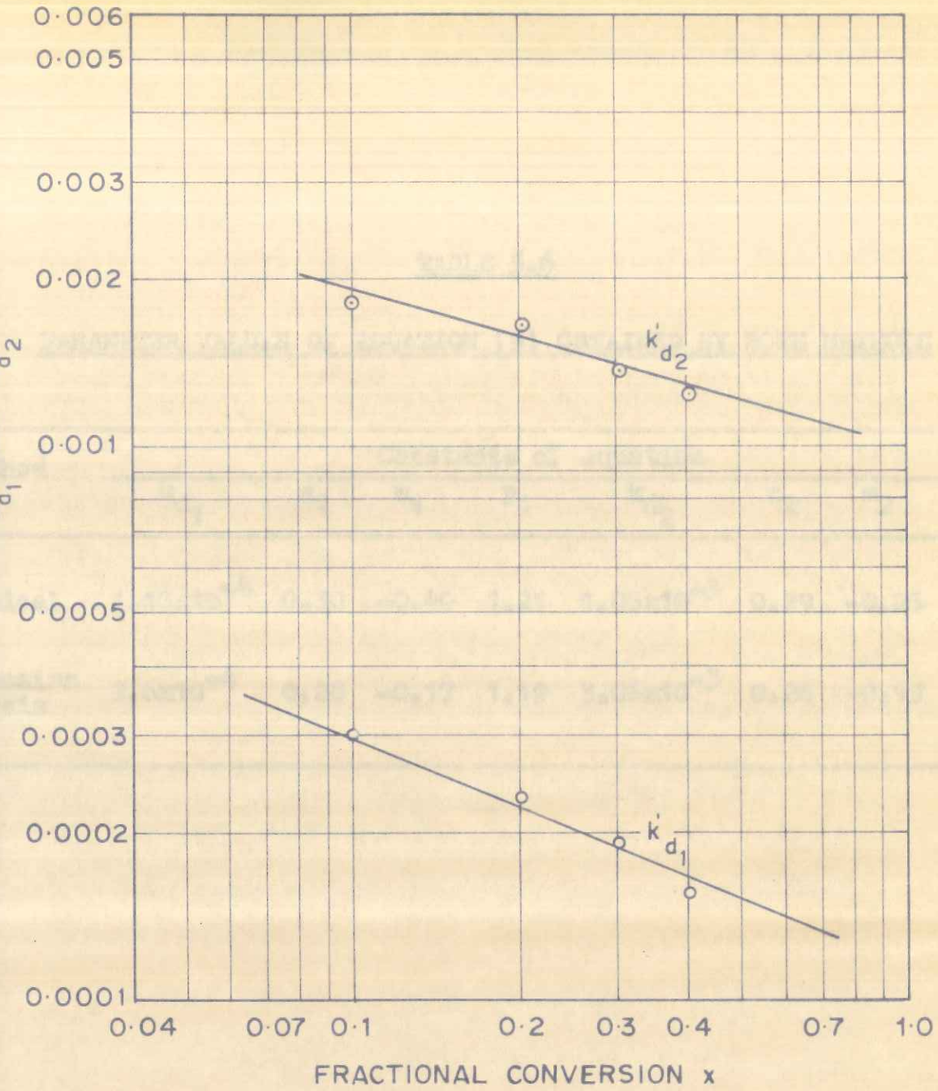

FIGURE 3·10: PLOTS FOR EQUATION (11)

$$r_t = r_o \exp\left(-1.05\times10^{-3}\ C_p^{0.29} \cdot x^{0.26} \cdot t^{0.75}\right) \qquad (14)$$

where

$$r_o = \frac{k\ p_{NB}}{(1 + K_A\ p_A)^2}$$

The rates of reaction for different time intervals were calculated from equations (13) and (14) and are compared with observed rates and are summarized in Table 3.7. The validity of the above equations was further confirmed by plotting observed rates vs. calculated rates for different poison concentrations and time (Fig. 3.11). The average percent deviation shown is for the entire concentration range studied.

3.4.2 Linear regression analysis

The deactivation equation

$$a = \exp\left(-k_d\ C_p^n\ x^m\ t^p\right) \qquad (6)$$

or

$$\log(\ln(a)) = \log k_d + n \log C_p + m \log x + p \log t \qquad (6)$$

can be rewritten as

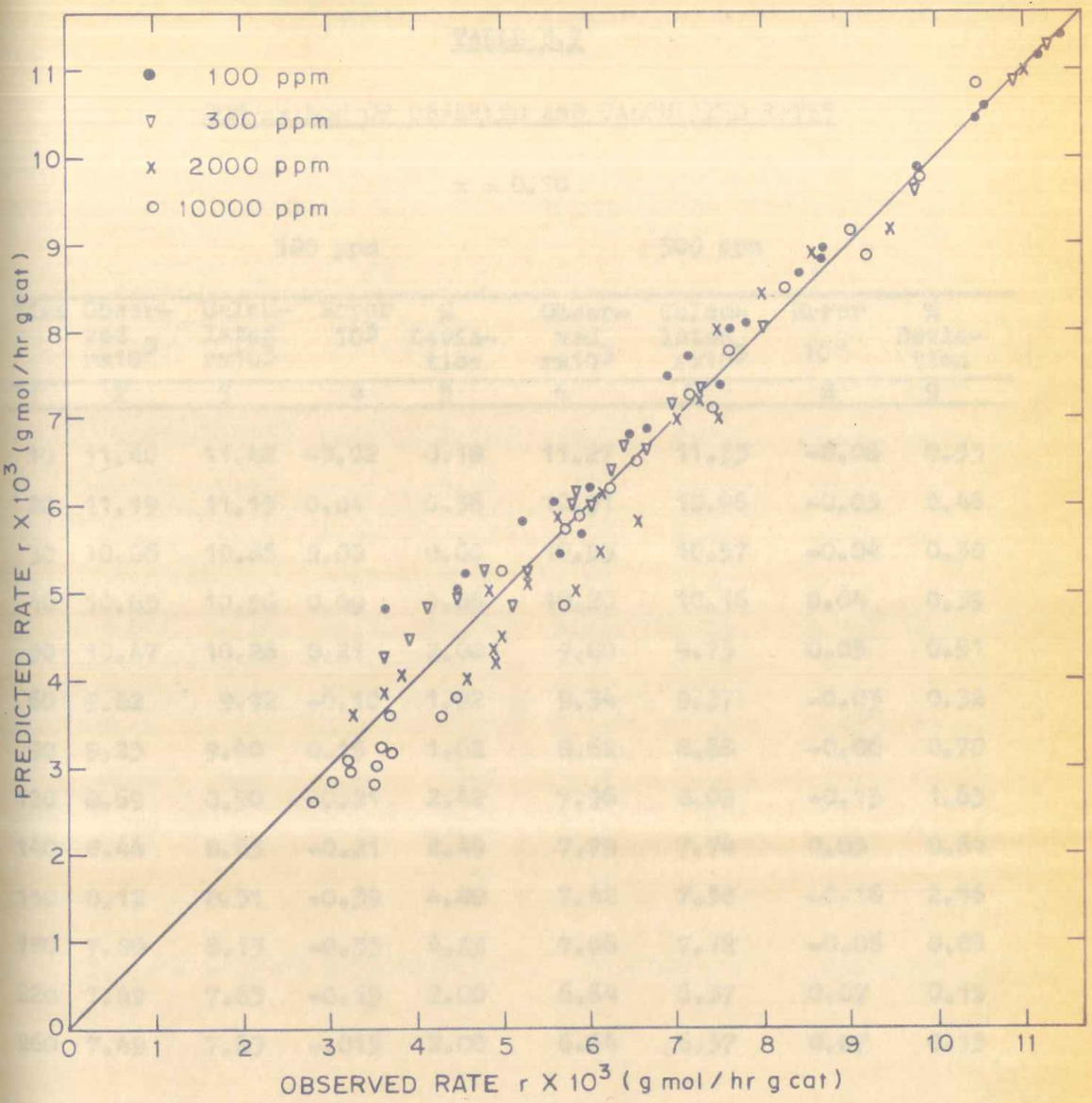

FIGURE 3·11: COMPARISON BETWEEN OBSERVED AND PREDICTED RATES

TABLE 3.7

COMPARISON OF OBSERVED AND CALCULATED RATES

x = 0.10

	100 ppm				300 ppm			
Time	Observed $rx10^3$	Calculated $rx10^3$	Error 10^3	% Deviation	Observed $rx10^3$	Calculated $rx10^3$	Error 10^3	% Deviation
1	2	3	4	5	6	7	8	9
10	11.40	11.42	-0.02	0.18	11.27	11.33	-0.06	0.53
20	11.19	11.15	0.04	0.36	10.91	10.96	-0.05	0.46
30	10.86	10.86	0.00	0.00	10.53	10.57	-0.04	0.38
40	10.65	10.56	0.09	0.85	10.20	10.16	0.04	0.39
50	10.47	10.26	0.21	2.00	9.80	9.75	0.05	0.51
60	9.82	9.92	-0.10	1.02	9.34	9.37	-0.03	0.32
90	9.25	9.40	0.15	1.62	8.62	8.68	-0.06	0.70
120	8.69	8.90	-0.21	2.42	7.96	8.09	-0.13	1.63
140	8.44	8.65	-0.21	2.49	7.79	7.74	0.05	0.64
150	8.12	8.51	-0.39	4.80	7.42	7.58	-0.16	2.16
180	7.80	8.13	-0.33	4.23	7.06	7.12	-0.06	0.85
220	7.49	7.63	-0.15	2.00	6.64	6.57	0.07	0.15
260	7.49	7.63	-.015	2.00	6.64	6.57	0.07	0.15

Average percent deviation (1.84) Average percent deviation(0.68)

.....

x = 0.10

	2000 ppm				10000 ppm			
1	2	3	4	5	6	7	8	9
10	11.04	11.10	-0.06	0.54	10.52	10.81	-0.29	2.76
20	10.52	10.48	0.04	0.38	9.82	9.84	-0.02	0.20
30	9.90	9.82	0.08	0.81	9.15	9.86	0.29	3.16
40	9.52	9.16	0.36	3.78	8.20	7.91	0.29	3.52
50	9.06	8.52	0.54	5.96	7.42	7.08	0.34	4.58
60	8.28	8.01	0.27	3.26	6.78	6.46	0.32	4.72
90	7.49	7.01	0.48	6.41	5.66	5.20	0.46	8.12
120	7.06	6.31	0.75	10.61	4.63	4.20	0.43	9.28
140	6.58	5.95	0.63	9.57	4.36	3.88	0.48	11.00
150	6.13	5.73	0.40	6.52	4.28	3.72	0.56	13.08
180	5.78	5.27	0.51	8.82	3.52	3.15	0.37	10.51
220	5.78	5.27	0.51	8.82	3.52	3.15	0.37	10.51
260	5.78	5.27	0.51	8.82	3.52	3.15	0.37	10.51

Average percent deviation(5.71) Average percent deviation(7.08)

.....

x = 0.20

	100 ppm				300 ppm			
1	2	3	4	5	6	7	8	9
10	9.46	9.46	0.00	0.00	9.39	9.42	-0.03	-0.32
20	9.22	9.29	-0.07	-0.76	9.15	9.18	-0.03	-0.33
30	8.98	9.11	-0.13	-1.45	8.84	8.93	-0.09	-1.08
40	8.70	8.90	-0.20	-2.29	8.52	8.66	-0.14	-1.64
50	8.43	8.70	-0.27	-3.20	8.02	8.40	-0.38	-4.74
60	7.78	8.41	-0.63	-8.09	7.73	8.02	-0.29	-3.76
90	7.56	8.00	-0.44	-5.82	7.29	7.52	-0.23	-3.16
120	7.11	7.70	-0.59	-8.29	6.90	7.09	-0.19	-2.75
140	6.90	7.50	-0.60	-8.69	6.63	6.83	-0.20	-3.00
150	6.77	6.78	-0.01	-0.15	6.43	6.71	-0.28	-4.35
180	6.63	7.10	-0.47	-7.00	6.18	6.37	-0.19	-3.07
220	6.49	6.75	-0.26	-4.01	5.88	5.96	-0.08	-1.34
260	6.49	6.75	-0.26	-4.01	5.88	5.96	-0.08	-1.34

Average percent deviation(4.15) Average percent deviation(2.37)

.....

x = 0.20

	2000 ppm				10000 ppm			
1	2	3	4	5	6	7	8	9
10	9.12	9.28	-0.16	-1.75	8.99	9.08	-0.09	1.00
20	8.60	8.87	-0.27	-3.14	8.34	8.45	-0.11	1.32
30	8.02	8.44	-0.42	5.23	7.56	7.81	-0.25	3.31
40	7.48	8.00	-0.52	6.95	7.04	7.17	-0.13	1.85
50	7.11	7.58	-0.47	6.61	6.57	6.56	0.01	0.15
60	7.04	7.02	0.02	0.28	6.12	5.84	0.28	4.57
90	6.63	6.29	0.34	5.12	5.37	4.89	0.48	8.93
120	5.94	5.68	0.26	4.38	4.53	4.16	0.37	8.17
140	5.71	5.38	0.33	5.78	4.14	3.76	0.38	9.17
150	5.35	5.20	0.14	2.62	3.70	3.57	0.13	3.51
180	5.27	4.82	0.45	8.53	3.16	3.09	0.07	2.21
220	4.90	4.40	0.50	10.20	3.16	3.09	0.07	2.21
260	4.90	4.40	0.50	10.20	3.16	3.09	0.07	2.21

Average percent deviation(5.44) Average percent deviation(3.74)

.....

x = 0.30

	100 ppm				300 ppm			
1	2	3	4	5	6	7	8	9
10	7.37	7.41	-0.04	0.54	7.32	7.38	-0.06	0.82
20	7.24	7.30	-0.06	0.83	7.13	7.22	-0.09	1.26
30	7.02	7.17	-0.15	2.14	6.89	7.05	-0.16	2.32
40	6.89	7.04	-0.16	2.32	6.70	6.88	-0.18	2.69
50	6.72	6.90	-0.18	2.68	6.48	6.69	-0.21	3.24
60	6.65	6.66	-0.01	0.15	6.33	6.37	-0.04	0.64
90	6.52	6.39	0.13	1.99	6.02	6.02	0.00	0.00
120	6.23	6.15	0.08	1.28	5.72	5.71	0.01	0.17
140	6.14	6.00	0.14	2.28	5.56	5.52	0.04	0.72
150	6.00	3.93	0.07	1.17	5.45	5.43	0.02	0.37
180	5.90	5.73	0.17	2.88	5.29	5.18	0.11	2.08
220	5.67	5.49	0.18	3.17	5.13	4.88	0.25	4.87
260	5.67	5.49	0.18	3.17	5.13	4.88	0.25	4.87

Average percent deviation(1.89) Average percent deviation(1.85)

.....

x = 0.30

	2000 ppm			10000 ppm				
1	2	3	4	5	6	7	8	9
10	7.26	7.28	-0.02	0.28	7.13	7.16	-0.03	0.42
20	7.00	7.02	-0.02	0.29	6.70	6.74	-0.04	0.59
30	6.72	6.73	-0.01	0.15	6.15	6.30	-0.15	2.43
40	6.52	6.44	0.08	1.23	5.84	5.86	-0.02	0.34
50	6.20	6.14	0.06	0.97	5.39	5.43	-0.04	0.74
60	5.96	5.68	0.28	4.69	5.28	4.79	0.49	9.28
90	5.69	5.22	0.45	7.94	4.83	4.49	0.34	7.03
120	5.23	4.78	0.45	8.60	4.29	3.83	0.46	10.72
140	5.03	4.58	0.45	8.94	3.95	3.52	0.43	10.88
150	4.87	4.40	0.47	9.65	3.65	3.37	0.28	7.69
180	4.64	4.12	0.52	11.20	3.54	3.25	0.29	8.19
220	4.64	4.12	0.52	11.20	3.54	3.25	0.29	8.19
260	4.64	4.12	0.52	11.20	3.54	3.25	0.29	8.19

Average percent deviation(5.87) Average percent deviation(5.75)

.....

$$y = b_0 + b_1 x_1 + b_2 x_2 + b_3 x_3$$

The above equation was solved for its constants by linear regression.

The values of the constants thus obtained are given in Table 3.6. By knowing the constants of the equation, the rates were calculated and are compared with the observed rates (Table 3.8). The adequacy of the equation was further tested by plotting observed rates vs. predicted rates (Fig.3.12).

3.5 DISCUSSION

It can be seen from Figs. 3.11 and 3.12 that the values of rates obtained from the constants evaluated by the graphical method are more scattered around the central line than from the constants evaluated by the regression method.

Plots of fractional conversion (x) vs. time of operation (t) for different reciprocal space velocities and poison concentrations (Figs. 3.1, 3.2, 3.3, 3.4) showed that there is a rapid fall of conversion in the initial period (for about 60-80 minutes) which subsequently slows down and attains a constant nonzero value. Similar behaviour has been observed in many cases viz. in the conversion of benzene to cyclohexane (4) which was contaminated by addition of thiophene

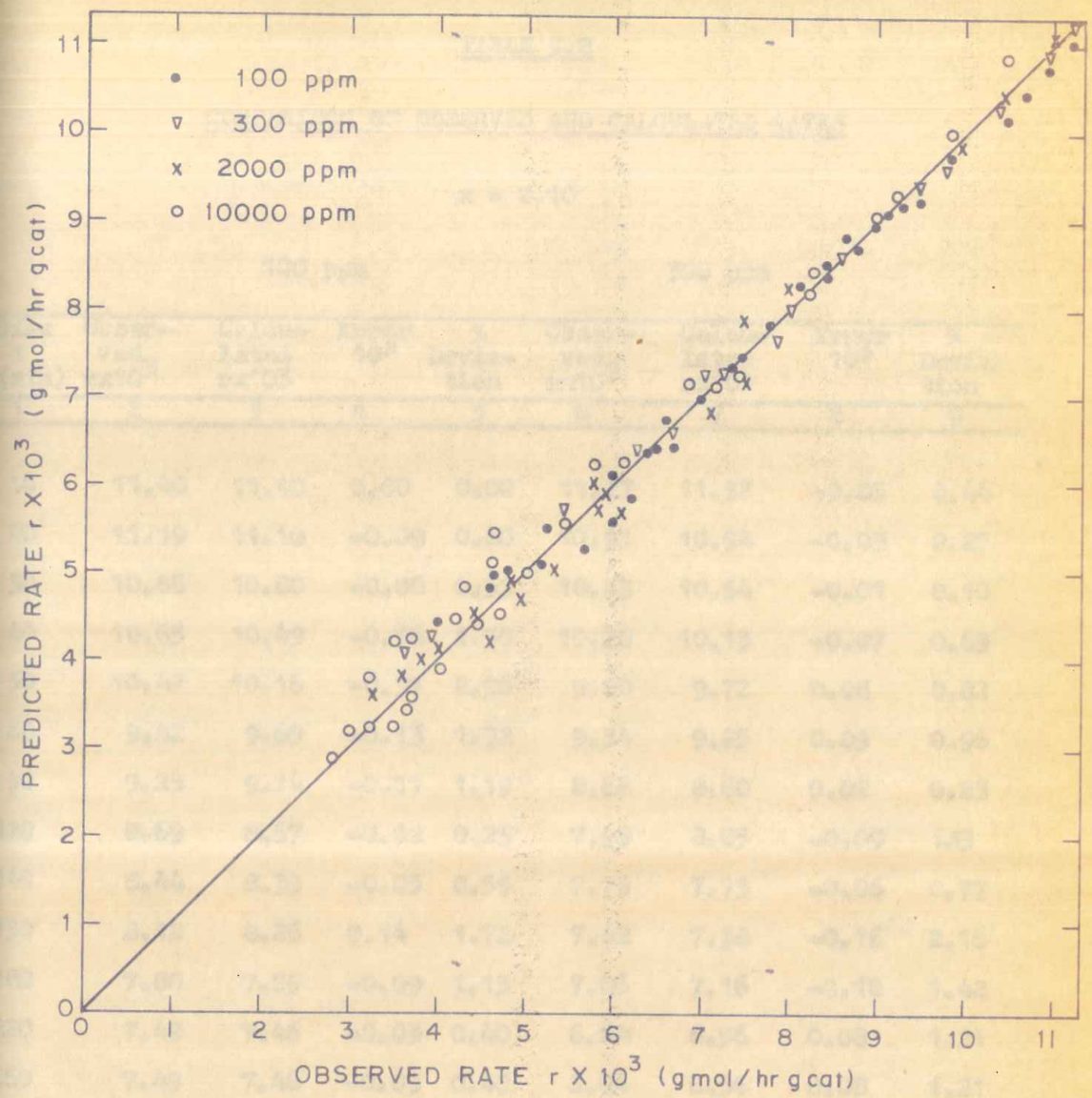

FIGURE 3.12: COMPARISON BETWEEN OBSERVED AND PREDICTED RATES

TABLE 3.8

COMPARISON OF OBSERVED AND CALCULATED RATES

x = 0.10

	100 ppm				300 ppm			
Time t (min)	Observed $r \times 10^3$	Calculated $r \times 10^3$	Error 10^3	% Deviation	Observed $r \times 10^3$	Calculated $r \times 10^3$	Error 10^3	% Deviation
1	2	3	4	5	6	7	8	9
10	11.40	11.40	0.00	0.00	11.27	11.32	-0.05	0.44
20	11.19	11.10	-0.09	0.80	10.91	10.94	-0.03	0.27
30	10.86	10.80	-0.06	0.55	10.53	10.54	-0.01	0.10
40	10.65	10.49	-0.16	1.50	10.20	10.13	-0.07	0.69
50	10.47	10.16	-0.31	2.96	9.80	9.72	0.08	0.82
60	9.82	9.69	-0.13	1.32	9.34	9.25	0.09	0.96
90	9.25	9.14	-0.11	1.19	8.62	8.60	0.02	0.23
120	8.69	8.67	-0.02	0.23	7.96	8.05	-0.09	1.13
140	8.44	8.39	-0.05	0.59	7.79	7.73	-0.06	0.77
150	8.12	8.26	0.14	1.72	7.42	7.58	-0.16	2.16
180	7.80	7.89	-0.09	1.15	7.06	7.16	-0.10	1.42
220	7.49	7.46	-0.03	0.40	6.64	6.56	0.08	1.21
260	7.49	7.46	-0.03	0.40	6.64	6.56	0.08	1.21
	Average percent deviation(0.98)				Average percent deviation(0.88)			

.....

x = 0.10

	2000 ppm				10000 ppm			
1	2	3	4	5	6	7	8	9
10	11.00	11.13	-0.09	0.82	10.52	10.88	-0.36	3.42
20	10.52	10.53	-0.01	0.10	9.82	10.00	-0.18	1.83
30	9.90	9.90	0.00	0.00	9.15	9.11	0.04	0.44
40	9.52	9.28	0.24	2.52	8.20	8.25	-0.05	0.61
50	9.06	8.67	0.39	4.30	7.42	7.43	-0.01	0.13
60	8.28	8.29	-0.01	0.12	6.78	7.08	-0.30	4.42
90	7.49	7.44	0.05	0.67	5.66	6.14	-0.48	8.48
120	7.06	6.75	0.31	4.39	4.63	5.20	-0.57	12.31
140	6.58	6.36	0.22	3.34	4.36	4.66	-0.30	6.88
150	6.13	6.17	-0.04	0.65	4.28	4.30	-0.02	0.47
180	5.78	5.67	0.11	1.90	3.52	3.60	-0.08	2.27
220	5.78	5.67	0.11	1.90	3.52	3.60	-0.08	2.27
260	5.78	5.67	0.11	1.90	3.52	3.60	-0.08	2.27

Average percent deviation(1.74) Average percent deviation(3.52)

.....

x = 0.20

	100 ppm				300 ppm			
1	2	3	4	5	6	7	8	9
10	9.46	9.43	0.03	0.32	9.39	9.38	0.01	0.11
20	9.22	9.22	0.00	0.00	9.15	9.09	0.06	0.66
30	8.98	8.99	-0.01	0.11	8.84	8.80	0.04	0.45
40	8.70	8.75	-0.05	0.57	8.52	8.49	0.03	0.35
50	8.43	8.51	-0.08	0.95	8.02	8.18	-0.16	1.99
60	7.78	8.10	-0.32	4.11	7.73	7.80	-0.07	0.91
90	7.56	7.72	-0.16	2.12	7.29	7.30	-0.01	0.14
120	7.11	7.36	-0.25	3.52	6.90	6.89	0.01	0.15
140	6.90	7.15	-0.25	3.62	6.63	6.64	-0.01	0.15
150	6.77	7.00	-0.23	3.39	6.43	6.50	-0.07	1.09
180	6.63	6.73	-0.10	1.51	6.18	6.19	-0.01	0.16
220	6.49	6.42	-0.07	1.08	5.88	5.81	0.07	1.19
260	6.49	6.42	-0.07	1.08	5.88	5.81	0.07	1.19

Average percent deviation(1.72) Average percent deviation(.66)

.....

x = 0.20

	2000 ppm				10000 ppm			
1	2	3	4	5	6	7	8	9
10	9.12	9.23	-0.11	-1.21	8.99	9.05	-0.06	0.67
20	8.60	8.79	-0.19	-2.21	8.34	8.39	-0.05	0.59
30	8.02	8.32	-0.30	-3.74	7.56	7.73	-0.17	2.25
40	7.48	7.85	-0.37	-4.95	7.04	7.08	-0.04	0.57
50	7.11	7.39	-0.28	-3.94	6.57	6.45	0.12	1.83
60	7.04	7.07	-0.03	-0.43	6.12	6.20	-0.08	1.31
90	6.63	6.41	0.22	3.32	5.37	5.47	-0.10	1.86
120	5.94	5.87	0.07	1.18	4.53	4.84	-0.31	6.84
140	5.71	5.56	0.15	2.63	4.14	4.42	-0.28	6.76
150	5.34	5.41	-0.07	-1.31	3.70	4.00	-0.30	8.11
180	5.27	5.02	0.25	4.74	3.16	3.41	-0.25	7.91
220	4.90	4.68	0.22	4.49	3.16	3.41	-0.25	7.91
260	4.90	4.68	0.22	4.49	3.16	3.41	-0.25	7.91

Average percent deviation(2.97) Average percent deviation(4.19)

.....

x = 0.30

	100 ppm				300 ppm			
1	2	3	4	5	6	7	8	9
10	7.37	7.38	-0.01	0.14	7.32	7.34	-0.02	0.27
20	7.24	7.22	-0.02	0.28	7.13	7.13	0.00	0.00
30	7.02	7.06	-0.04	0.57	6.89	6.92	-0.03	0.43
40	6.89	6.88	0.01	0.15	6.70	6.69	0.01	0.15
50	6.72	6.71	0.01	0.15	6.48	6.46	0.02	0.31
60	6.65	6.42	0.23	3.46	6.33	6.17	0.16	2,52
90	6.52	6.11	0.41	6.28	6.02	5.80	0.22	3.65
120	6.23	5.84	0.39	6.26	5.72	5.49	0.23	4.02
140	6.14	5.68	0.46	7.49	5.56	5.30	0.26	4.67
150	6.08	5.60	0.48	7.89	5.45	5.22	0.23	4.22
180	5.90	5.39	0.51	8.64	5.29	4.96	0.33	6.23
220	5.67	5.25	0.42	7.40	5.13	4.76	0.37	7.21
260	5.67	5.25	0.42	7.40	5.13	4.76	0.37	7.21

Average percent deviation(4.32) Average percent deviation(3.14)

.....

x = 0.30

	2000 ppm			10000 ppm				
1	2	3	4	5	6	7	8	9
10	7.26	7.23	0.03	0.41	7.13	7.09	0.04	0.56
20	7.00	6.91	0.09	1.28	6.70	6.62	0.08	1.19
30	6.72	6.57	0.15	2.23	6.15	6.13	0.02	0.32
40	6.52	6.22	0.30	4.60	5.84	5.64	0.20	3.42
50	6.20	5.88	0.32	5.16	5.39	5.17	0.22	4.08
60	5.96	5.65	0.31	5.20	5.28	5.02	0.26	4.92
90	5.67	5.15	0.52	9.17	4.83	4.41	0.42	8.69
120	5.23	4.75	0.48	9.18	4.29	3.95	0.34	7.92
140	5.03	4.50	0.50	9.94	3.95	3.72	0.23	5.82
150	4.87	4.40	0.47	9.65	3.65	3.55	0.10	2.74
180	4.64	4.27	0.37	7.97	3.54	3.25	0.29	8.19
220	4.64	4.27	0.37	7.97	3.54	3.25	0.29	8.19
260	4.64	4.27	0.37	7.97	3.54	3.25	0.29	8.90

Average percent deviation(6.21) Average percent deviation(4.94)

---

in feed a rapid fall of conversion occurred for the initial one or two hours which then attained a constant nonzero value. Gioia (3) observed a rapid fall of conversion during the deactivation of Cu-MgO catalysts for the hydrogenation of ethylene. Water vapour acted as a poison. After the first rapid fall of conversion he observed a constant nonzero value. It can be said that the first rapid decrease in activity or conversion may be due to the irreversible adsorption of thiophene on the catalysts surface. During its initial contact with the catalyst surface, thiophene attacks the active centres thereby reducing the activity of the catalyst. This process continues till a stage is reached when thiophene in the gas phase remains in equilibrium with that adsorbed on the catalyst surface, which is indicated by the constant nonzero value of the conversion obtained. Nearly constant conversion obviously indicates reversible adsorption of thiophene.

Adsorption of thiophene on the catalyst surface during the reaction occurs in two stages. The first stage corresponds to irreversible adsorption of thiophene in which the activity is reduced rapidly, and the second stage to reversible adsorption in which the active sites are saturated with thiophene species or the thiophene species on the catalyst surface remains in equilibrium with that in the gas phase (as shown by the constant conversion). In short, in the case of

feed poisoning the poison can be adsorbed by both the modes, irreversible as well as reversible.

The equation presented for the deactivation kinetics is simple in form. The poison concentration, fractional conversion and time of operation are easily obtainable parameters.

As seen earlier the constants of the deactivation equation have two sets of values for two different time intervals ($0 < t < 50$ min and $t > 50$ min). This shows that the activity decay is not uniform throughout the time intervals.

....

NOMENCLATURE

a	Activity of the catalyst
a_o	Initial activity of the catalyst
C_p	Thiophene concentration (ppm)
F	Feed rate of reactant (g mol/hr)
K_A	Adsorption equilibrium constant for aniline (atm^{-1})
k_d	Deactivation constant in Eqn. (5)
k	Reaction rate constant (g mol/hr g cat)
m	Conversion dependency term in equation (5)
n	Thiophene concentration dependency term in equation (5)
p	Time dependency term in equation (5)
p_A	Partial pressure of aniline (atm)
p_{NB}	Partial pressure of nitrobenzene (atm)
r_o	Rate of reaction on unpoisoned catalyst (g mol/hr g cat)
r_t	Rate of reaction at time t on poisoned catalyst (g mol/hr g cat)
T	Absolute temperature (°K)
t	Time (min)
W	Weight of the catalyst (g)
x	Fractional conversion

REFERENCES

1. Andersen R.B., Whitehouse, A.M.
Ind. Eng. Chem., 53, 1011 (1961)

2. Almauist, J.A., Blank, C.A.,
J. Am. Chem. Soc. 48, 2814 (1926)

3. Emmett, P.H. Brunauner, S.,
J. Am. Chem. Soc., 52, 2682 (1930)

4. Gioia, F.,
Ind. Eng. Chem. (Fundl) 10, 204 (1971)

5. Minachev k.h.M., Isagulyants, G.V.,
Proccd. 3rd Int. Cong. Cat., Part I, 309 (1965)

6. Stephen Szepe and O. Levenspiel,
Chem. Rea. Eng., Sept. 265 (1968)

....

CHAPTER 4

USE OF GAS CHROMATOGRAPHY IN STUDYING ADSORPTION

CHAPTER 4

USE OF GAS CHROMATOGRAPHY IN STUDYING ADSORPTION

4.1 INTRODUCTION

Copper chromite catalyst which is extensively used in the hydrogenation of nitrobenzene is known to be poisoned by thiophene. It can be seen from the results presented in Chapter 3 that the adsorption of thiophene (both reversible and irreversible) plays an important role in poisoning the catalyst. It is necessary therefore to study the adsorption behaviour of thiophene on this catalyst.

4.2 METHOD FOR THE MEASUREMENT OF ADSORPTION

4.2.1 Static methods

Volumetric methods: In the commonly used volumetric methods successive doses of the gas to be adsorbed are passed on to the surfaces of the adsorbent. After equilibrium is attained, the pressure of the gas in the dead space is measured by monometer and the quantity of gas adsorbed is then calculated assuming the applicability of the ideal gas law. For this purpose volume of the dead space must be known accurately.

Gravimetric methods: In this method the adsorbent is kept in a closed tube and provision is made for weighing the adsorbent intermittently, either by attaching the adsorbent

tube to a spring or a beam balance or by removing tube and weighing it.

4.2.2 Dynamic methods

Older dynamic methods (2) consisted of passing the pure gas through a bubbler-saturator, and maintaining the partial pressure by admixing the pure gas with the saturated gas. The mixture of the gas was then passed through the adsorption tube immersed in the constant temperature bath. The attainment of the adsorption equilibrium was then checked by removing and weighing the tube intermittently. The method is however laborious and lacks precision. With the recent development in gas liquid chromatography the dynamic methods for measuring the adsorption have become easier and yield results of high accuracy.

4.3 USE OF GAS-LIQUID CHROMATOGRAPHY

Advantages of studying the catalytic properties under conditions close to those of reaction conditions have been emphasized by Heinemann (20). The use of gas liquid chromatography has become handy in the measurement of many of the physico-chemical properties of the solid catalyst (24, 25, 33, 6, 1, 17).

The advantages of the gas chromatographic methods over the static methods are: (1) measurements can be made

rapidly, (2) no vacuum system is required, and (3) the operations can be conducted over a wide range of temperature. Use of gas chromatography in studying the catalysis have been reviewed by Choudhary et al. (5), (7).

4.3.1 Gas chromatographic data

Gas chromatographic data can generally be obtained by three basic techniques: (1) Elution analysis, (2) Frontal analysis and (3) Displacement method.

Elution analysis: In the elution method, the sample is passed over the column along with inert carrier gas. The concentration of sample at the outlet of the column is recorded against time. Distribution of the given component takes place in a constant ratio between gas and immobile phase. At the fixed conditions of temperature and pressure the time of emergence of band is a characteristic of the system. The repeated distribution of the material between two phases give Gaussian-type concentration profile along the column for each component which give rise to the bell-shaped chromatograms.

Frontal analysis: In the frontal analysis, constant flow of sample is introduced into the carrier gas stream. Since the sample flow is continuous, instead of a symmetrical chromatogram an S-shaped front developes. The front breaks through the column only when the entire column is saturated.

This breakthrough is characteristic of the material under study.

Displacement method

In this method the sample is injected into the column and pushed through the column by means of a displacer vapour which is carried at a constant concentration in a stream of carrier gas. The displacer vapour must be more strongly adsorbed than any of the components of mixture. Each component then forms a band of constant concentration along the column and produces a step in the chromatogram.

4.3.2 Nature of adsorption

The pulse technique can be used (18) to detect the occurrence of irreversible adsorption provided the process occurs at such a rate that a measurable number of molecules are adsorbed within the contact time allotted. Eberly Jr.(11) used a mixture of helium and the adsorbate under investigation and every time the area of the chromatogram obtained by passing the mixture through an empty column is compared with that obtained with the packed column to determine the irreversible adsorption. For the detection of reversible adsorption a pulse consisting of argon and adsorbate was injected into the helium stream. Nil adsorption was indicated by the presence of only one recorded pulse, while the occurrence of adsorption was shown by the presence of two peaks. Reversible

adsorption has been studied by this technique for hydrogen on nickel (29) (30), cobalt and copper (32) and on iron (30).

4.3.3 Adsorption isotherms

Adsorption isotherms, isobars and isosters can be calculated from a knowledge of the adsorption behaviour. Many methods have been used to calculate adsorption isotherms.

Gluckauf's method: This is one of the commonest method (16) in which the isotherms are calculated from the shape of the diffused boundary of an elution peak (13), (9) or a desorption curve (18). In this method a continuous stream of adsorbate is introduced into the column until saturation occurs, and the adsorbate is then eluted with a pure carrier gas stream. The adsorption isotherm is then calculated from the shape of the desorption curve (10, 34).

Frontal method: This method (2, 22) involves the determination of the retention volume of a given concentration of sample by the switching the mixture of sample and the carrier gas into an empty column, and measuring the retention volume of the sample front.

Displacement method: In this technique adsorption isotherms of gases on the catalyst can be obtained (21) by altering the nature of the displacer or its concentration. This method is useful only for reversible adsorption.

Peak maxima method: In cases where the retention volumes of the diffused edges are independent of the amount of adsorbate added, the single injection method can be used. When this is not the case, the peak maxima method developed by Kipping and Winter (23) can be used. In this method the isotherm is obtained by injecting a number of samples, measuring their peak-maxima and determining the retention volume for zero concentration by extrapolating the curve down through the maxima of the superimposed peaks.

The pulse-flow method: This technique is useful to measure the adsorption at high temperatures (11). The concentration of the adsorbate in the effluent stream is continuously measured.

4.3.4 Heat of adsorption

Heat of adsorption can be evaluated from a knowledge of retention time and adsorbate temperature (12). Heat of adsorption obtained by the above method has certain limitations. Carberry (4) has pointed out that isotherms can give the heat of adsorption (from retention data) only when the concentration falls in the linear portion of the isotherm i.e. at low surface coverages.

4.4 STUDIES OF ADSORPTION ON COPPER CHROMITE CATALYST

Adsorption of CO and O_2 on copper chromite catalyst has been studied with the help of static methods by Frazer and Albert (14) and Frazer and Heard (15). Rate of adsorption of oxygen was determined in the temperature range 100-200°C, and was found to increase with temperature due to activated adsorption. Adsorption of CO was found to reduce with temperature, except in the neighbourhood of 150°C where there was a sharp maximma. The maxima observed was again due to activated adsorption. Recently adsorption of hydrogen was studied on copper chromite catalyst (8) with the help of dynamic gas-chromatographic method. Both the adsorptions, irreversible as well as reversible were studied in the temperature range 30° - 350°C. The reversible adsorption was found to be an activated process.

4.5 PRESENT STUDY

In the present case adsorption of thiophene has been studied on copper chromite catalyst under reaction conditions (in the temperature range 150° to 300°C and in the presence of hydrogen, which is one of the reactants) using the pulse flow technique. Both the adsorptions, reversible as well as irreversible, have been considered and the isotherms have been obtained from which the heat of adsorption has been calculated.

REFERENCES

1. Arita, K., Kuge, Y., Yoshikawa, Y.,
Bull. Chem. Soc. Japan; 38, 632 (1965)

2. Beebe, R.A., Evans, P.L., Klinstenber, T.C.W.,
J. Phy. Chem., 70, 1009 (1966)

3. Brunaner, S.,
'Physical adsorption of gases and vapours',
p. 36, Oxford University Press (1942)

4. Carberry, J.J.,
Nature, 189, 391 (1961)

5. Choudhary, V.R., Doraiswamy, L.K.,
Ind. Eng. Chem. (Prod. R.D.), 10, 218 (1971)

6. Choudhary, V.R., Menon, P.G.,
J. Chromatogr; 116, 431 (1976)

7. Choudhary, V.R., Parande, M.G.,
Chem. Eng. Commun., 3, 21-27, (1979)

8. Choudhary, V.R., Srinivasan, K.R.,
J. Chromatogr, 148, 373 (1978)

9. Cremer, E., Huber, H.F.,
Angewchem., 73, 461 (1961)

10. de, Vault D.,
J. Am. Chem. Soc., 65, 532 (1943)

11. Eberly, P.E., Jr.,
J. Phys. Chem., 65, 68 (1961)

12. Eberly, P.E., Jr., Spencer, E.M.,
Trans. Far. Soc., 56, 289 (1961)

...

13. Faucher, J.A. Jr., Southworth, R.W., Thomas, H.C.,
J. Chem. Phys. 20, 157 (1952)

14. Frazer, J.C.W., Albert, C.C.,
J. Phys. Chem. 40, 101 (1936)

15. Frazer, J.C.W., Meard, L.,
J. Phys. Chem. 42, 855 (1938)

16. Gluckaur, E.,
Nature, 156, 748 (1945)

17. Greens, A., Pust, H.,
J. Phys. Chem. 62, 55 (1958)

18. Gregg, S.J., Stock, R.,
'Gas Chromatography' Desty, D.M. Ed.
Butterworths, London, p. 90 (1958)

19. Haley, A.J.,
J. Appl. Chem. 13, 392 (1963)

20. Heinemann, H.,
Int. Cong. Cat. Paris, France, July 4-9 (1960)

21. James, D.H., Phillips, C.S.G.,
J. Chem. Soc., 1066 (1954)

22. Keulemans, A.J.M.,
'Gas Chromatography', 2nd Ed.,
Reinhold, New York, N.Y. (1959)

23. Kipping, P.J., Winter, D.G.,
Nature, 205, 1002 (1965)

24. Kobayashi, R., Chappelear, P.S., Deans, H.A.,
Ind. Eng. Chem. 59, 63 (1967)

25. Littlewood, A.B., Phillips, C.S.G., Price, D.T.,
J. Chem. Soc., 148 (1955)

....

26. Nelsen, F.M., Eggertsen, F.T.,
Analyt. Chem. 30, 1387 (1958)

27. Owens, D.R., Hamlin, A.C., Phillips, T.R.,
Nature, 201, 901 (1964)

28. Ozaki, A., Kimura, T., Motohashi, M.,
J. Chem. Soc., Japan, 88, 834 (1967)

29. Ozaki, A., Nozaki, F., Maruya, K., Ogasawara, S.,
J. Catal, 7, 234 (1967)

30. Ozaki, A., Shigehara, Y.,
ibid, 8, 41 (1967)

31. Roth, J.F., Ellwood, R.J.,
Analyt. Chem. 31, 1738 (1959)

32. Shigehara, Y., Ozaki, A.,
J. Chem. Soc. Japan, 88, 844 (1967)

33. White, D., Cowan, C.T.,
Tran. Far. Soc., 54, 557 (1958)

34. Wilson, J.N.,
J. Am. Chem. Soc., 62, 1583 (1940)

.....

CHAPTER 5

ADSORPTION OF THIOPHENE ON COPPER CHROMITE CATALYST

CHAPTER 5

ADSORPTION OF THIOPHENE ON COPPER CHROMITE CATALYST

5.1 STUDIES IN ADSORPTION OF THIOPHENE

Many people have reported the adsorption of thiophene on various catalysts with different techniques for adsorption measurements. Most of the thiophene adsorption studies include the adsorption of thiophene during hydrodesulphurization reaction (20, 19) on sulphided catalysts such as chromia and supported cobalt molybdenum catalysts. The adsorption has been studied along with the reactant and products of reaction. The adsorption of thiophene has been studied on Ni-Al_2O_3 catalyst (18) and the adsorption-desorption isotherms have also been evaluated. Studies of adsorption of thiophene on silica gel, alumina gel and zeolites have also been carried out under static conditions (8). Improved volumetric adsorption systems have been used to investigate the adsorption isotherms on graphite (7). Infra red spectroscopy has been used (17) to study the thiophene adsorption on Al_2O_3 and zeolite.

In the present case, adsorption of thiophene on copper chromite catalyst has been investigated.

5.2 EXPERIMENTAL

5.2.1 Experimental set-up

The chromatographic adsorption data were collected using an NCL-AMIL dual column gas chromatograph equipped with a flame isonization detector after suitably modifying the instrument. The experimental arrangement is shown in Fig. 5.1. The carrier gas flow rate and the pressure drop across the catalyst column were measured with a calibrated capillary flow meter and two mercury manometers as shown in Fig. 5.1. Glass rods were introduced into the column connections in order to minimize the dead space in them. A two way stop cock was used to introduce the carrier gas either through empty capillary column or through the catalyst column. A Hamilton microliter syringe was used to inject accurate quantities of thiophene into the column.

5.2.2 Detector response

Experiments were carried out to test the linearity of the detector response with respect to the sample size. Varying amounts of thiophene (1 to 10 μl) were injected using Hamilton microliter syringe and their chromatograms were recorded. The plot of peak area vs. amount of thiophene injected was found to be linear (Fig. 5.2).

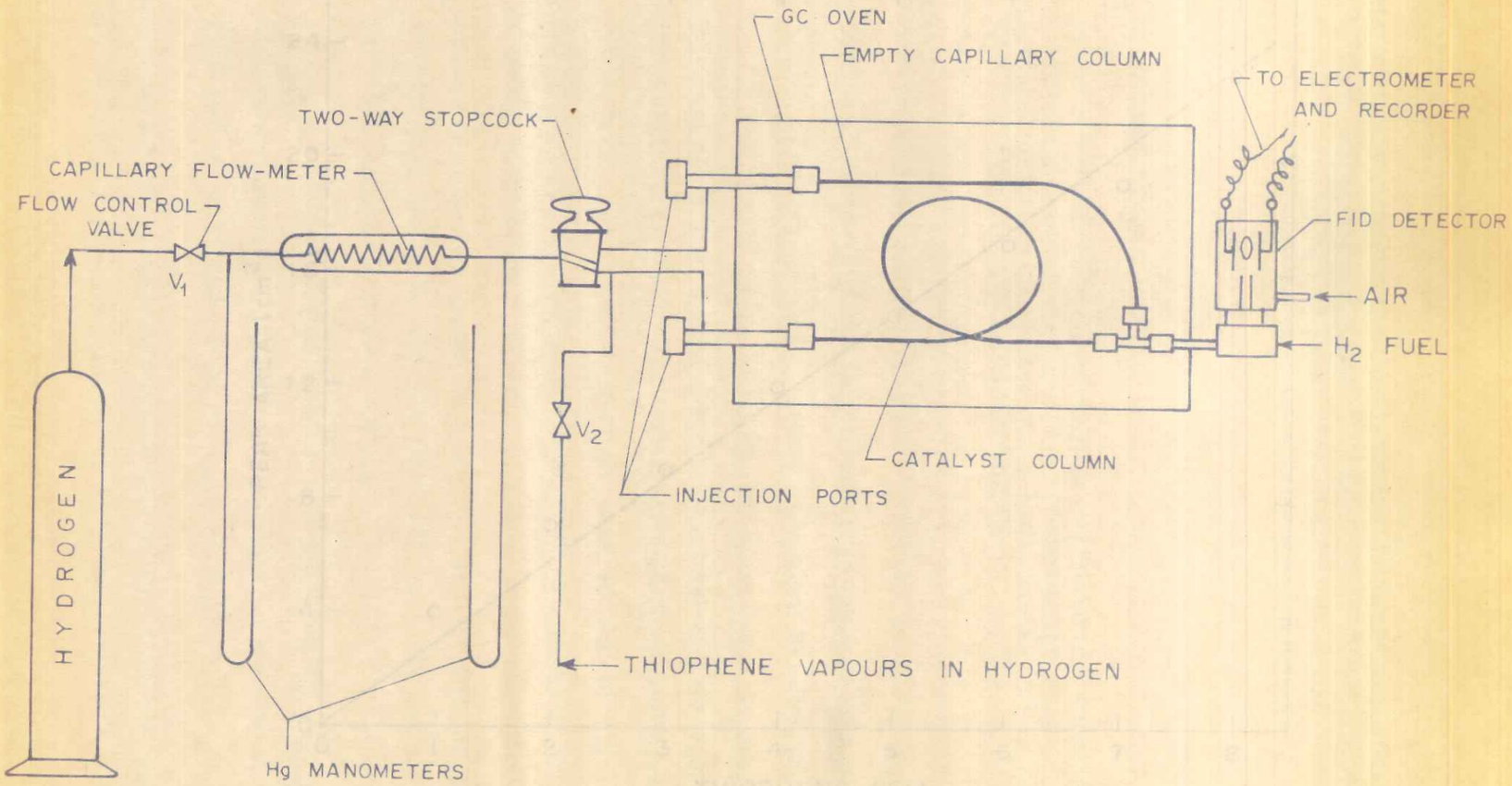

FIG. 5.1. EXPERIMENTAL SET-UP FOR ADSORPTION STUDIES

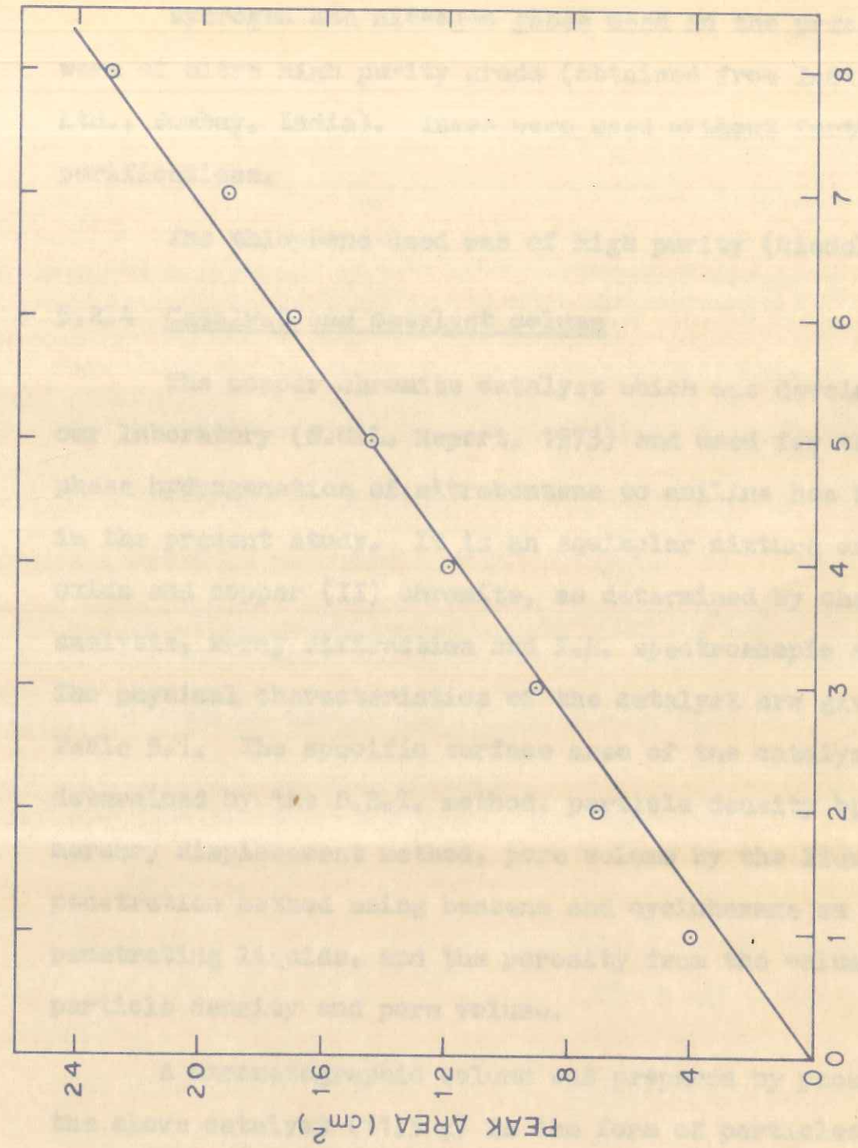

FIGURE 5·2: DETECTOR RESPONSE

5.2.3 Gases and chemicals

Hydrogen and nitrogen gases used in the present study were of ultra high purity grade (obtained from Indian Oxygen Ltd., Bombay, India). These were used without further purifications.

The thiophene used was of high purity (Riedel) grade.

5.2.4 Catalyst and catalyst column

The copper chromite catalyst which was developed in our laboratory (N.C.L. Report, 1975) and used for the vapour phase hydrogenation of nitrobenzene to aniline has been used in the present study. It is an equimolar mixture of copper oxide and copper (II) chromite, as determined by chemical analysis, x-ray diffraction and I.R. spectroscopic studies. The physical characteristics of the catalyst are given in Table 5.1. The specific surface area of the catalyst was determined by the B.E.T. method, particle density by the mercury displacement method, pore volume by the liquid penetration method using benzene and cyclohexane as the penetrating liquids, and the porosity from the values of particle density and pore volume.

A chromatographic column was prepared by packing the above catalyst (11.5 g) in the form of particles (size 0.34 mm) in a stainless steel tube of 6.0 mm O.D.

TABLE 5.1

PROPERTIES OF CATALYST AND CATALYST COLUMN

Catalyst	Copper chromite ($CuO.CuCr_2O_4$)
Particle diameter	av. 0.34 (mm)
Particle density	2.161 (g/c.c)
Particle pore volume	0.293 (c.c/g)
Particle porosity	0.63
Specific surface area of unreduced catalyst	54.0 (m^2/g)
Length of the packed column	60.0 (cm)
Internal cross sectional area of the column	0.212 (cm^2)
Weight of the unreduced catalyst	11.53 (g)
Weight of the reduced catalyst	10.32 (g)
Void fraction of the packed column (F_1)	0.63
Solid fraction of the packed column (F_2)	0.37

5.2.5 Catalyst pretreatment

After connecting the catalyst column to the gas chromatographic unit, the catalyst was reduced by passing a stream of hydrogen, initially at 200°C for 2 hours and then finally at 300°C for 12 hours. Nitrogen was also passed through the column during reduction in order to remove the high heat of reduction. The loss in the catalyst weight due to reduction was about 10.5 wt %. No change in weight was observed when the catalyst was heated further in the stream of hydrogen at 300°C. The reduced catalyst was always kept in an atmosphere of hydrogen by constantly maintaining a positive flow of the gas through the column to prevent its reoxidation.

5.2.6 Experimental procedure

The pulse flow technique was employed to observe the occurrence of irreversible as well as reversible adsorption. Hydrogen gas was used as the carrier (to achieve reaction conditions) as well as the fuel for FID. During the experiments: (i) the elution chromatographic peaks were recorded on a chart until the recorder pen reached the base line, (ii) sufficient time was allowed between two successive pulses for desorption of thiophene adsorbed reversibly during the passage of the first pulse, (iii) the adsorption of thiophene was found to be negligible on the column wall,

(iv) the pressure drop across the column was within 5 to 6% of the outlet pressure, and (v) carrier gas flow rate was maintained about 40 ml/min.

The area under an elution chromatogram was determined by cutting and weighing the chromatogram.

Irreversible adsorption

Test of irreversibility: In order to test the occurrence of irreversible adsorption of thiophene on the catalyst, thiophene pulses were injected through the catalyst column as well as through the empty column under identical experimental conditions. A comparison of the area under the resulting elution peaks revealed whether irreversible adsorption had taken place or not.

Measurement of irreversible adsorption: In order to determine the amount of irreversibly adsorbed thiophene, the carrier gas flow was switched to position 2 (Fig. 5.1) with the help of a two-way stop cock and the pulse experiments were carried out by injecting 5.0 μl of thiophene into the catalyst column using a Hamilton microliter syringe and recording the elution chromatograms. The area under the peak of the pulse in the absence of catalyst was obtained by directing the carrier gas into the empty column by switching over to position 1 (Fig. 5.1) and injecting same amount of thiophene pulse into the empty column under identical experimental

conditions. Sufficient time was allowed between two successive introductions of pulses. Thiophene pulses were injected into the catalyst column until the area of four peaks in succession remained constant for identical sample size. In all, about 15-20 pulses were required to be injected at each temperature of study.

Reversible adsorption

Before starting the experiments for reversible adsorption, the irreversible adsorption sites on the catalyst surface were saturated with thiophene, by passing the thiophene vapours with the carrier gas for about 3.0 hours at each temperature of study. Saturation of the irreversible adsorption sites was confirmed by comparing the area under the elution peak in presence of catalyst with that obtained in absence of the catalyst.

Measurement of reversible adsorption: Pulses of thiophene varying from 0.1 to 40 μl were injected one after another into the catalyst column and the elution chromatograms were recorded. The reproducibility of the catalyst surface was checked from time to time by injecting the same quantity of thiophene under identical experimental conditions and measuring the pulse retention time.

5.3 RESULTS

Carrier gas rate (F) was corrected to column temperature and pressure drop across it using the expression:

$$F' = F \cdot \frac{T_c}{T_f} \cdot \frac{3}{2} \left\{ \frac{(p_1/p_o)^2 - 1}{(p_1/p_o)^3 - 1} \right\} \qquad (1)$$

5.3.1 Irreversible adsorption

The amount of irreversibly adsorbed thiophene was calculated from the relation:

$$q_i = \frac{V\rho}{W M} \left(\frac{A^* - A}{A^*} \right) \qquad (2)$$

Elution peaks of the successive thiophene pulses obtained on the catalyst at four temperatures of study are presented in Figs. (5.3a, 5.3b, 5.3c and 5.3d). The quantity q_i represents the amount of thiophene which is not eluted from the catalyst column because of the strong bonding between the adsorption sites and the adsorbate, and it therefore represents the irreversible adsorption.

Peak areas of the effluent pulses, amount of irreversibly adsorbed thiophene and pulse numbers are given in Tables (5.2a, 5.2b, 5.2c and 5.2d).

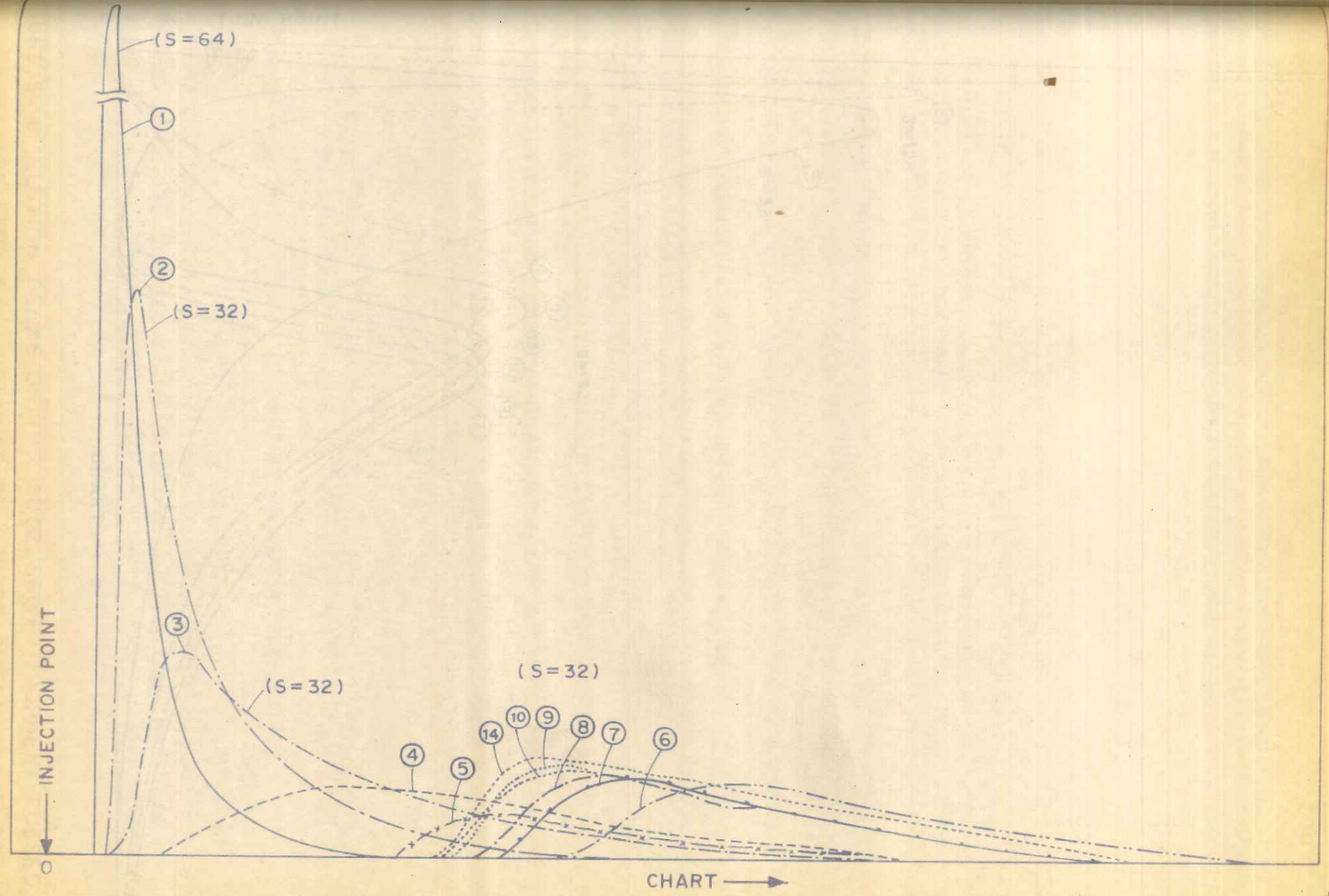

FIGURE 5·3a: ELUTION PEAKS OF THE SUCCESSIVE THIOPHENE PULSES (EACH OF SIZE: 5 μl) OBTAINED ON COPPER CHROMITE AT 150 °C (S = Sensitivity or attenuation)

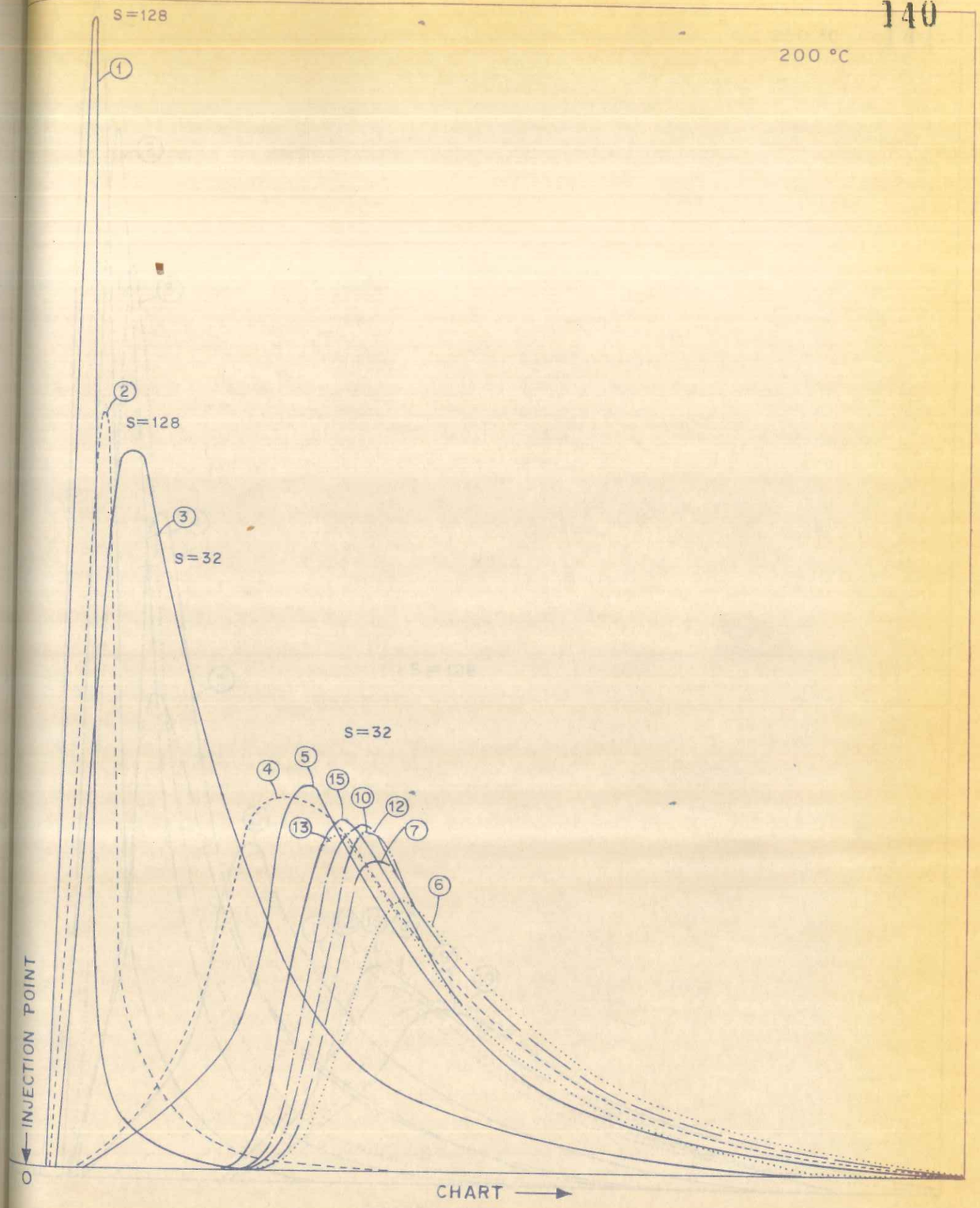

FIGURE 5·3b: ELUTION PEAKS OF THE SUCCESSIVE THIOPHENE PULSES (EACH OF SIZE: 5 µl) OBTAINED ON COPPER CHROMITE AT 200 °C
(S = Sensitivity of attenuation)

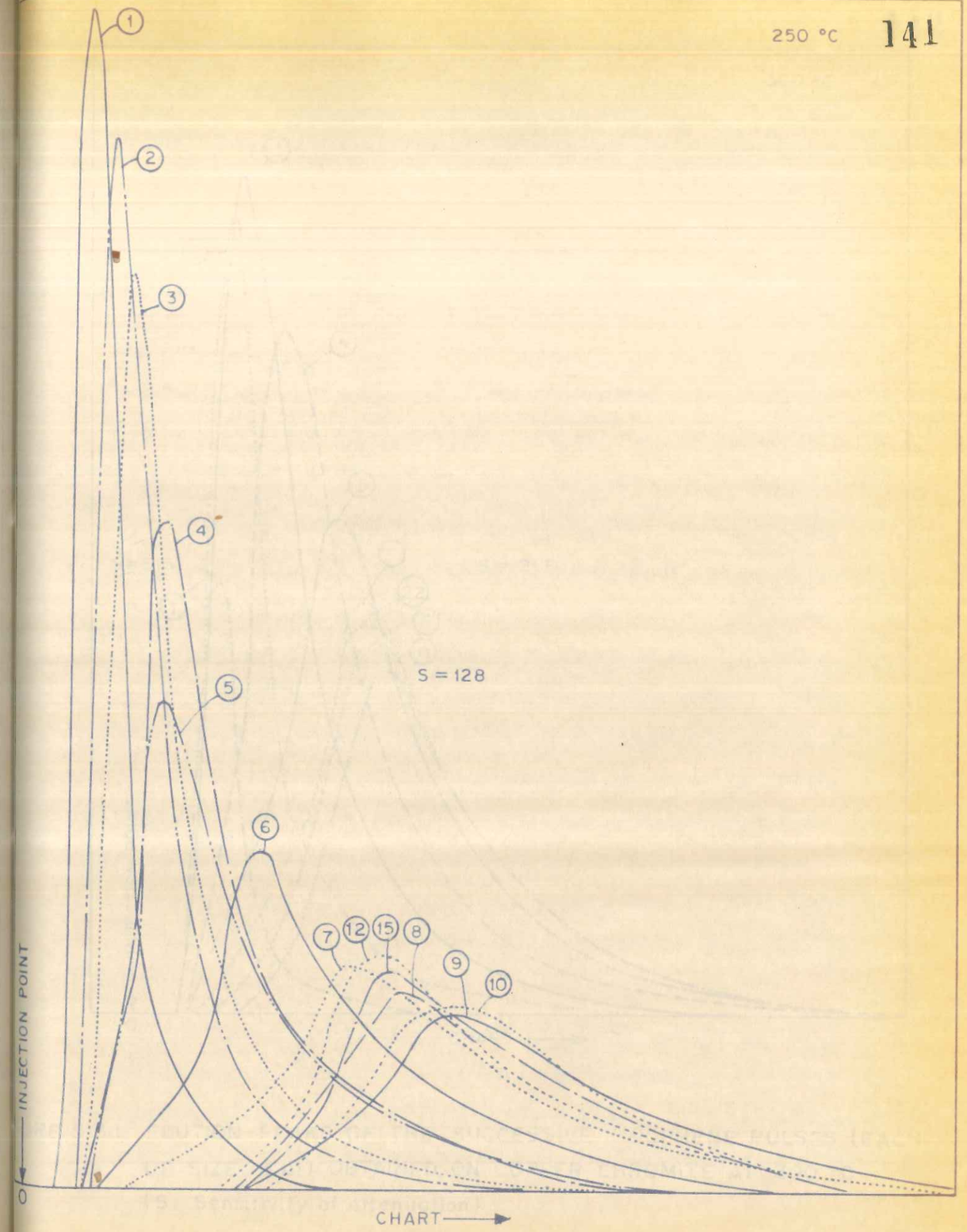

FIGURE 5·3c: ELUTION PEAKS OF THE SUCCESSIVE THIOPHENE PULSES (EACH OF SIZE: 5 μl) OBTAINED ON COPPER CHROMITE AT 250 °C (S = Sensitivity of attenuation)

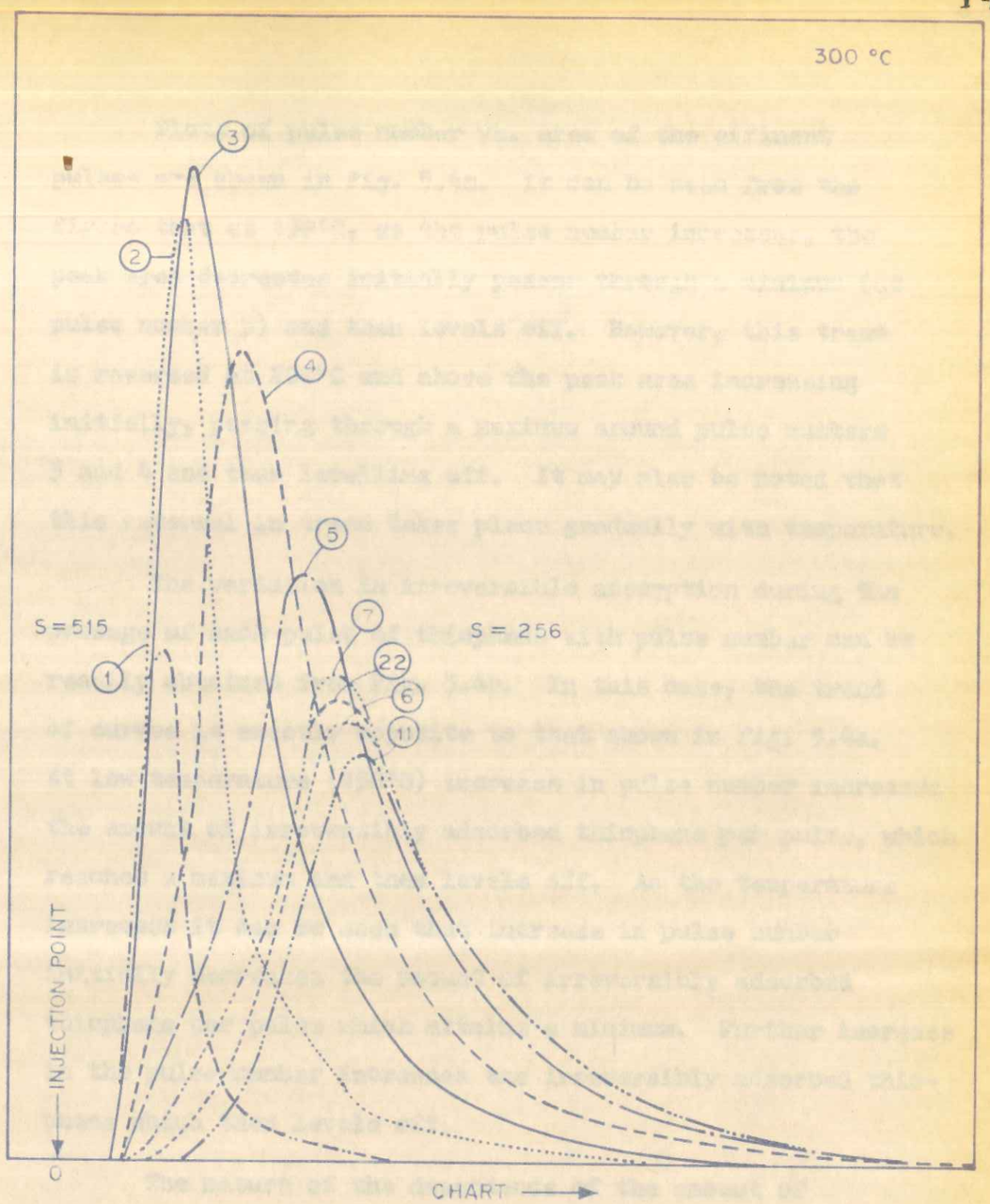

URE 5·3d: ELUTION PEAKS OF THE SUCCESSIVE THIOPHENE PULSES (EACH OF SIZE: 5 μl) OBTAINED ON COPPER CHROMITE AT 300 °C (S Sensitivity of attenuation)

Plots of pulse number vs. area of the effluent pulses are shown in Fig. 5.4a. It can be seen from the figure that at 150°C, as the pulse number increases, the peak area decreases initially passes through a minimum (at pulse number 5) and then levels off. However, this trend is reversed at 200°C and above the peak area increasing initially, passing through a maximum around pulse numbers 3 and 4 and then levelling off. It may also be noted that this reversal in trend takes place gradually with temperature.

The variation in irreversible adsorption during the passage of each pulse of thiophene with pulse number can be readily obtained from Fig. 5.4b. In this case, the trend of curves is exactly opposite to that shown in Fig. 5.4a. At low temperature (150°C) increase in pulse number increases the amount of irreversibly adsorbed thiophene per pulse, which reaches a maximum and then levels off. As the temperature increases it can be seen that increase in pulse number initially decreases the amount of irreversibly adsorbed thiophene per pulse which attains a minimum. Further increase in the pulse number increases the irreversibly adsorbed thiophene which then levels off.

The nature of the dependence of the amount of irreversibly adsorbed thiophene on pulse number (or extent of initial surface coverage) is quite unusual. A previous study (6) involving the adsorption of hydrogen on the same catalyst

TABLE 5.2 (a)

EXPERIMENTAL DATA FOR IRREVERSIBLE ADSORPTION

Temperature 150°C

Hydrogen flow rate (F) = 0.9569 ml/sec (corrected)

P_i = 715 mm P_o = 745 mm Chart speed C = 0.05 cm/sec μ_1(inert) = 18.62 sec

Thiophene sample size = 5.0 μl

Sr. No.	Sensitivity S	Peak area (cm^2)	* A -An (cm^2)	Irreversibly adsorbed Thiophene ($q_i \times 10^6$ (g mol/g)	Initial surface coverage $q_{it} \times 10^6$ (g mol/g)	μ_1 sec	Retention volume (ml/g) $F(\mu_1 - \mu_{(inert)})$ / (ml W/ g)
1	2	3	4	5	6	7	8
1	256	17.68	27.02	2.55	2.55	62.0	3.03
2	64	40.05	138.95	3.56	6.11	100.0	5.68
3	32	66.58	291.42	3.76	9.87	174.0	10.86
4	32	40.11	317.87	4.07	13.94	302.0	19.80
5	32	15.52	342.47	4.43	18.37	406.0	27.07
6	32	36.26	321.74	4.11	22.48	592.0	40.08
7	32	41.16	316.84	4.06	26.54	542.0	36.58
8	32	38.87	319.13	4.09	30.63	504.0	33.93
9	32	39.77	318.23	4.08	34.71	464.0	31.13
10	32	41.25	316.75	4.07	38.78	468.0	31.41
11	32	50.81	307.19	3.94	42.72	494.0	33.23
12	32	55.61	302.39	3.88	46.60	514.0	34.63
13	32	52.12	305.88	3.92	50.52	496.0	33.37
14	32	55.59	302.41	3.88	54.40	498.0	33.51
15	32	56.29	301.71	3.87	58.27	474.0	31.83

...

TABLE 5.2 (b)

EXPERIMENTAL DATA FOR IRREVERSIBLE ADSORPTION

Temperature 200°C

Hydrogen flow rate (F) = 1.0686 ml/sec (corrected)

P_1 = 715 mm P_o = 747 mm Chart speed C = 0.05 cm/sec $\mu_{1(inert)}$ = 16.67 sec

Thiophene sample size = 5.0 μl

1	2	3	4	5	6	7	8
1	256	18.91	27.31	2.75	2.75	28.0	0.88
2	128	38.72	52.28	2.64	5.39	36.0	1.51
3	128	33.88	57.12	2.88	8.27	104.0	6.81
4	64	67.60	114.40	2.89	11.16	234.0	16.95
5	64	47.01	134.94	3.41	14.57	216.0	15.55
6	64	37.16	144.84	3.66	18.23	290.0	21.32
7	32	72.24	291.76	3.68	21.91	272.0	19.92
8	32	73.94	290.06	3.66	25.57	266.0	19.45
9	32	86.56	277.44	3.49	29.06	264.0	19.29
10	32	77.96	286.04	3.61	32.67	262.0	19.14
11	32	78.50	285.50	3.59	36.26	256.0	18.67
12	32	77.06	286.06	3.61	39.87	252.0	18.36
13	32	78.05	285.95	3.61	43.48	254.0	18.51
14	32	78.50	285.50	3.39	47.07	256.0	18.67
15	32	78.80	285.20	3.59	50.65	256.0	18.67
16	32	79.17	284.83	3.59	54.25	256.0	18.67
17	32	78.56	285.44	3.59	57.84	256.0	18.67
							....

TABLE 5.2 (c)

EXPERIMENTAL DATA FOR IRREVERSIBLE ADSORPTION

Temperature 250°C

Hydrogen flow rate (F) = 1.1784 ml/sec (corrected)

P_i = 715 mm P_o = 751 mm Chart speed C = 0.1 cm/sec $t_{1(inert)}$ = 15.12 sec

Thiophene sample size = 5.0 µl

1.	2	3	4	5	6	7	8
1	512	16.24	9.46	1.69	1.69	27	1.02
2	256	44.29	7.21	0.64	2.33	38	1.97
3	256	40.80	10.70	0.96	3.29	41	2.23
4	256	38.81	12.69	1.13	4.42	57	3.60
5	256	37.45	14.05	1.26	5.68	63	4.12
6	128	61.88	41.12	1.83	7.51	85	6.01
7	128	62.03	40.97	1.82	9.33	125	9.45
8	128	54.92	48.08	2.15	11.48	137	10.48
9	128	49.65	53.35	2.38	13.86	141	10.83
10	128	50.70	52.30	2.33	16.19	156	11.09
11	128	50.12	52.88	2.36	18.55	145	11.17
12	128	55.59	47.41	2.11	20.66	127	8.60
13	128	53.40	49.60	2.21	22.87	128	9.71
14	128	50.54	52.46	2.34	25.21	140	10.74
15	128	53.10	49.90	2.23	27.44	139	10.65
16	128	50.88	52.12	2.32	29.76	141	10.83
17	128	52.59	50.41	2.25	32.01	147	11.34
18	128	52.50	50.50	2.25	34.26	143	10.99

...

TABLE 5.2 (d)

EXPERIMENTAL DATA FOR IRREVERSIBLE ADSORPTION

Temperature 300°C

Hydrogen flow rate (F) = 1.2874 ml/sec (corrected)

P_i = 715 mm P_o = 755 mm Chart speed C = 0.1 cm/sec $\mu_{1(inert)}$ = 13.84 sec

Thiophene sample size = 5.0 μl

1	2	3	4	5	6	7	8
1	512	10.58	11.77	2.42	2.42	18	0.39
2	256	29.95	14.75	1.52	3.94	24	0.96
3	256	42.81	1.89	0.19	4.13	29	1.43
4	256	43.98	0.72	0.07	4.21	40	2.46
5	256	39.99	4.71	0.48	4.69	49	3.31
6	256	31.25	13.46	1.38	6.07	56	3.96
7	256	29.87	14.83	1.53	7.59	57	4.06
8	256	32.42	12.28	1.26	8.86	56	3.96
9	256	31.56	13.14	1.35	10.21	57	4.06
10	256	28.69	16.01	1.64	11.85	59	4.25
11	256	28.34	16.36	1.68	13.53	58	4.15
12	256	30.09	14.61	1.50	15.03	58	4.15
13	256	29.44	15.26	1.57	16.59	60	4.34
14	256	25.99	18.71	1.92	18.52	61	4.43
15	256	28.74	15.96	1.64	20.16	60	4.34
16	256	26.84	17.86	1.83	21.99	60	4.34
17	256	28.92	15.78	1.62	23.61	61	4.43
18	256	28.89	15.81	1.62	25.23	61	4.43
19	256	29.26	15.44	1.58	26.81	60	4.34

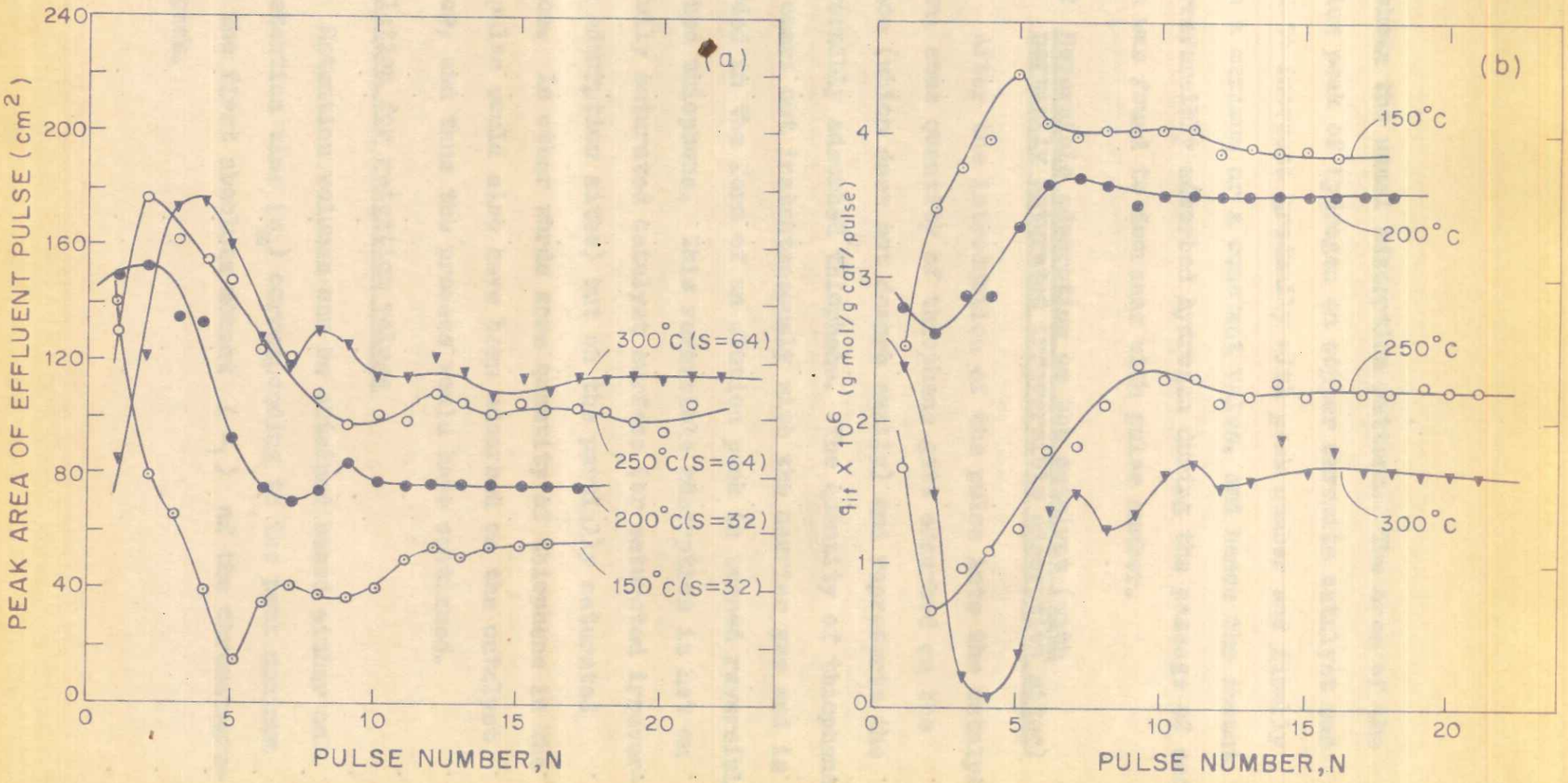

FIGURE 5·4: EFFECT OF INITIAL SURFACE COVERAGE ON THE IRREVERSIBLE ADSORPTION OF THIOPHENE DURING THE PASSAGE OF EACH PULSE

had shown the usual adsorption pattern. The area of the elution peak of hydrogen on copper chromite catalyst was found to increase gradually with peak number and finally reach a maximum or a constant value, and hence the amount of irreversibly adsorbed hydrogen during the passage of each pulse was found to decrease with pulse number.

5.3.2 Reversible adsorption on the catalyst (with partially saturated irreversible adsorption sites)

After the introduction of the pulse into the catalyst column, some quantity of thiophene gets adsorbed on the surface (which does not desorb easily) and represents the irreversibly adsorbed thiophene. The quantity of thiophene that comes out instantaneously with the carrier gas and is recorded in the form of an elution peak is termed reversibly adsorbed thiophene. This reversible adsorption is not on the fully saturated catalyst surface (or saturated irreversible adsorption sites) but on the partially saturated surface. In other words some quantity of thiophene in the next pulse would also have been adsorbed on the catalyst surface, and thus the process would have continued.

Calculation for retention volume

Retention volumes can be obtained based either on the retention time (t_m) corresponding to the peak maximum or on the first absolute moment (μ_1) of the chromatographic peak.

For the symmetrical peaks, the peak maxima method can be used to calculate retention volume, while retention data based on the first absolute moment (μ_1) gives a more correct picture of reversible adsorption (6) for non-symmetrical peaks.

First absolute moment (μ_1)

The chromatographic elution curve is a typical distribution curve which describes the concentration of a species as the number of particles in a certain volume having a given property, i.e. breakthrough time. The moment μ_1 gives the location of the arithmatic mean of distribution curve on the axis of quantitative property. Hence the first absolute moment μ_1 indicates the location of the centroid of the area under the chromatographic curve, which is the position of the mean of the time axis. The property of the centroid of the area under the curve which is the time of breakthrough into the detector, has a definite physical meaning. Breakthough time of the maximum (t_m) is less significant, because it is not possible to give to this point a simple physical interpretation, and it is also influenced by longitudinal diffusion (10). The first absolute moment does not depend upon any kinetic constant, but upon the equilibrium constants of adsorption, and the porosity of the adsorbent.

In the present study, the retention volume calculation is based on the first absolute moment (μ_1) of the chromatographic curve.

The first absolute moment of the chromatographic peak (μ_1) is given by the relation:

$$\mu_1 = m_1/m_o \qquad (3)$$

where

$$m_n = \int_o^\infty t^n C(t)\, dt \qquad (4)$$

C(t) is the concentration or the height of the abcissa at time t.

$$n = 0 \text{ or } 1$$

Hence

$$\mu_1 = \int_o^\infty t\, C(t)\, dt \Big/ \int_o^\infty C(t)\, dt \qquad (5)$$

The integral in the above equation is evaluated from chromatographic data [C (t) vs. t] numerically using the Trapezoidal rule.

The first absolute moment (μ_1) thus calculated includes the moment for the adsorbent (catalyst) as well as the moment for the non-adsorbent (dead spaces) ($\mu_{1(inert)}$). When gas flows through the column it passes through the catalyst as well as the dead spaces between the joints and detector, and through the void speces between the catalyst particles. The absolute moment μ_1 gives the total retention of the gas (through adsorbent and non-adsorbent) in the column. To evaluate the retention due to the dead spaces (non-adsorbent) one has to pass a non-adsorbing gas or inert through the catalyst column and calculate the retention due to non-adsorbent.

In the present study it was not possible to obtain $\mu_{1(inert)}$ experimentally by using inert gas (because of the use of the flame ionization detector), hence values of $\mu_{1(inert)}$ were calculated from the relation (10):

$$\mu_{1(inert)} = \frac{L}{U}\left(1 + \frac{\varepsilon_i}{\varepsilon_e}\right) \qquad (6)$$

The values of retention volume thus calculated, i.e. $[F(\mu_{1(thiophene)} - \mu_{1(inert)})]$, the surface coverage as well as pulse numbers for four temperatures are included in Table (5.2a, 5.2b, 5.2c and 5.2d).

The variation of the retention volume of thiophene, i.e. $[\ F\ (\mu_{1(\text{thiophene})} - \mu_{1(\text{inert})})\ ]$, with pulse number is shown in Fig. 5.5a, and the dependence of the total amount of irreversibly adsorbed thiophene on pulse number are shown in Fig. 5.5b. It can be seen that as the initial surface coverage (due to the irreversible adsorption) increases, the retention volume (which is the measure of the extent of reversible adsorption) increases initially, passes through a maximum (except at 300°C) and then levels off. It is also noticed that the curves show a typical trend which gradually changes with temperature.

Reversible adsorption

After the confirmation of the saturation with respect to the irreversible adsorption sites (as stated earlier), different amounts of thiophene pulses (ranging from .1 to 8 μl) were injected into the catalyst column. The chromatograms were then obtained for four temperatures of study and are given in the Figs. (5.6a, 5.6b, 5.6c and 5.6d).

The retention time (t_m) was calculated by the peak maxima method and the retention time for the inert (t_d) was evaluated by the usual method (10). The experimental data are given in Tables (5.3a, 5.3b, 5.3c and 5.3d).

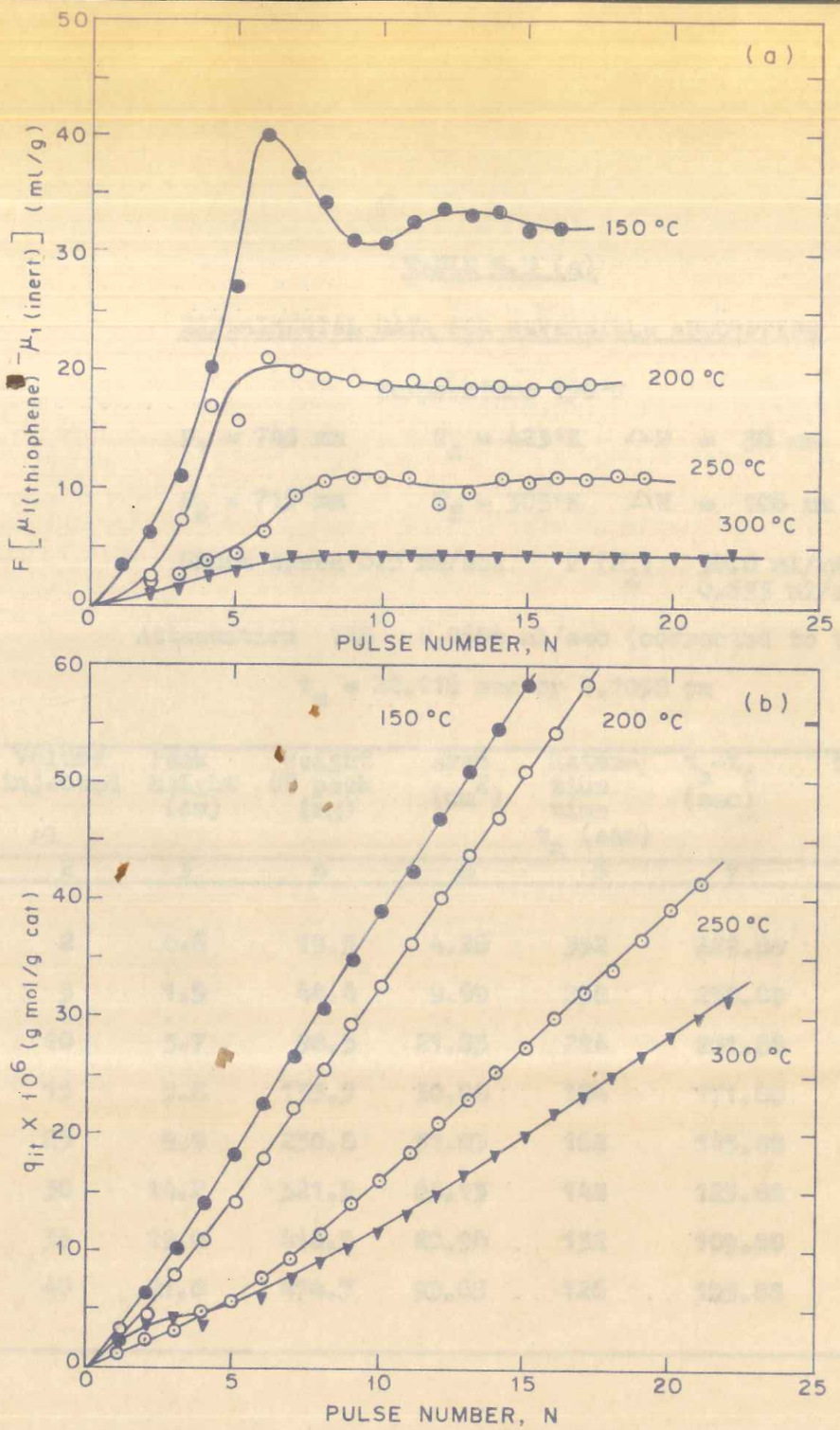

GURE 5·5: EFFECT OF INITIAL SURFACE COVERAGE OF IRREVERSIBLY ADSORBED THIOPHENE ON THE EXTENT OF REVERSIBLE ADSORPTION OF THIOPHENE ON COPPER CHROMITE.

TABLE 5.3 (a)

EXPERIMENTAL DATA FOR REVERSIBLE ADSORPTION

Temperature 150°C

P_1 = 745 mm T_c = 423°K ΔP = 30 mm

P_2 = 715 mm T_f = 303°K ΔH = 106 mm

Chart speed 0.5 mm/sec F (H_2) 38.0 ml/min
0.633 ml/sec

Attenuation 128 0.8654 ml/sec (corrected to t and p)

t_d = 22.116 sec or 1.1058 cm

Sr. No.	Volume injected μl	Peak height (cm)	Weight of peak (mg)	Area (cm^2)	Retention time t_a (sec)	$t_a - t_d$ (sec)	$t_a - t_d$ (cm)
1	2	3	4	5	6	7	8
1	2	0.6	19.5	4.26	352	329.88	16.494
2	5	1.9	44.4	9.69	258	235.88	11.79
3	10	3.7	98.3	21.83	224	201.88	10.09
4	15	5.8	135.5	30.08	194	171.88	8.59
5	25	9.9	230.8	51.03	168	145.88	7.29
6	30	14.2	321.5	63.13	148	125.88	6.29
7	35	19.0	416.5	80.94	132	109.88	5.50
8	40	21.8	474.7	93.65	126	103.88	5.19

TABLE 5.3 (b)

EXPERIMENTAL DATA FOR REVERSIBLE ADSORPTION

Temperature 200°C

P_1 = 747 mm T_c = 473°K ΔP = 32 mm

P_2 = 715 mm T_f = 303°K ΔH = 107 mm

Chart speed 0.5 mm/sec $F(H_2)$ 39.0 ml/min
0.65 ml/sec

Attenuation 128 or 0.9923 ml/sec
(corrected to t and p)

t_d = 19.28 sec or 0.962 cm

1	2	3	4	5	6	7	8
1	5	2.5	37.55	8.14	158	138.72	6.94
2	10	5.5	77.00	15.94	131	111.71	5.59
3	20	12.7	155.95	34.62	92	72.71	3.64
4	30	18.6	231.30	51.14	79	59.72	2.98
5	35	24.2	281.90	61.49	70	50.72	2.54

TABLE 5.3 (c)

EXPERIMENTAL DATA FOR REVERSIBLE ADSORPTION

Temperature 250°C

P_1 = 750 mm T_c = 523°K ΔP = 35 mm

P_2 = 715 mm T_f = 303°K ΔH = 107 mm

Chart speed 0.5 mm/sec $F(H_2)$ 39 ml/min

Attenuation 256 or 0.65 ml/sec

1.095 ml/sec

(corrected to t and p)

t_d = 17.4 sec or 0.874 cm

1	2	3	4	5	6	7	8
1	5	4.10	29.50	6.37	67	49.54	2.48
2	10	7.15	64.60	13.51	62	44.52	2.23
3	12.5	9.20	88.70	18.36	60	42.52	2.13
4	15	11.00	98.00	21.76	58	40.52	2.02
5	17.5	12.50	115.00	25.54	50	32.52	1.63
6	20	13.60	119.50	26.53	46	28.52	1.43

TABLE 5.3 (d)

EXPERIMENTAL DATA FOR REVERSIBLE ADSORPTION

Temperature 300°C

P_1 = 715 mm T_c = 573°K ΔP = 36 mm

P_2 = 715 mm T_f = 303°K ΔH = 107 mm

Chart speed 1.0 mm/sec $F(H_2)$ 39 ml/min

Attenuation 32 0.65 ml/sec or 1.198 ml/sec (corrected to t and p)

t_d = 15.98 sec or 1.598 cm

1	2	3	4	5	6	7	8
1	1	0.2	3.0	0.57	97	81.02	8.10
2	2	1.0	12.2	3.32	82	66.03	6.60
3	3	2.1	32.6	6.67	76	60.02	6.00
4	4	3.5	41.2	10.93	72	56.02	5.60
5	5	5.3	67.4	14.95	66	50.04	5.00
6	6	7.9	97.0	21.53	61	45.03	4.50
7	7	10.6	129.0	28.64	57	41.02	4.10
8	8	13.2	162.1	35.84	54	38.02	3.80
9	9	16.0	191.2	42.15	51	35.02	3.50
10	10	19.25	231.3	50.15	48	32.02	3.20

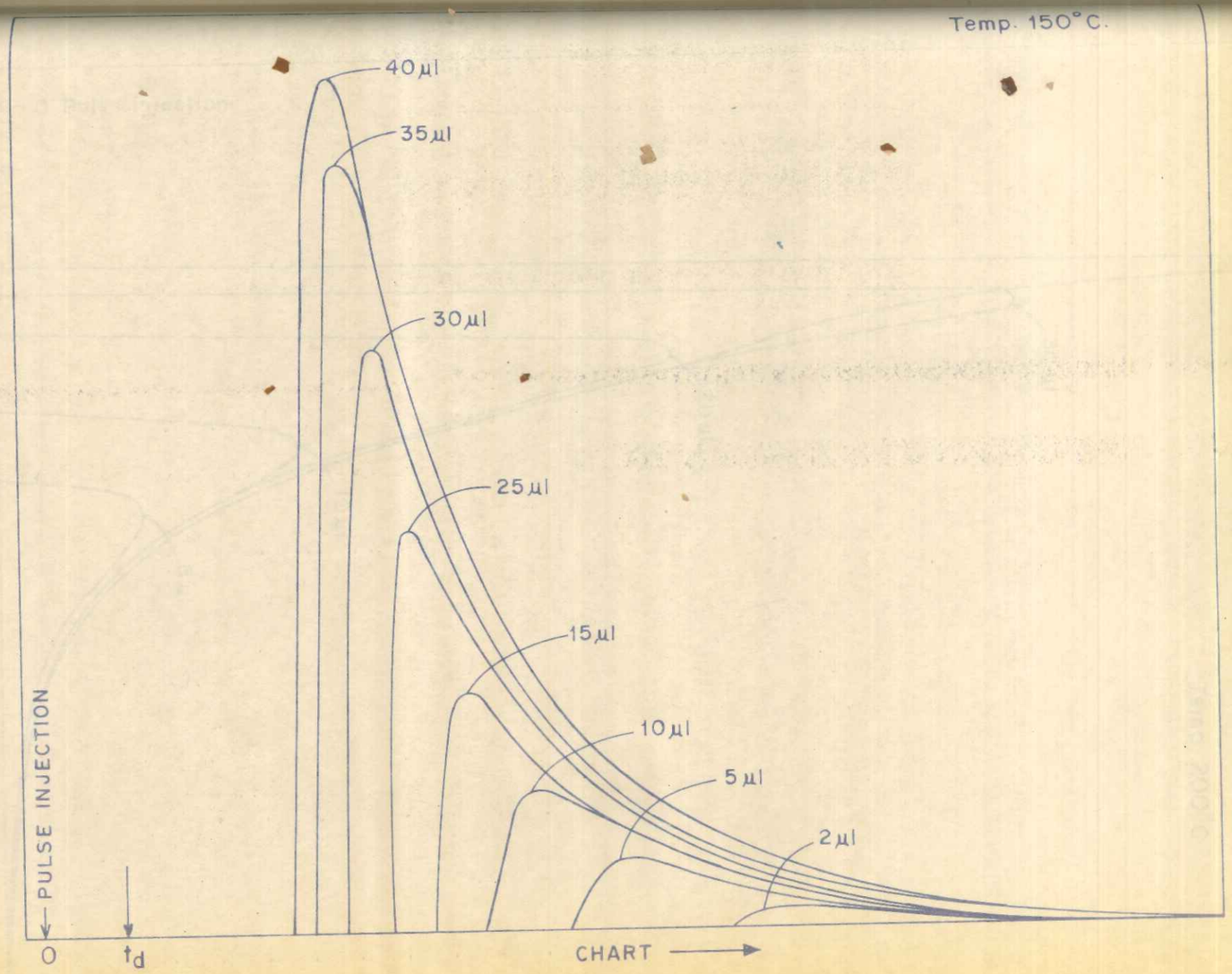

FIGURE 5·6a: ELUTION PEAKS OF PULSES OF THIOPHENE OF VARIABLE SIZES

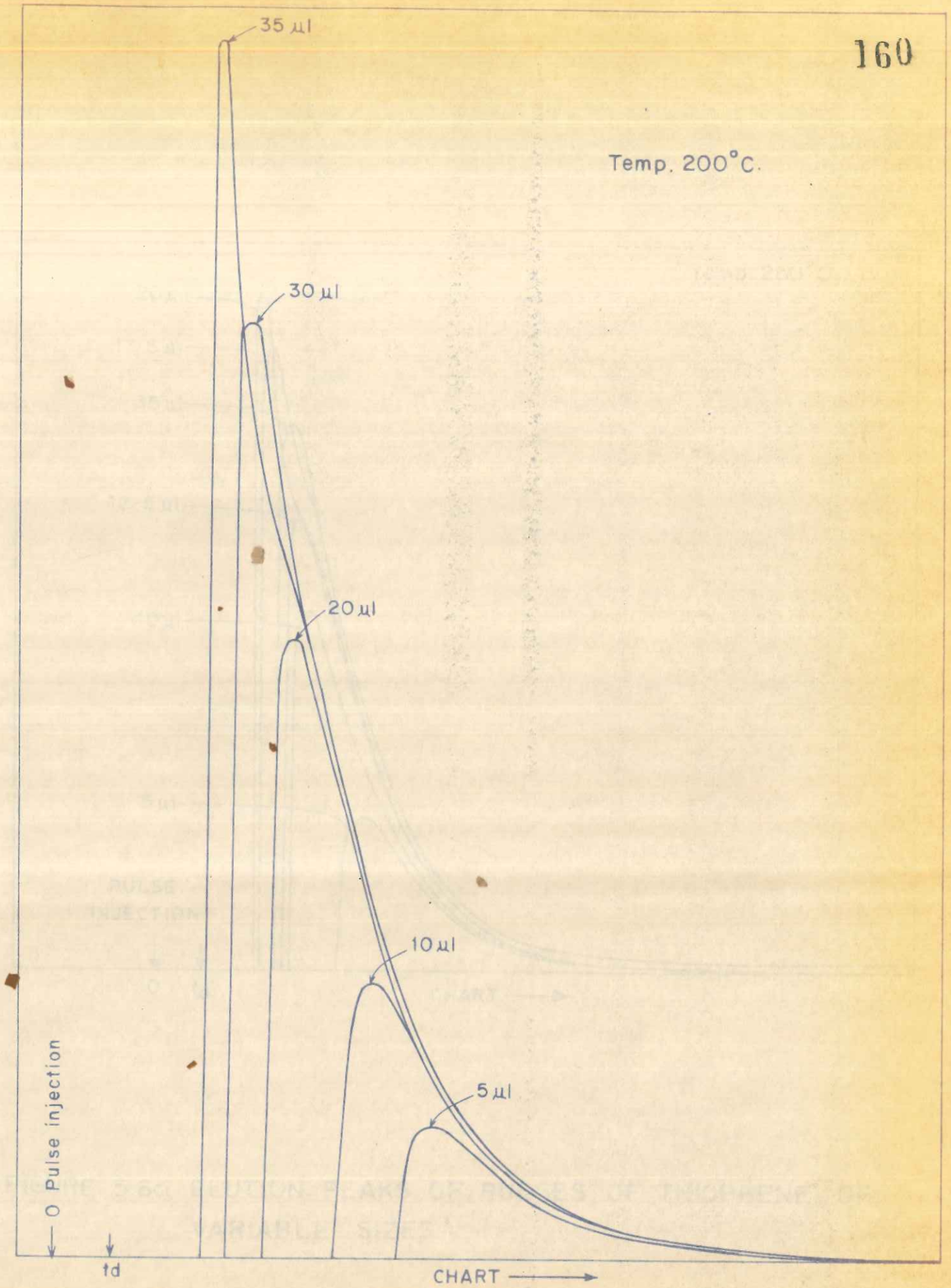

FIGURE 5·6b: ELUTION PEAKS OF PULSES OF THIOPHENE OF VARIABLE SIZES

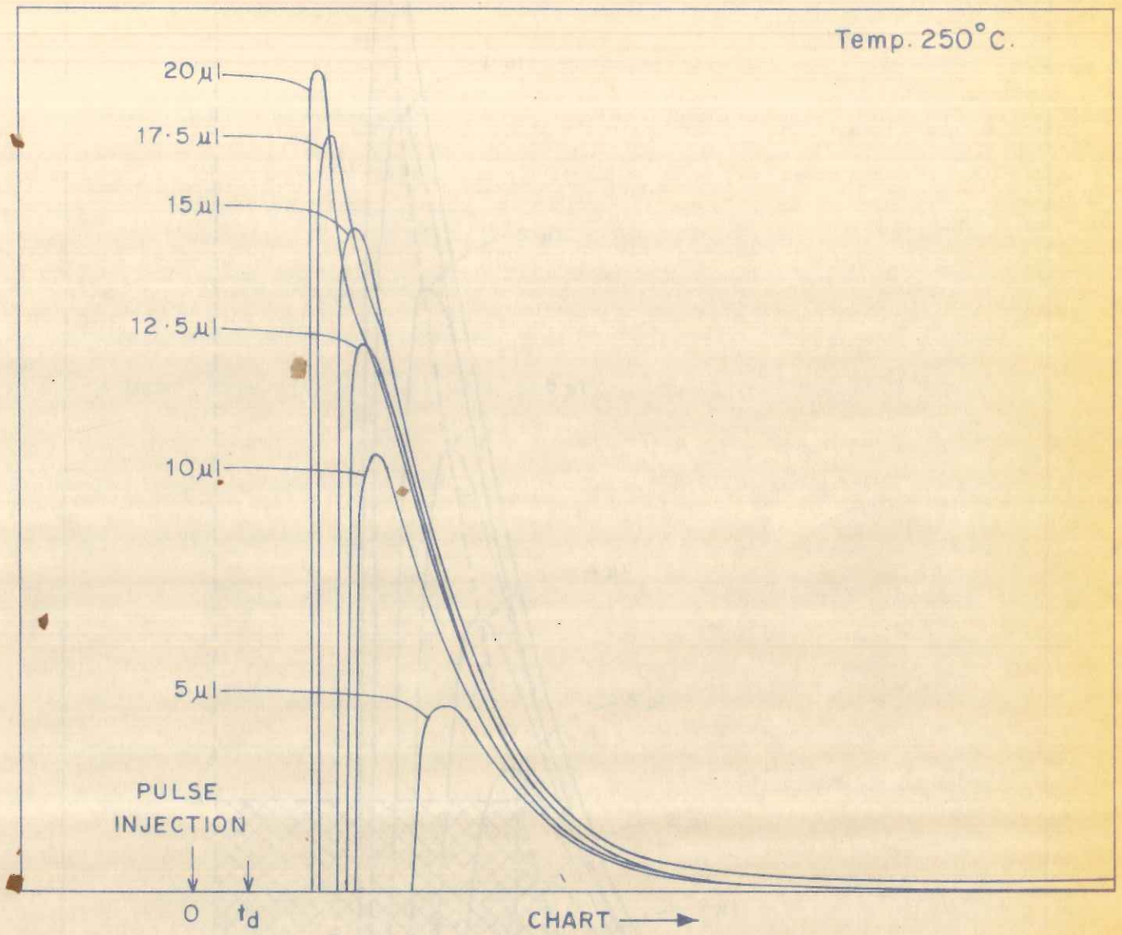

FIGURE 5·6c: ELUTION PEAKS OF PULSES OF THIOPHENE OF VARIABLE SIZES

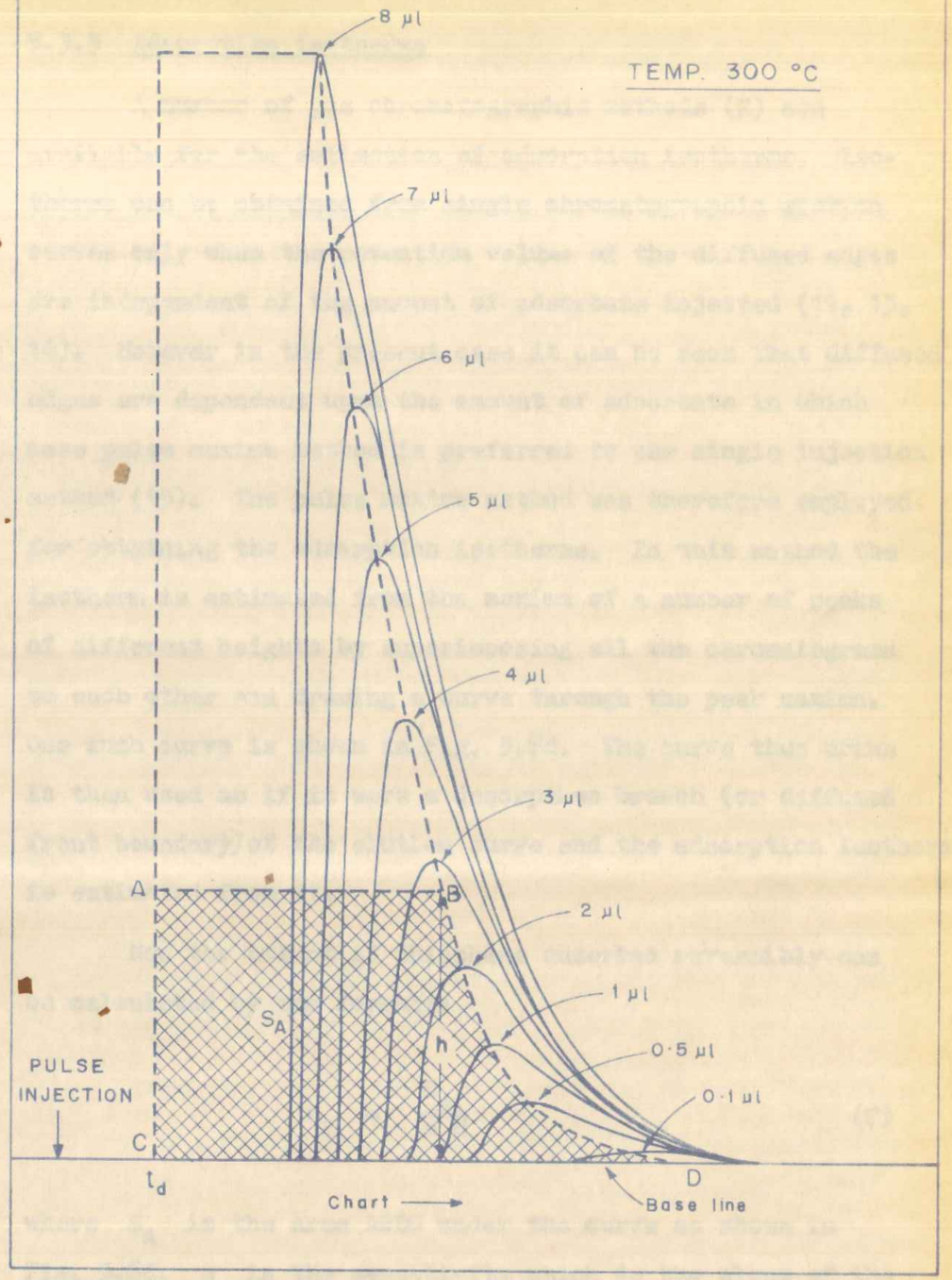

FIG. 5·6d: ELUTION PEAKS OF PULSES OF THIOPHENE OF VARIABLE SIZES

5.3.3 Adsorption isotherms

A number of gas chromatographic methods (2) are available for the estimation of adsorption isotherms. Isotherms can be obtained from single chromatographic elution curves only when the retention volume of the diffused edges are independent of the amount of adsorbate injected (11, 13, 14). However in the present case it can be seen that diffused edges are dependent upon the amount of adsorbate in which case pulse maxima method is preferred to the single injection method (15). The pulse maxima method was therefore employed for obtaining the adsorption isotherms. In this method the isotherm is estimated from the maxima of a number of peaks of different heights by superimposing all the chromatograms on each other and drawing a curve through the peak maxima. One such curve is shown in Fig. 5.6d. The curve thus drawn is then used as if it were a desorption branch (or diffused front boundary) of the elution curve and the adsorption isotherm is estimated from it.

Now the amount of thiophene adsorbed reversibly can be calculated by the formula:

$$q_r = \frac{S_A}{s\,W} \qquad (7)$$

where S_A is the area ABDC under the curve as shown in Fig. 5.6d. s is the sensitivity which is the slope of the

plot peak area vs. amount of thiophene injected and is shown in Fig. 5.7.

The partial pressure (p) of thiophene in the mobile phase is estimated from the relation:

$$p = C R T \qquad (8)$$

where

$$C = \frac{h C}{F s} \qquad (9)$$

hence

$$p = \frac{h C R T}{F s} \qquad (8)$$

or

$$p = 6.236 \times 10^4 \left(\frac{h C T}{F s} \right) \qquad (8)$$

The values thus obtained, i.e. area (S_A) partial pressure of thiophene (p), and amount of reversibly adsorbed (q_r) thiophene for four temperatures of study are tabulated in Tables (5.4a, 5.4b, 5.4c and 5.4d).

From the above tables isotherms are plotted (q_r vs. p) for four temperatures and these plots are shown in Fig. 5.8. The shape of the isotherms suggests that these are of the Freundlich type. Indeed the adsorption data could very well

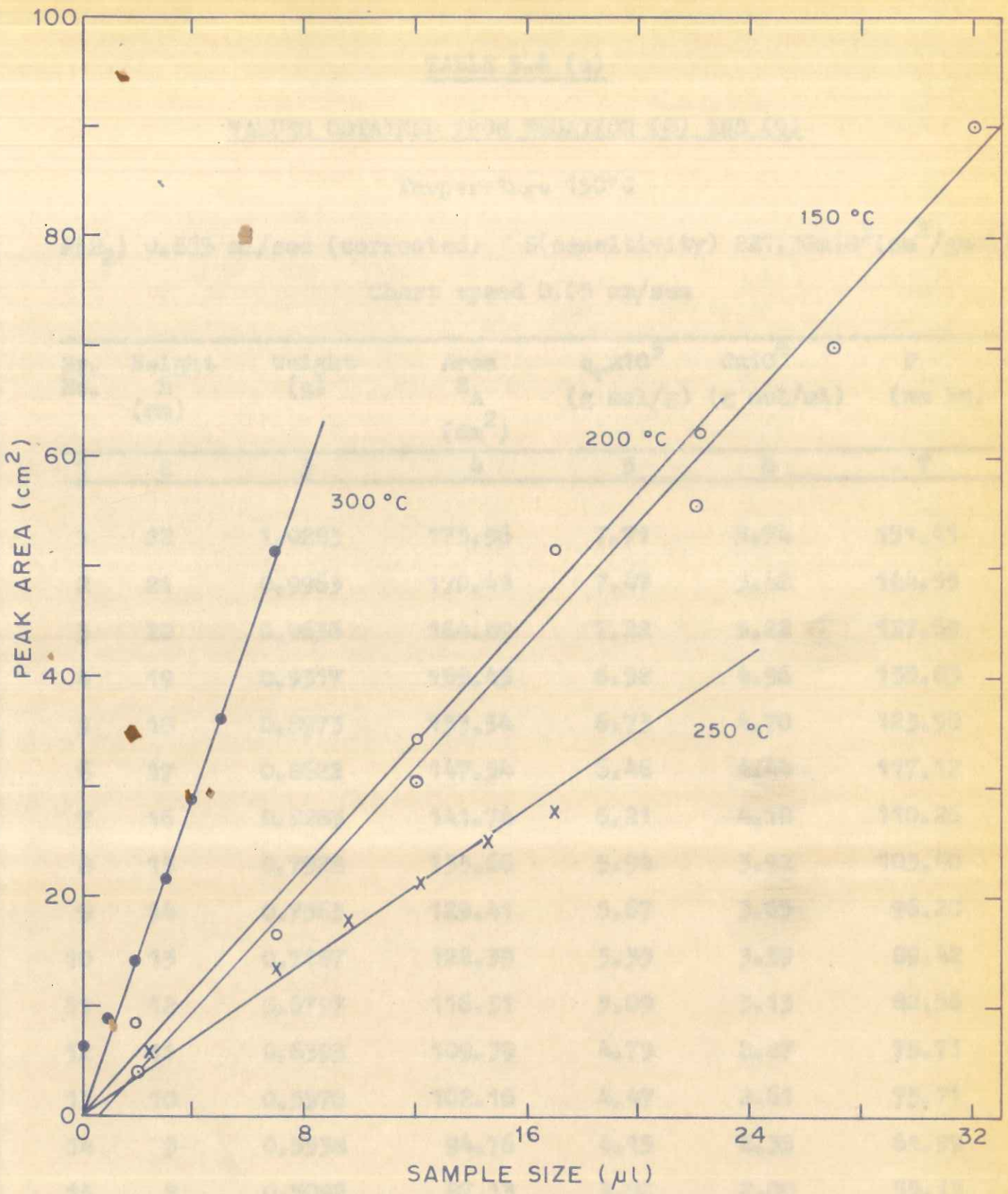

FIGURE 5·7: PLOTS TO DETERMINE SENSITIVITY s IN Eq (7)

TABLE 5.4 (a)

VALUES OBTAINED FROM EQUATION (8) AND (9)

Temperature 150°C

$F(H_2)$ 0.865 ml/sec (corrected) S(sensitivity) $221.30 \times 10^3 (cm^2/gmol)$

Chart speed 0.05 cm/sec

Sr. No.	Height h (cm)	Weight (g)	Area S_A (cm^2)	$q_r \times 10^5$ (g mol/g)	$C \times 10^6$ (g mol/ml)	P (mm Hg)
1	2	3	4	5	6	7
1	22	1.0283	175.96	7.71	5.74	151.41
2	21	0.9963	170.48	7.47	5.48	144.55
3	20	0.9636	164.89	7.22	5.22	137.69
4	19	0.9317	159.43	6.98	4.96	130.83
5	18	0.8973	153.54	6.73	4.70	123.98
6	17	0.8622	147.54	6.46	4.44	117.12
7	16	0.8283	141.74	6.21	4.18	110.26
8	15	0.7928	135.66	5.94	3.92	103.40
9	14	0.7563	129.41	5.67	3.65	96.28
10	13	0.7187	122.39	5.39	3.39	89.42
11	12	0.6797	116.31	5.09	3.13	82.56
12	11	0.6393	109.39	4.79	2.87	75.71
13	10	0.5970	102.16	4.47	2.61	75.71
14	9	0.5538	94.76	4.15	2.35	61.99
15	8	0.5092	87.13	3.82	2.09	55.13
						.....

1	2	3	4	5	6	7
16	7	0.4614	78.95	3.46	1.83	48.27
17	6	0.4127	70.62	3.09	1.57	41.41
18	5	0.3594	61.49	2.69	1.31	34.56
19	4	0.3045	52.10	2.28	1.04	27.43
20	3	0.2450	41.50	1.82	0.78	20.58
21	2.5	0.2113	35.79	1.57	0.65	17.15
22	2	0.1771	28.50	1.25	0.52	13.72
23	1.5	0.1398	22.86	1.00	0.39	10.29
24	1	0.1002	17.13	0.75	0.26	6.86

TABLE 5.4 (b)

VALUES OBTAINED FROM EQUATIONS (8) AND (9)

Temperature 200°C

$F(H_2)$ 0.9923 ml/sec (corrected) S(sensitivity) $227.15 \times 10^3 (cm^2/gmol)$

Chart speed .05 cm/sec

1	2	3	4	5	6	7
1	25	0.6023	103.06	4.40	5.50	162.23
2	24	0.5875	100.53	4.29	5.30	156.33
3	23	0.5726	97.98	4.18	5.08	149.84
4	22	0.5571	95.33	4.07	4.86	143.35
5	21	0.5414	92.64	3.96	4.64	136.86
6	20	0.5256	89.94	3.84	4.42	130.37
7	19	0.5098	87.23	3.72	4.20	123.88
8	18	0.4934	84.43	3.60	3.98	117.39
9	17	0.4762	81.49	3.48	3.76	110.91
10	16	0.4589	78.52	3.35	3.54	104.42
11	15	0.4398	75.26	3.21	3.32	97.33
12	14	0.4201	71.89	3.07	3.09	91.14
13	13	0.4001	68.46	2.92	2.87	84.65
14	12	0.3793	64.90	2.77	2.65	78.17
15	11	0.3571	61.10	2.61	2.43	71.68
16	10	0.3345	57.24	2.44	2.21	65.87
17	9	0.3106	53.15	2.27	1.99	58.69
18	8	0.2846	48.22	2.06	1.77	52.21
						.....

1	2	3	4	5	6	7
19	7	0.2575	43.63	1.86	1.54	45.52
20	6	0.2289	38.78	1.66	1.33	39.23
21	5	0.1970	31.71	1.35	1.10	32.45
22	4	0.1640	26.81	1.14	0.88	25.96
23	3.5	0.1473	24.08	1.03	0.77	22.71
24	3	0.1295	21.71	0.93	0.66	19.47
25	2.5	0.1103	18.49	0.79	0.55	16.22
26	2	0.0914	15.62	0.67	0.44	12.98
27	1.5	0.0709	11.74	0.50	0.33	9.734
28	1.0	0.0490	8.17	0.35	0.22	6.49
29	0.5	0.0260	4.08	0.17	0.11	3.24

TABLE 5.4 (c)

VALUES OBTAINED FROM EQUATIONS (8) AND (9)

Temperature 250°C

$F(H_2)$ 1.0950 ml/sec (corrected) S(sensitivity) 139.39 x 10^3 (cm^2/g mol)

Chart speed .05 ml/sec

1	2	3	4	5	6	7
1	14	0.2280	38.62	2.68	4.58	149.37
2	13	0.2184	37.00	2.57	4.25	138.61
3	12	0.2079	35.22	2.45	3.92	127.85
4	11	0.1959	33.19	2.31	3.59	117.09
5	10	0.1831	31.02	2.16	3.27	106.65
6	9	0.1699	27.34	1.90	2.94	95.89
7	8	0.1570	25.67	1.79	2.62	85.45
8	7	0.1427	23.33	1.62	2.29	74.09
9	6	0.1281	20.95	1.46	1.96	63.92
10	5	0.1130	18.94	1.32	1.64	53.49
11	4.5	0.1052	17.64	1.23	1.47	47.94
12	4	0.0974	16.65	1.16	1.31	42.72
13	3.5	0.0910	15.55	1.08	1.14	37.18
14	3	0.0822	14.05	0.98	0.98	31.96
15	2.5	0.0717	11.87	0.83	0.82	26.74
16	2	0.0609	10.08	0.70	0.65	21.20
17	1.5	0.0475	7.92	0.55	0.49	15.98
18	1	0.0354	5.55	0.39	0.33	10.76
19	.5	0.0180	2.82	0.19	0.16	5.32

TABLE 5.4 (d)

VALUES OBTAINED FROM EQUATIONS (8) AND (9)

Temperature 300°C

$F(H_2)$ 1.198 ml/sec (corrected) S(sensitivity) $571.44 \times 10^3 (cm^2/g\ mol)$

Chart speed 0.1 cm/sec

1	2	3	4	5	6	7
1	20	0.5330	94.63	1.6	2.92	104.34
2	19	0.5343	91.43	1.54	2.77	98.98
3	18	0.5145	88.04	1.49	2.63	93.98
4	17	0.4942	84.57	1.43	2.48	88.62
5	16	0.4732	80.97	1.37	2.34	83.61
6	15	0.4518	77.31	1.31	2.19	78.25
7	14	0.4288	73.37	1.24	2.04	72.89
8	13	0.4057	69.42	1.17	1.90	67.89
9	12	0.3830	64.89	1.09	1.75	62.53
10	11	0.3557	60.26	1.02	1.61	57.53
11	10	0.3297	55.86	0.94	1.46	52.17
12	9	0.3033	51.39	0.87	1.31	46.81
13	8	0.2747	46.54	0.79	1.17	41.81
14	7	0.2478	41.98	0.71	1.02	36.45
15	6	0.2177	36.88	0.62	0.88	31.44
16	5	0.1873	30.14	0.51	0.73	26.08
17	4	0.1552	25.38	0.43	0.58	20.72
18	3.5	0.1383	22.61	0.38	0.51	18.22
						.....

1	2	3	4	5	6	7
19	3	0.1212	20.32	0.34	0.44	15.72
20	2.5	0.1037	17.38	0.29	0.37	13.22
21	2	0.0859	14.68	0.25	0.29	10.36
22	1.5	0.0670	11.09	0.19	0.22	7.86
23	1	0.0470	7.83	0.13	0.15	5.36
24	.5	0.0255	4.00	0.07	0.07	2.51

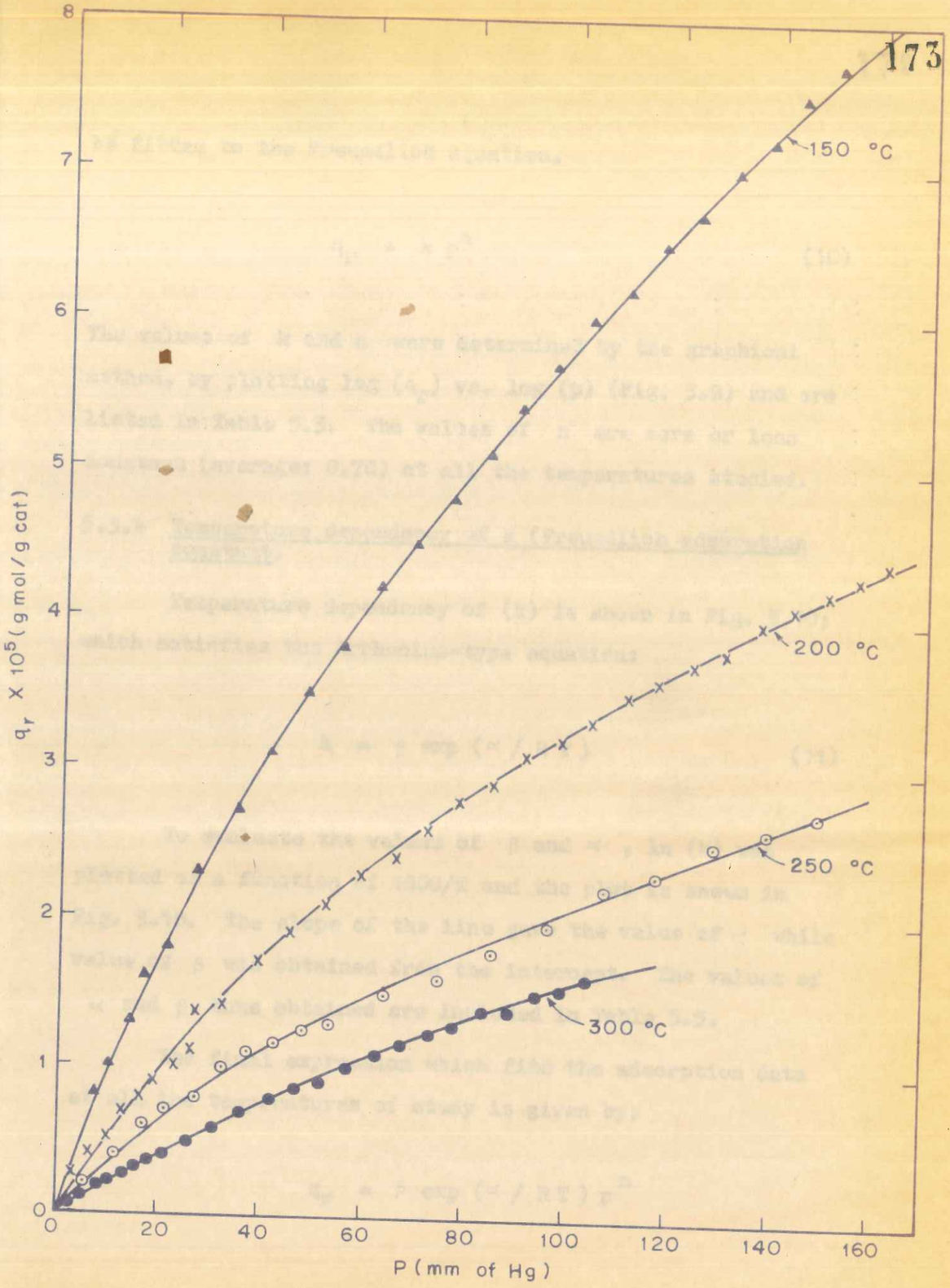

G.5.8: ADSORPTION ISOTHERMS OF THIOPHENE ON COPPER CHROMITE

be fitted to the Freundlich equation,

$$q_r = k\, p^n \qquad (10)$$

The values of k and n were determined by the graphical method, by plotting log (q_r) vs. log (p) (Fig. 5.9) and are listed in Table 5.5. The values of n are more or less constant (average: 0.78) at all the temperatures studied.

5.3.4 Temperature dependency of k (Freundlich adsorption constant)

Temperature dependency of (k) is shown in Fig. 5.10; which satisfies the Arrhenius-type equation:

$$k = \beta \exp(\alpha / RT) \qquad (11)$$

To evaluate the values of β and α, ln (k) was plotted as a function of 1000/T and the plot is shown in Fig. 5.10. The slope of the line gave the value of α while value of β was obtained from the intercept. The values of α and β thus obtained are included in Table 5.5.

The final expression which fits the adsorption data at all the temperatures of study is given by:

$$q_r = \beta \exp(\alpha / RT)\, p^n$$

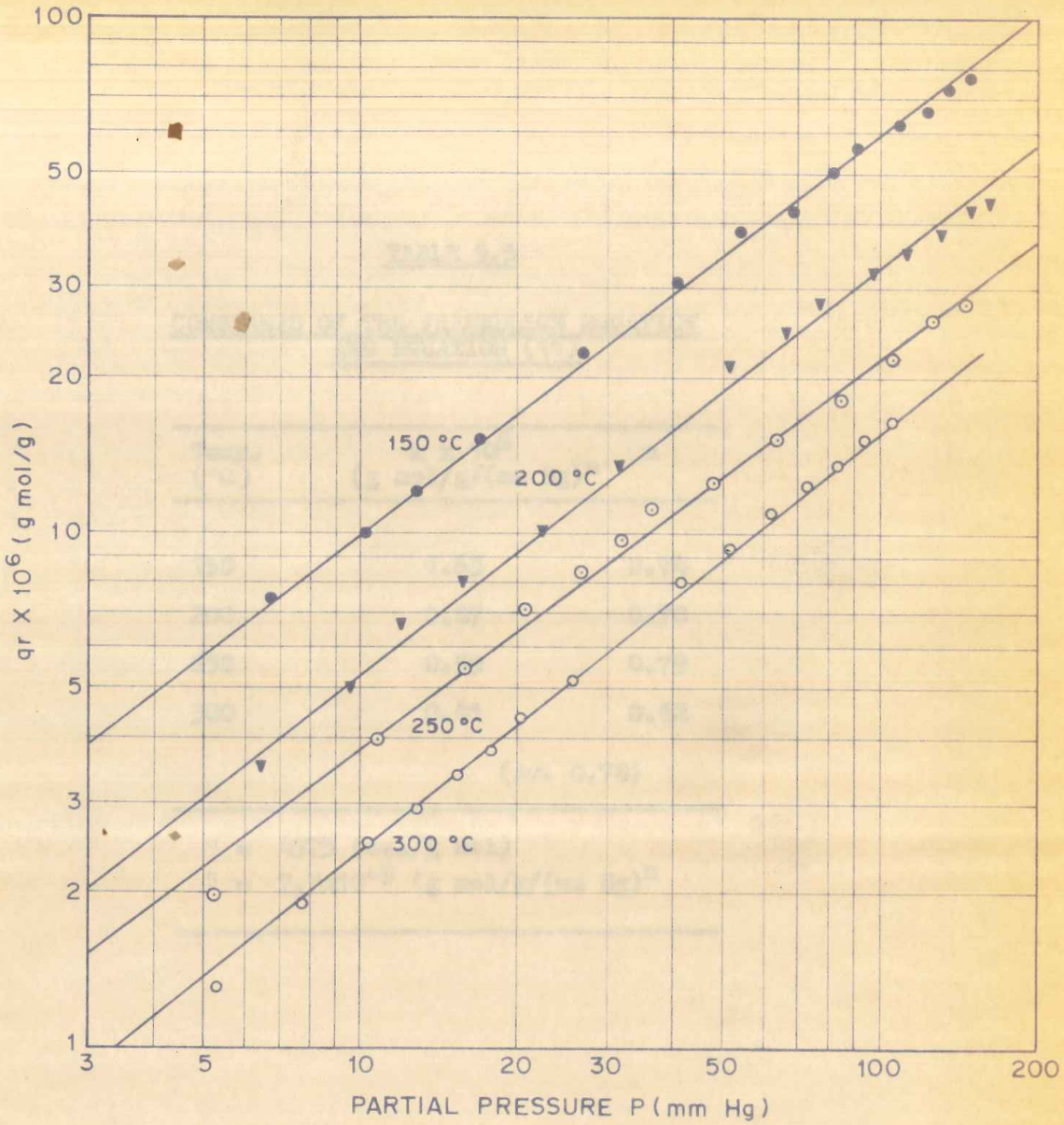

FIGURE 5·9: PLOTS FOR FREUNDLICH Eq. (10)

TABLE 5.5

CONSTANTS OF THE FREUNDLICH EQUATION AND EQUATION (11)

Temp. (°C)	$k \times 10^6$ (g mol/g/(mm Hg)^n	n
150	1.63	0.74
200	0.87	0.78
250	0.59	0.79
300	0.41	0.82
		(Av. 0.78)

α = 4575 (cal/g mol)

$\beta = 7.3 \times 10^{-9}$ (g mol/g/(mm Hg)^n

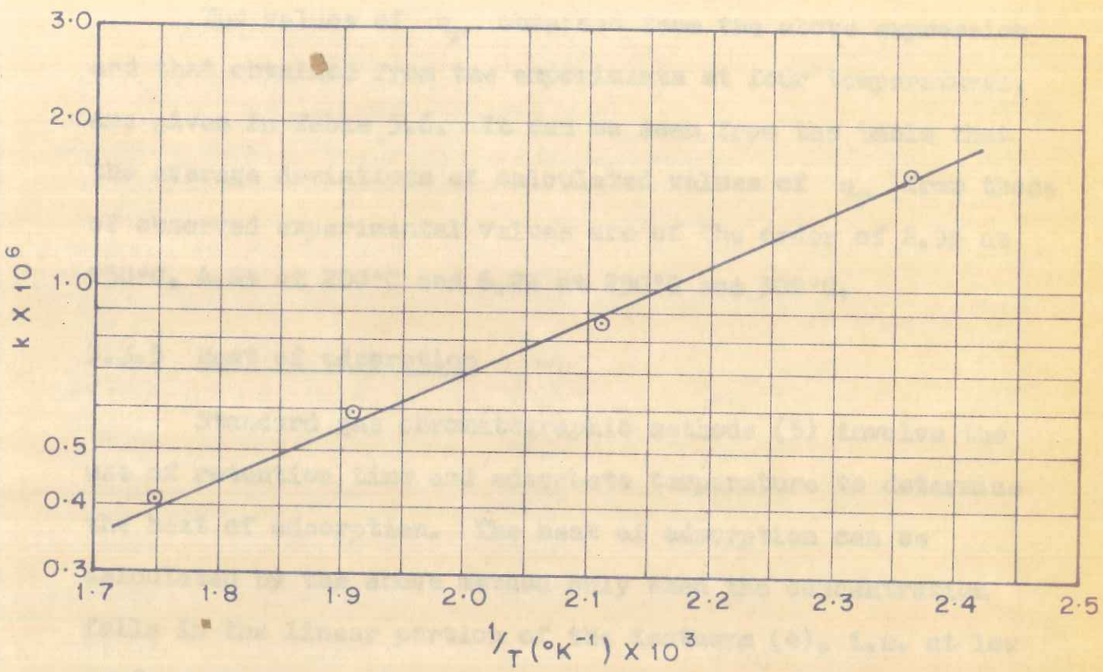

FIG. 5·10: TEMPERATURE DEPENDENCE OF FREUNDLICH ADSORPTION CONSTANT (k)

or

$$= 7.3 \times 10^{-9} \exp (2288/T)\ p^{0.78} \qquad (12)$$

The values of q_r obtained from the above expression and that obtained from the experiments at four temperatures, are given in Table 5.6. It can be seen from the table that the average deviations of calculated values of q_r from those of observed experimental values are of the order of 2.9% at 150°C, 4.8% at 200°C and 6.2% at 250°C and 300°C.

5.3.5 Heat of adsorption

Standard gas chromatographic methods (5) involve the use of retention time and adsorbate temperature to determine the heat of adsorption. The heat of adsorption can be calculated by the above method only when the concentration falls in the linear portion of the isotherm (4), i.e. at low surface coverage. In the present study, it can be seen that the retention time of the effluent pulses is dependent upon the amount of adsorbate injected. This fact, together with the measured adsorption isotherm, indicates that adsorption under chromatographic conditions does not correspond to the linear portion of the adsorption isotherm, which is the essential condition required for the applicability of the gas chromatographic methods in determining the heat of adsorption. Hence the heat of adsorption was calculated from the adsorption isotherm obtained at different temperatures.

TABLE 5.6

COMPARISON BETWEEN OBSERVED AND CALCULATED q_T (FROM EQUATION 12)(g mol/g)

P (mm Hg)	$q_T \times 10^5$ (observed)	$q_T \times 10^5$ (calculated)	$q_T \times 10^5$	% Deviation
1	2	3	4	5
		Temperature 150°C		
151.41	7.71	8.18	-0.46	6.08
137.69	7.22	7.59	-0.37	5.12
123.98	6.73	6.99	-0.26	3.86
110.26	6.21	6.39	-0.18	2.89
96.28	5.67	5.75	-0.08	1.41
82.56	5.09	5.09	0.0	0.12
68.85	4.47	4.42	0.05	1.12
55.13	3.82	3.72	0.10	2.61
41.41	3.09	2.98	0.11	3.56
27.43	2.28	2.16	0.12	5.26
17.15	1.57	1.50	0.07	4.45
13.72	1.25	1.26	0.01	0.80
10.29	1.00	1.00	0.00	0.00
6.86	0.75	0.73	0.02	2.66

Average percent deviation (2.86)

....

1	2	3	4	5
		Temperature 200°C		
162.23	4.40	4.89	-0.49	11.13
149.84	4.18	4.59	-0.41	9.80
130.37	3.84	4.12	-0.28	7.29
110.91	3.48	3.64	-0.16	4.59
97.93	3.21	3.30	-0.09	2.80
78.17	2.77	2.77	0.00	0.00
65.87	2.44	2.43	0.01	0.41
52.21	2.06	2.02	0.04	1.94
32.45	1.35	1.39	-0.04	2.96
22.71	1.03	1.06	-0.03	2.91
16.22	0.79	0.81	-0.02	2.53
12.98	0.67	0.68	-0.01	1.49
9.73	0.50	0.54	-0.04	8.00
6.49	0.35	0.39	-0.04	11.40

Average percent deviation (4.80)

....

1	2	3	4	5
		Temperature 250°C		
149.37	2.68	2.86	-0.18	6.70
127.85	2.45	2.53	-0.08	3.26
106.65	2.16	2.20	-0.04	1.85
85.45	1.79	1.85	-0.06	3.35
63.92	1.46	1.48	-0.02	1.37
47.94	1.23	1.18	0.05	4.06
37.18	1.08	0.97	0.11	10.18
31.96	0.98	0.86	0.12	12.20
26.74	0.83	0.75	0.08	9.63
21.20	0.70	0.63	0.07	10.00
15.98	0.55	0.50	0.04	7.27
10.76	0.39	0.37	0.02	5.12
5.32	0.19	0.21	-0.01	5.10
	Average percent deviation (6.16)			

....

1	2	3	4	5
		Temperature 300°C		
104.34	1.65	1.48	0.17	10.3
93.98	1.49	1.37	0.12	8.05
83.61	1.37	1.25	0.12	8.76
72.89	1.24	1.12	0.12	9.61
62.53	1.09	0.99	0.10	9.17
52.17	0.94	0.87	0.07	7.45
41.81	0.79	0.73	0.06	7.59
26.08	0.51	0.50	0.01	1.96
20.72	0.43	0.42	0.01	2.32
18.22	0.38	0.38	0.0	0.00
15.72	0.34	0.34	0.0	0.00
13.22	0.29	0.30	-0.01	3.45
10.36	0.25	0.24	0.01	4.00
7.86	0.19	0.20	-0.01	5.26
5.36	0.13	0.14	-0.01	7.69
		Average percent deviation (6.24)		

The isosteric heat of adsorption (Q_a) is defined as

$$Q_a = -R \left[\delta(\ln p)/\delta(1/T)\right]_{q_r} \qquad (13)$$

or

$$\log p = C' - \frac{Q_a}{2.3\,R}\left(\frac{1}{T}\right) \qquad (14)$$

log (p) was plotted vs. (1/T) for different surface coverages (ranging from .2 to 4.5×10^{-5} g mol/g cat) as shown in Fig. 5.11. Heats of adsorption were calculated from the slopes and for different surface coverages and are summarised in Table 5.7.

5.3.6 Dependence of heat of adsorption (Q_a) on surface coverage

To study the effect of surface coverage (q_r) on the heat of adsorption (Q_a), surface coverage was plotted vs. heat of adsorption (Fig. 5.12). It can be seen from the figure that as the surface coverages increase, heat of adsorption (Q_a) decreases initially, passes through a minimum at a coverage of about $.6 \times 10^{-5}$ g mol/g cat of thiophene and then increases monotonocally with coverage. In other words, the heat of adsorption (Q_a) is dependent upon surface coverage.

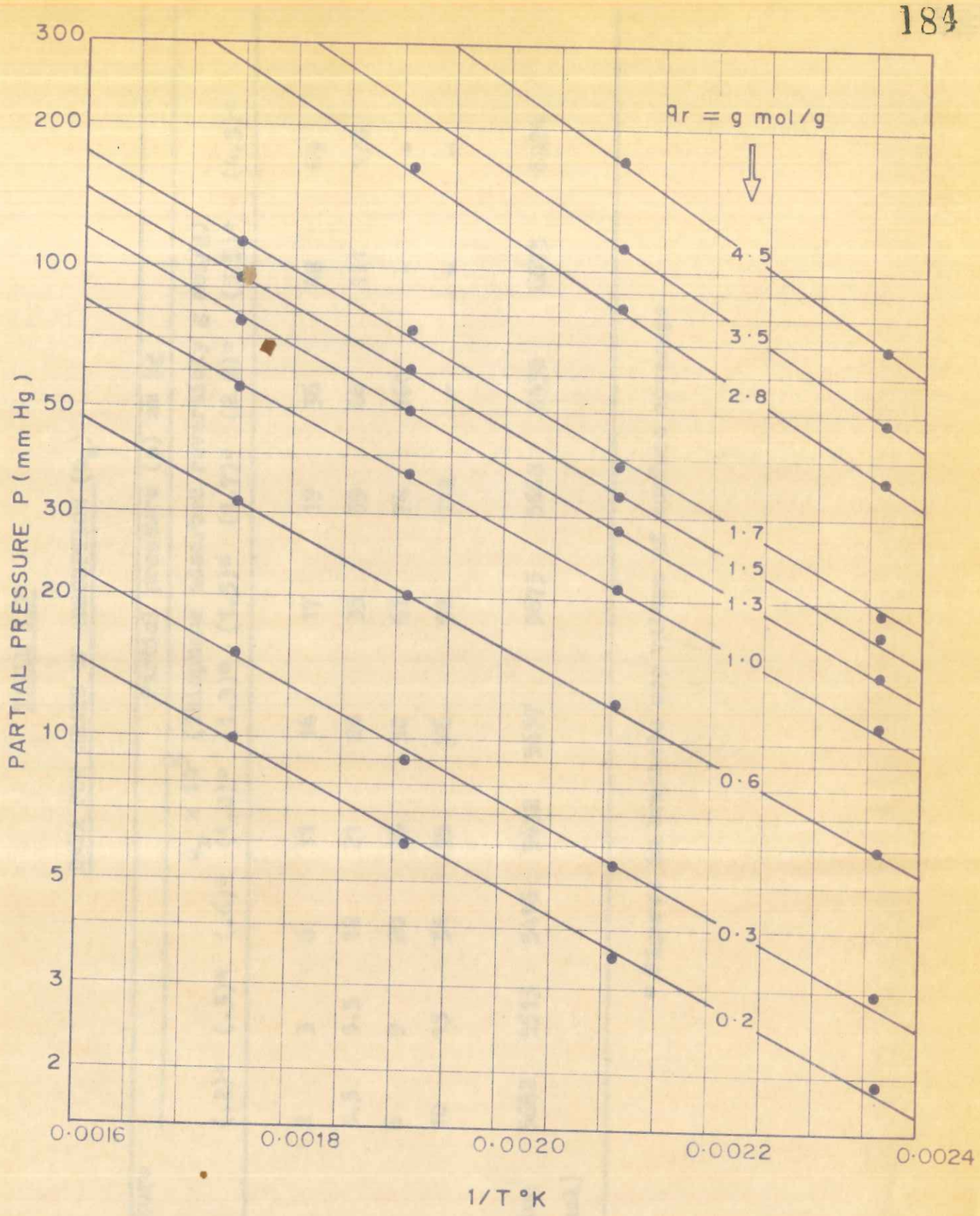

FIGURE 5·11: PLOT FOR EQUATION (14)

TABLE 5.7

DATA FOR HEATS OF ADSORPTION (Q_a)

Temperature °K	Partial pressure (p) mm Hg									
	$q_r \times 10^5$ (Thiophene adsorbed reversibly g mol/g)									
	(.2)*	(.3)*	(.6)*	(1.0)*	(1.3)*	(1.5)*	(1.7)*	(2.8)*	(3.5)*	(4.5)*
423	2	3	6	11	14	17	19	36	48	69
473	3.5	5.5	12	21	28	33	39	66	111	170
523	6	9	20	36	50	61	74	160	-	-
573	10	15	31	55	76	92	112	-	-	-
Heat of adsorption (Q_a) (cal/g mol)	5662	5513	5416	5452	5657	5673	5668	6430	6673	6924

* Figures in brackets are values of surface coverage

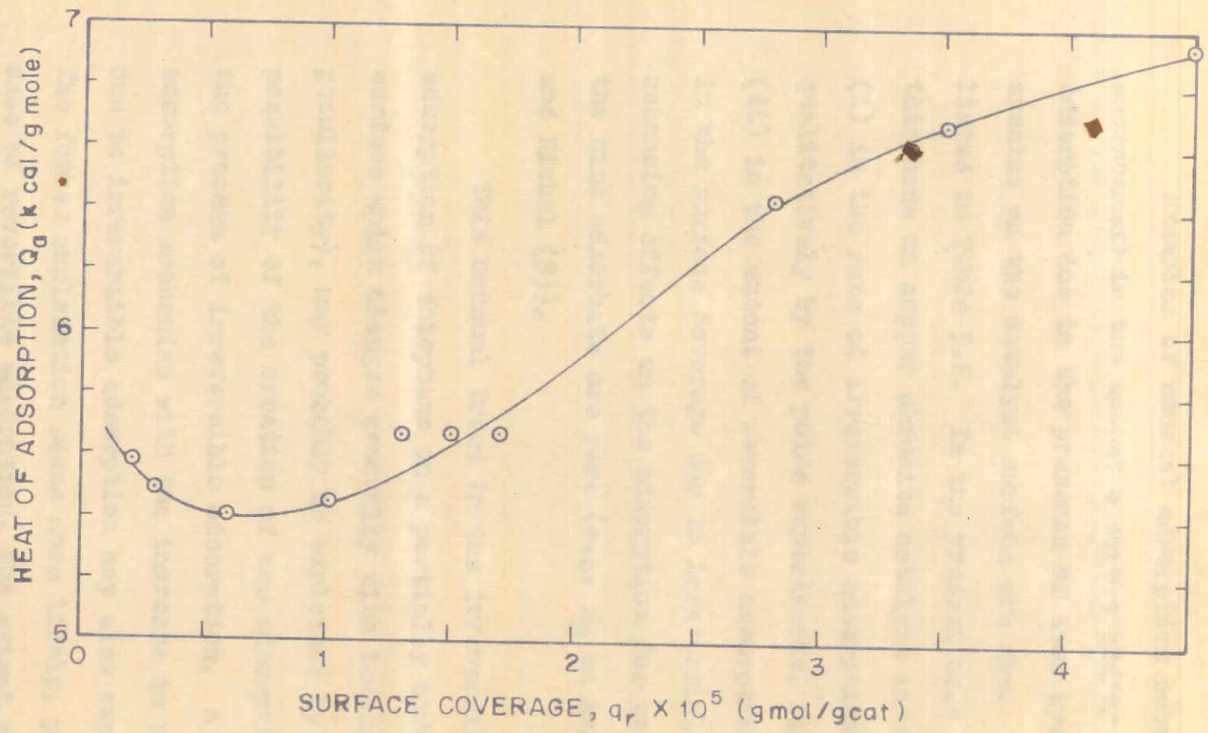

FIG. 5·12: EFFECT OF SURFACE COVERAGE ON HEAT OF ADSORPTION OF THIOPHENE ON COPPER CHROMITE

5.4 DISCUSSION

Examples of unusual adsorption behaviour such as enhancement in the amount adsorbed and/or of the rate of adsorption due to the presence of same species or some other species on the catalyst surface are few. Some of these are listed in Table 5.8. In the present case the adsorption of thiophene on copper chromite catalyst involves an enhancement (i) in the rate of irreversible adsorption (as indicated qualitatively by the pulse experiments, Fig. 5.4b), and (ii) in the extent of reversible adsorption with the increase in the surface coverage due to irreversible adsorption. Such enhancing effects on the adsorption due to the presence of the same adsorbate are rare (e.g. H_2 on iron (3), copper (2) and Nickel (9)).

This unusual trend in the irreversible and reversible adsorption of thiophene on a partially covered catalyst surface which changes gradually with temperature (an additional peculiarity), may probably be explained by considering the possibility of the creation of new adsorption sites during the process of irreversible adsorption. A change in the adsorption mechanism with the increase in surface coverage due to irreversible adsorption may also explain this behavior. The former explanation seems more likely, particularly in the case of reversible adsorption, the extent of which increases

TABLE 5.8

EXAMPLES OF UNUSUAL ADSORPTION BEHAVIOUR

Adsorbate 1	Catalyst 2	Observation 3	Reference 4
H_2	Iron	After rapid initial adsorption, the adsorption rate declined almost to zero within 2-3 hours, remained roughly constant for a further 50 hours, then increased for a further 50 hours and then again declined.	(3)
H_2 and D_2	Copper	Adsorption rate was found to increase with amount adsorbed	(2)
H_2	Nickel	When the catalyst was pretreated with H_2, the initial rate of adsorption of H_2 was found to be enhanced due to pretreatment, but there was decrease in the total adsorption and the ambient adsorption rate.	(9)
H_2	Nickel (with preadsorbed CO)	With an increase in the amount of preadsorbed CO, there was an increase in the rate of initial adsorption of H_2, but the total amounts of adsorption and the ambient adsorption rate of H_2 was decreased.	(12)
H_2	Fischer-Tropsch catalyst (with preadsorbed CO)	The presence of CO on the surface enhanced the adsorption of H_2.	(21)

....

1	2	3	4
H_2	Cobalt (with pre-adsorbed CO)	Total amount of H2 adsorbed was less but the rate of adsorption was found to be faster than that on clean (or untreated with CO) catalyst.	(1)
H_2	$Ru-Al_2O_3$ (with pre-adsorbed CO)	With an increase in the amount of CO on the surface, total amount adsorbed (after 100 min) and rate of adsorption of H_2 was found to be increased, while the initial adsorption rate of H_2 was retarded.	(16)
H_2	$Ru-Al_2O_3$ (with pre-adsorbed O_2)	Due to the presence of pre-adsorbed O_2, the adsorption of H_2 was found to enhanced.	(16)
H_2 + CO (25:1)	Cobalt	The adsorption of the mixture (CO + H_2) was, at first, faster than that of pure H_2.	(1)
H_2 + CO (1:1)	Cobalt	Mutual enhancement in both the rates and the amounts of adsorption was observed.	(22)
Thiophene	Copper chromite	GC pulse experiments indicated an enhancement in the rate of irreversible adsorption and the amounts of reversible adsorption with the increase in surface coverage; a very complex but peculiar trend observed.	Present study

with initial surface coverage. This increase is most probably due to an increase in the number of active sites, involved in the reversible adsorption process. However, it is not possible to give a more satisfactory explanation of this complex trend, which also changes gradually with temperature, both in respect of irreversible and reversible adsorption on the catalyst surface with its partially covered irreversible adsorption sites.

The reversible adsorption of thiophene on copper chromite, with its irreversible sites already saturated with thiophene was found to follow the Freundlich adsorption isotherm. The isosteric heat of adsorption estimated from the adsorption isotherms, showed that it is significantly influenced by surface coverage. The initial decrease in the heat of adsorption (Fig. 5.12) may be due to site heterogeneity, while the continuous increase in its value above a certain surface coverage may be due to the surface heterogeneity induced or caused by interaction between the adsorbed species.

NOMENCLATURE

A	Peak area under elution peak in presence of catalyst (cm^2)
A^*	Peak area under elution peak in absence of catalyst (cm^2)
C (t)	Concentration of adsorbate as a function of time (i.e. height of abcissa at time t)
C'	Constant of Eqn. (9)
F	Volumetric flow rate corrected for column temperature and pressure drop across it (ml/sec)
h	Recorder deflection (cm)
k	Freundlich adsorption constant
L	Length of the packed column (cm)
M	Molecular weight
n	Constant of Eq. (6)
p	Partial pressure of thiophene (mm Hg)
Q_a	Isosteric heat of adsorption (cal/g mol)
q_i	Amount of thiophene adsorbed irreversibly (g mol/g cat)
q_{it}	Total amount of irreversible adsorption (g mol/g cat)
q_r	Amount of thiophene adsorbed reversibly (g mol/g cat)
R	Gas constant

....

S_A	Area under the curve ABCD (Fig. 5) (cm^2)
s	Sensitivity (cm^2/g mol)
T	Column temperature (°K)
t	Time (sec)
U	Interstitial carrier gas velocity (cm/sec)
V	Pulse size (cm^3)
W	Weight of catalyst (g)
α and β	Constant of Eqn. (7)
ε_i	Intraparticle void fraction
ε_e	External void fraction
μ_1	First absolute moment (sec)
ρ	Density of thiophene (g/cm^3)

.....

REFERENCES

1. Agliardi, N., and Marelli, S., Giazz. Chim. Ital., 78, 707 (1948)

2. Beebe, R.A., Low, G.W. (Jr), Willdner, E.L. and Goldwasser, S., J. Am. Chem. Soc., 57, 2527 (1935)

3. Benton, A.F., White, T.A., J. Am. Chem. Soc., 54, 1820 (1932)

4. Carberry, J.J., Nature, 189, 391 (1961)

5. Choudhary, V.R., Doraiswamy, L.K., Ind. Eng. Chem. Prod. Res. Dev., 10, 218 (1971)

6. Choudhary, V.R., Srinivasan, K.R., J. Chromatogr., 148, 373 (1978)

7. Conway, Pierce, Bland, Iwing, J. Phys. Chem. 71, 3408 (1967)

8. E'ltekov Yu. A., Semenova, V.N., Akad, Nauk. SSSR, 6, 243 (1964)

9. Eucken, A., Z. Electrochem., 53, 285 (1949)

10. Grubner, O., Advan. Chromatogr., 6, 173 (1968)

11. Huber, J.F., Keulemans, A.J.M., Procd. 44th Symp. Gas Chromatogr. Hamburg, p. 26 (1962)

12. Iijima, S.I., Rev. Phys. Chem., Japan, 12, 1 (1938)

....

13. Kieselev, A.V., Yashin, Y.I.,
'Gas-Adsorption Chromatography', Plenum Press,
New York, London (1969)

14. Kipping, P.J., Jeffery, P.G.,
Nature, 200, 1314 (1963)

15. Kipping, P.J., Winter, D.G.,
Nature, 205, 1002 (1965)

16. Low, M.J.D., Taylor, H.A.,
J. Electrochem. Soc., 106, 138 (1959)

17. Lygin, V.I., Romanovskii, B.V., Topehieva, K.V.,
Thanh, Ho, Chi,
Z.h. Fiz. Khim. 42 (1), 289 (1968)

18. Mardashev, Yu. S., Agronomos, A.E.,
Z.h. Fiz. Khim. 36, 1785 (1962)

19. Owens, P.J., Amberg, C.H.,
Cand. J. Chem. 40, 947 (1962)

20. Owens, P.J., Amberg, C.H.,
Ad. Chem. Ser. 33, 182 (1961)

21. Sastri, M.V.C., Vishwanathan, T.S.,
J. Am. Chem. Soc., 77, 3967 (1955)

22. Sastri, M.V.C., Gupta, R.B., Vishwanathan, T.S.,
J. Catal., 32, 325 (1974)

.....

PUBLICATION

Part of the work in Chapter 5 have been published in "Journal of Catalysis", Vol. 60, 21-26 (1979). A reprint of the above article is attached at the end.

...

JOURNAL OF CATALYSIS 60, 21–26 (1979)

Some Unusual Observations Concerning the Adsorption of Thiophene on Copper Chromite

S. D. SANSARE, V. R. CHOUDHARY, AND L. K. DORAISWAMY

National Chemical Laboratory, Poona-411 008, India

Received August 11, 1978; revised April 3, 1979

Adsorption of thiophene, a poison, on copper chromite catalyst has been studied at conditions close to those used in the reduction of nitrobenzene to aniline (i.e., at temperatures of 150° to 300°C and in the presence of excess hydrogen) by using pulse gas chromatographic technique. Both irreversible and reversible adsorption on a surface partially saturated with irreversibly adsorbed thiophene showed unusual behaviour: the rate of irreversible adsorption and the extent of reversible adsorption increased with initial surface coverage due to irreversible adsorption.

INTRODUCTION

Copper chromite catalyst is known to be poisoned by thiophene which is invariably present in traces in feeds of petrochemical origin. Earlier studies (*1*) on the poisoning of copper chromite catalyst by thiophene for the reduction of nitrobenzene to aniline revealed that both irreversible and reversible adsorption of thiophene on the catalyst play an important role in the poisoning. The present study has been undertaken to investigate the adsorption behavior of thiophene on copper chromite catalyst under reaction conditions (in the temperature range 150–300°C and in the presence of hydrogen) using the gas chromatographic pulse technique.

EXPERIMENTAL TECHNIQUE

The chromatographic adsorption data were collected using an NCL-AMIL dual column gas chromatograph equipped with a flame ionization detector (FID). Hydrogen (ultrahigh purity) was used as the carrier gas (and also as fuel for the detector).

A stainless-steel chromatographic column (6.0 mm o.d. and 60 mm length) was prepared by packing copper chromite catalyst ($CuO \cdot CuCr_2O_4$, developed in our laboratory for the vapor phase reduction of nitrobenzene to aniline) in the form of particles of average size 0.34 mm. The catalyst had the following properties: specific surface area, 54.0 m^2/g; porosity, 0.63; average pore radius, 108 Å.

After connecting the catalyst column to the gas chromatographic unit, the catalyst was reduced by passing a mixture of hydrogen and nitrogen (ultrahigh purity) (10% H_2) at 200°C for 2 hr and then finally at 300°C for 12 hr. The reduced form of the catalyst was 2 $Cu–Cr_2O_3$ as indicated by its loss in weight (10.5%) after reduction.

For the study of irreversible adsorption, the carrier gas flow (40 ml/min) was switched to catalyst column with the help of a two-way stopcock and the pulse experiments were carried out by injecting

0021-9517/79/130021-06$02.00/0

5.0 μl of thiophene into the catalyst column using a Hamilton microliter syringe and recording the elution chromatograms. The area under the peak of the pulse of thiophene in the absence of catalyst was obtained by switching the carrier gas to empty column and injecting the same amount of thiophene pulse into the empty column under identical conditions.

RESULTS AND DISCUSSION

Irreversible Adsorption

Irreversible adsorption of thiophene was detected by comparing the areas under the elution peaks obtained with and without the catalyst. The area of the former peak was found to be less than that of the latter at all the temperatures studied, thus indicating irreversible adsorption of thiophene on the catalyst. In order to measure the extent of irreversible adsorption quantitatively, a number of peaks were recorded by passing successively pulses of thiophene (each of 5.0 μl size) over the catalyst under the same experimental conditions. The amount of irreversibly adsorbed thiophene q_i during the passage of each pulse was estimated from

$$q_i = \frac{Ve}{WM}\left[\frac{A^* - A}{A^*}\right] \qquad (1)$$

where A^* and A are the areas under the elution peaks in the presence and the absence of catalyst, respectively, V is the pulse size, W is the weight of catalyst, M is the molecular weight, and e is the density of thiophene.

Representative elution peaks of the successive thiophene pulses obtained on the catalyst at 150°C are presented in Fig. 1. At all the other temperatures of study, the elution curves obtained were generally similar to those at 150°C.

Figure 2a shows the variation of the peak area of the effluent pulse with pulse number at all the temperatures studied. At 150°C, as the pulse number increases, the peak area of the effluent pulse decreases initially, passes through a minimum (at pulse number 5) and then levels off. However, this trend is reversed at and above 200°C; the peak area of the effluent pulse increases initially, passes through a maximum near about a pulse number of $\frac{3}{4}$, and then levels off. It may also be noted that this reversal in trend takes place gradually with temperature.

The variation in irreversible adsorption during the passage of each pulse of thiophene with pulse number can be readily obtained from the above figure and is shown in Fig. 2b. In this case, the trend of the curves (q_i vs pulse number) is exactly opposite to that of those shown in Fig. 2a. The nature of dependence of irreversibly adsorbed thiophene on pulse number (or on the extent of initial surface coverage) is quite unusual. A previous study (2) involving the adsorption of hydrogen on this catalyst had shown the usual adsorption behavior: The area of the elution peak increased gradually with peak number and finally reached a maximum or a constant value; hence the amount of irreversibly adsorbed hydrogen during the passage of each pulse decreased with pulse number.

Reversible Adsorption on Catalyst with Partially Saturated Irreversible Adsorption Sites

The retention volume of the adsorbate is a convenient measure of reversible adsorption. In the present study, retention volume is based on the first absolute moment (μ_1) of the chromatographic curves instead of the retention time (which is based on the peak maximum) because the retention data based on the first absolute moment give a more correct picture of reversible adsorption (*2*), particularly when the elution curves are asymmetric.

The values of μ_1 for thiophene were calculated from the chromatographic data by the usual method (*2*). Since it was not possible to obtain μ_1 for the inert gas experi-

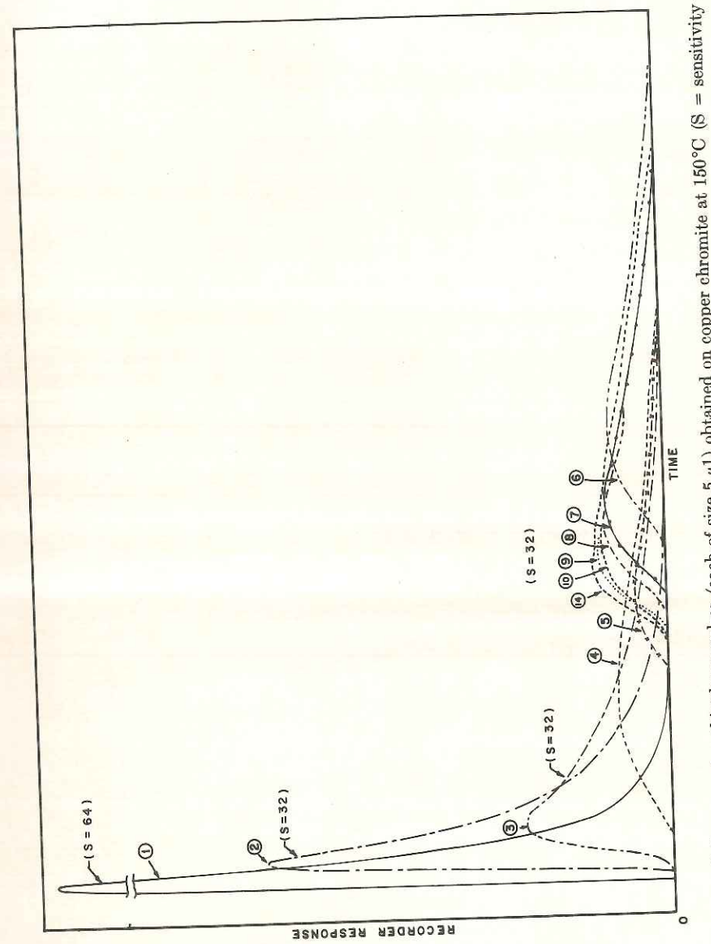

FIG. 1. Elution peaks of the successive thiophene pulses (each of size 5 μl) obtained on copper chromite at 150°C (S = sensitivity or attenuation).

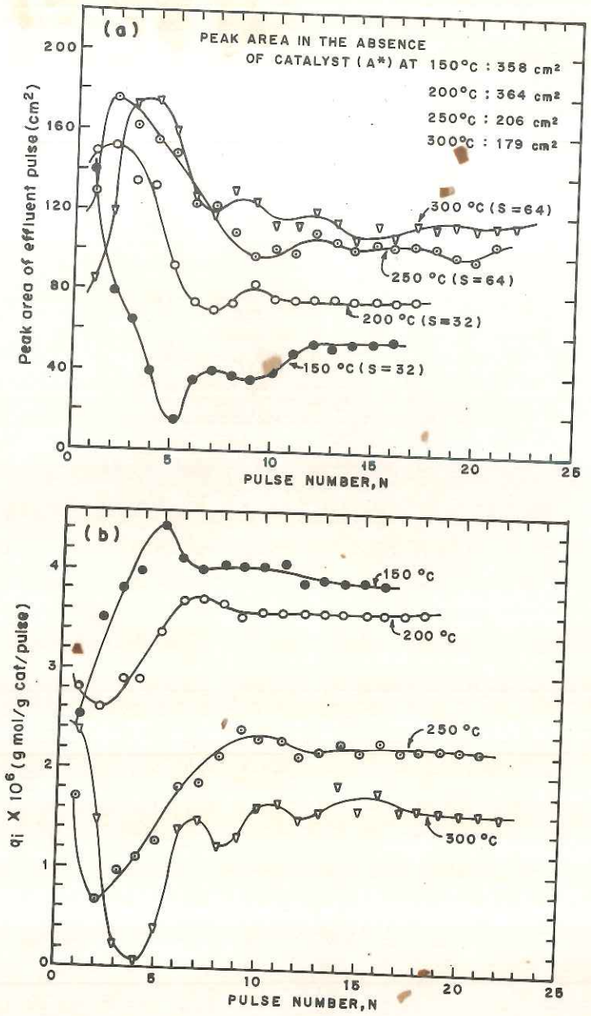

FIG. 2. Effect of initial surface coverage on the irreversible adsorption of thiophene during the passage of each pulse.

mentally (because of the use of FID), the values of $\mu_{1(\text{inert})}$ were calculated (*3*) from a knowledge of carrier gas flow rate and column characteristics.

The variation of the retention volume $[F(\mu_{1\,(\text{thiophene})} - \mu_{1\,(\text{inert})})]$ of thiophene with pulse number is shown in Fig. 3a. In order to emphasize the dependence of the retention volume on the initial surface coverage (due to irreversible adsorption), the total amount of irreversibly adsorbed thiophene (q_{it}) as a function of pulse

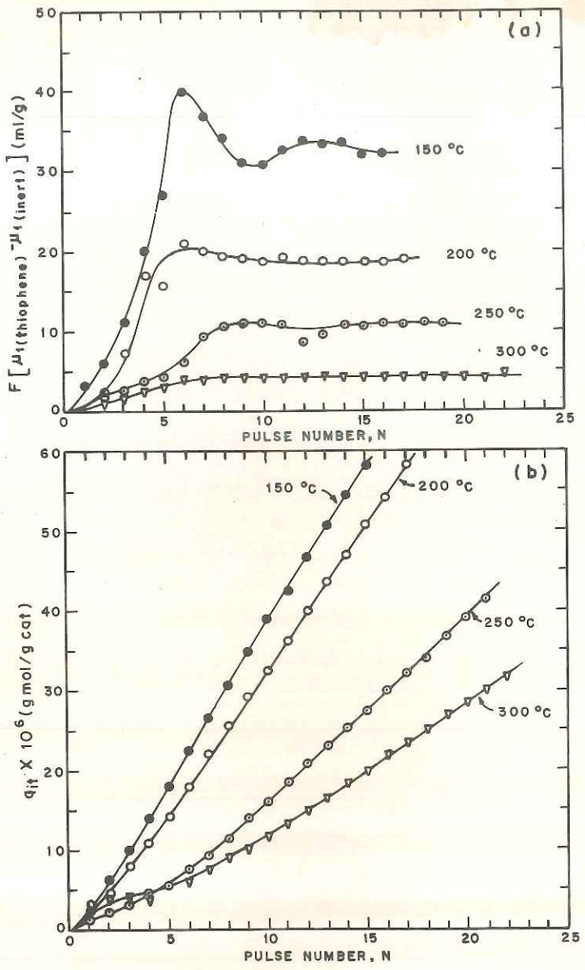

FIG. 3. Effect of initial surface coverage of irreversibly adsorbed thiophene on the extent of reversible adsorption of thiophene on copper chromite.

number is shown in Fig. 3b. It can be seen from these plots that, as the initial surface coverage increases, the retention volume (and therefore the extent of reversible adsorption) increases initially, passes through a maximum (except at 300°C) and then levels off. It may also be noticed that the plots of retention volume vs pulse number show a typical trend which gradually changes with temperature.

Examples of unusual adsorption behavior such as enhancement in the amount adsorbed and/or of the rate of adsorption due to the presence of the same species or some

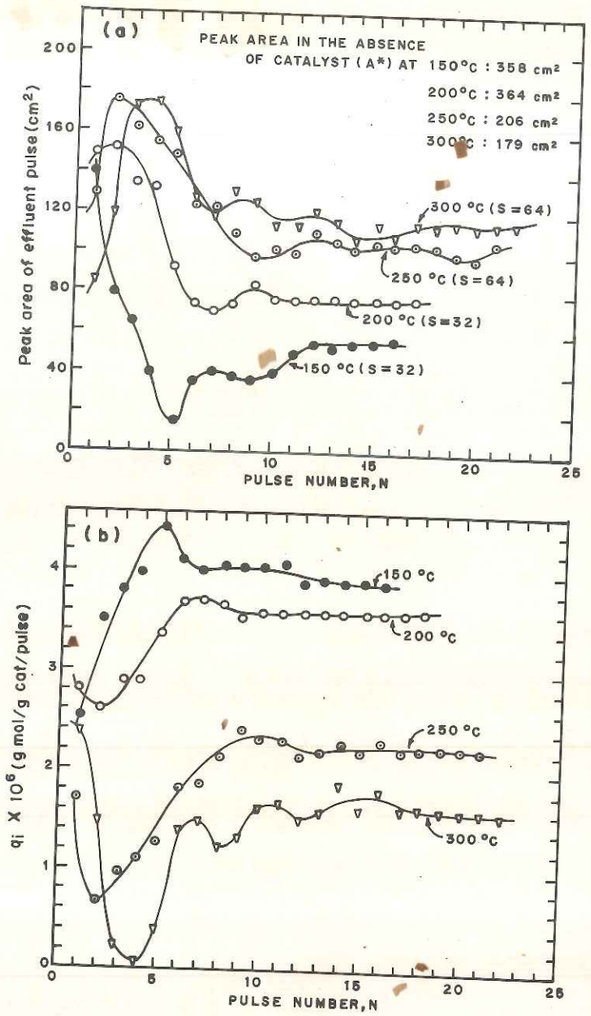

FIG. 2. Effect of initial surface coverage on the irreversible adsorption of thiophene during the passage of each pulse.

mentally (because of the use of FID), the values of $\mu_{1(\text{inert})}$ were calculated (*3*) from a knowledge of carrier gas flow rate and column characteristics.

The variation of the retention volume $[F(\mu_{1\ (\text{thiophene})} - \mu_{1\ (\text{inert})})]$ of thiophene with pulse number is shown in Fig. 3a. In order to emphasize the dependence of the retention volume on the initial surface coverage (due to irreversible adsorption), the total amount of irreversibly adsorbed thiophene (q_{it}) as a function of pulse

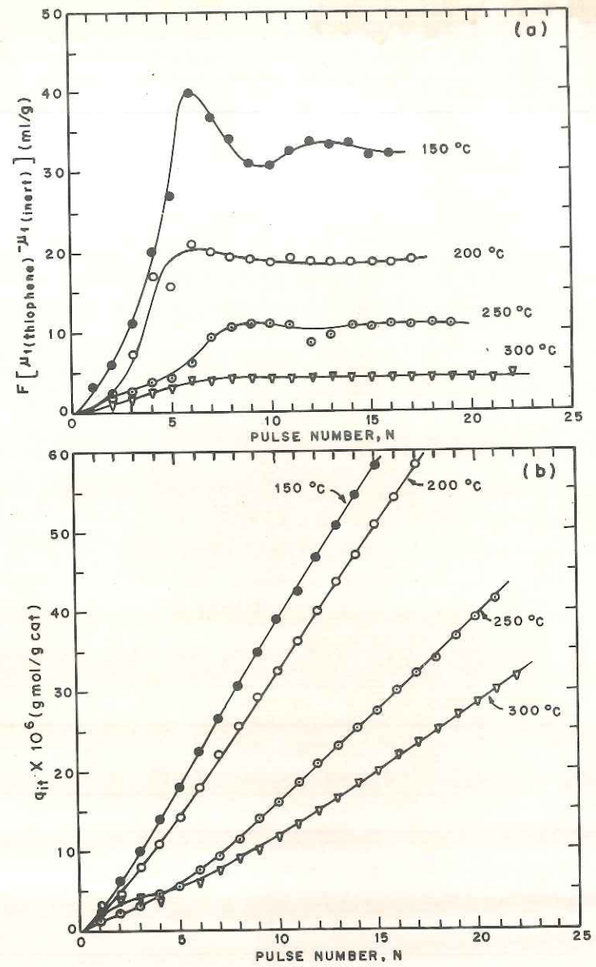

FIG. 3. Effect of initial surface coverage of irreversibly adsorbed thiophene on the extent of reversible adsorption of thiophene on copper chromite.

number is shown in Fig. 3b. It can be seen from these plots that, as the initial surface coverage increases, the retention volume (and therefore the extent of reversible adsorption) increases initially, passes through a maximum (except at 300°C) and then levels off. It may also be noticed that the plots of retention volume vs pulse number show a typical trend which gradually changes with temperature.

Examples of unusual adsorption behavior such as enhancement in the amount adsorbed and/or of the rate of adsorption due to the presence of the same species or some

other species on the catalyst surface are very few. In the present case, the adsorption of thiophene on copper chromite involves an enhancement (i) in the rate of irreversible adsorption as indicated qualitatively by the pulse experiments (Fig. 2b), and (ii) in the extent of reversible adsorption with increase in the surface coverage due to irreversible adsorption (Fig. 3a). Such enhancing effects on adsorption due to the presence of the same adsorbate are very rare, e.g., H_2 on iron (*4*), copper (*5*), and nickel (*6*).

The unusual trend in the irreversible and reversible adsorption of thiophene on a partially covered catalyst surface, which changes gradually with temperature (an additional peculiarity), may probably be explained by considering the possibility of the modification of existing sites and/or creation of new adsorption sites during the process of irreversible adsorption.

The gas chromatographic pulse flow technique seems to be unique, particularly in the study of reversible adsorption at various initial surface coverages due to the irreversible adsorption of the same species or some other species. It can also be conveniently employed for studying the effect of various preadsorbed species on the irreversible adsorption of a particular adsorbate.

REFERENCES

1. Sansare, S. D., and Doraiswamy, L. K., to appear.
2. Choudhary, V. R., and Srinivasan, K. R., *J. Chromatogr.* **148**, 373 (1978).
3. Grubner, O., *Adv. Chromatogr.* **6**, 173 (1968).
4. Benton, A. F., and White, T. A., *J. Amer. Chem. Soc.* **54**, 1820 (1932).
5. Beebe, R. A., Low, G. W., Jr., Wildner, E. L., and Goldwasser, S., *J. Amer. Chem. Soc.* **57**, 2527 (1935).
6. Eucken, A., *Z. Electrochem.* **53**, 285 (1949).